The Role of Kitlb on Development of Coordinated Muscular Contractions in the Zebrafish Gastrointestinal Tract

By
Brittany A. Heatherington

To
Graduate School in Partial Fulfillment of the Requirements
for the Degree of Master if Sciences in Biological Sciences

The College at Brockport

The College at
BROCKPORT
STATE UNIVERSITY OF NEW YORK
DEPARTMENT OF BIOLOGY

August 22, 2012 **Thesis Defense**

ittee Members	Approved	Not Approved	Comment
_____ Major Advisor	✓		
_____ Committee Member	✓		
_____ Committee Member	X		

ate Director: _____

tment Chair: _____

Abstract

Gastrointestinal (GI) motility is the spontaneous rhythmic contractions of smooth muscles that mix and propel the contents of the GI tract. Regulation of the complex muscular contractions is controlled by smooth muscles, interstitial cells of the Cajal (ICC) and enteric neurons. ICC act as pacemaker cells in the GI tract and set the frequency of spontaneous contractions. Altering ICC density results in uncoordinated GI muscular contractions. Our lab examines the role of ICC in GI motility and is focused on mechanisms that regulate ICC growth and development. Expression of the Kit receptor tyrosine kinase is used to identify ICC. Kit is stimulated by Kit ligand and stimulation is necessary for the growth and development of ICC. This project specifically examines the role of Kit - Kit ligand signaling on ICC development using the zebrafish model system. The zebrafish has two Kit genes (*kita* and *kitb*) that are orthologous to human *KIT*, and two Kit Ligand genes (*kitla* and *kitlb*). I will examine the role of *kitlb* on the development and maturation of ICC using morpholino oligonucleotides knockdown in zebrafish. Gene expression was quantified using reverse transcriptase PCR analysis. Digital imaging techniques was used to examine morphology of the GI tract. It is anticipated that continued stimulation of *kitb* by *kitlb* is necessary for development of the ICC network, and maintenance of the ICC network in adult animals.

Table of Contents

Abstract 2

Acknowledgments 8

Specific Goals of the Research 9

Introduction 16

KIT Ligand 19

How the KIT Gene Works 21

Anatomical and Functional Role of ICC 29

The Zebrafish Model 12

Zebrafish ICC 32

Morpholinos (MOs) 35

Fish Disease 37

Objective and Experimental Plan 38

Experimental Procedure 41

Aquaculture 41

Streamline Zebrafish Husbandry 42

Cleaning Larvae 43

Counting / Logging Larvae Viability 44

Morpholino 45

MO Design 46

Preparation / Storage of Stock Solution 47

Working Solution 47

Testing Efficacy of MO 48

GI Motility Assay 49

Fertilization and MO Injection 50

Screening of Embryos 50

Mounting 7dpf Larvae and Digital Imaging 51

Tiling Images 52

Digital Image Analysis 53

Motility Index 54

Statistical Analysis 55

RNA Isolation 55

Quantifying RNA by Spectral Absorption 56

cDNA Synthesis 56

Reverse Transcriptase Polymerase Chain Reaction (RT-PCR) 57

Potential Pitfalls 58

Results 59

Discussion/Conclusion 82

References 88

Appendix

1. Breeding Zebrafish Appendix 1

2. Larvae Care / Larvae Counting Appendix 2

3. Solutions Appendix 2

4. Micropipette Appendix 3

4.1: Pulling of Micropipette Appendix 3

4.2: Cutting Micropipette Appendix 4

4.3: Loading Micropipette for Injection Appendix 4

4.4: Attaching Micropipette in Pressure Injector Appendix 4

4.5: Prepping and Injection of Embryos Appendix 4

5. Primers Appendix 5

6. Mounting Agar / Standard Length Appendix 6

7. Standard Length Appendix 7

8. RNA Isolation (Qiagen Kit) Appendix 7

9. Synthesis of cDNA Appendix 8

9.1: Verification of RNA isolation and cDNA synthesis Appendix 8

10. Maintenance of the NanoDrop Appendix 11

10.1: Cleaning NanoDrop Appendix 11

10.2: Testing the NanoDrop Appendix 11

11. GI Motility Data Appendix 12

12. Motility Index Data Appendix 18

List of Figures

Figure 1, Genomic structure of zebrafish *kitla* and *kitlb* 61

Figure 2, Protein sequence comparison of zebrafish *kitla* and *kitlb* to mouse KL-1 and KL-2 62

Figure 3, Zebrafish *kitlb* amino acid sequence 63

Figure 4, Mouse KL-2 amino acid sequence 63

Figure 5, *kitlb* MO knockdown of *kitlb* expression 64

Figure 6, Verification of MO injection in embryos 66

Figure 7, Gel electrophoresis confirms *kitla / kitlb* MO knockdown in 5dpf larvae 67

Figure 8, Gel electrophoresis confirms *kitla / kitlb* MO knockdown in 7dpf larvae 69

Figure 9, Standard length of *kitla / kitlb* MO knockdown 5dpf larvae 71

Figure 10, Standard length of *kitla / kitlb* MO knockdown 7dpf larvae 72

Figure 11, Standard length of *kitlb* MO knockdown 7dpf larvae 73

Figure 12, Coordinated GI motor patterns inhibited with *kitla* and *kitlb* MO knockdown 75

Figure 13, Coordinated GI motor patterns in anterior GI region of 5dpf larvae inhibited with *kitla / kitlb* MO 76

Figure 14, Coordinated GI motor patterns in posterior GI region of 5dpf larvae inhibited with *kitla / kitlb* MO 77

Figure 15, Coordinated GI motor patterns in anterior GI region of 7dpf larvae inhibited with *kitla / kitlb* M0 78

Figure 16, Coordinated GI motor patterns inhibited in posterior GI region of 7dpf larvae by *kitla / kitlb* MO 79

Figure 17, Motility Index of 7dpf *kitlb* injected larvae 80

Figure 18, Motility Index of co – injected *kitla / kitlb* 5dpf and 7dpf MO injected larvae 81

Acknowledgments

I thank Dr. Rich, my advisor for giving me the opportunity to work in his laboratory, for his guidance, support and advice throughout my time at Brockport and with this project. I would like to express a special thanks to my committee members Dr. Tsubota and Dr. Pelletier for their assistance. I would also like to thank my fellow lab members for help caring for the zebrafish.

Specific Goals of the Research

The purpose of this study is to understand the role *kit ligand b (kitlb)* has on maturation and development of interstitial cells of Cajal (ICC) in the zebrafish. This is important because activation of Kit receptor by Kit ligand is necessary for growth and development of ICC in both humans and in mice (Hurst and Edwards 2004). ICC play an essential role in the regulation of complex motor patterns in the Gastrointestinal (GI) tract, a process called motility. Pathophysiological disturbances in motility, such as constipation and irritable bowel syndrome, are associated with decreased density of ICC. The zebrafish model system is used for experiments in this thesis because it is transparent during early developmental stages and GI motility can be directly observed in the intact animal.

Kit ligand is expressed in the GI tract by multiple cell types, including enteric neurons and smooth muscle cells (Ordog, Takayama, Cheung, Ward, & Sanders, 2000). Kit ligand functions as a growth factor and is expressed in two physiological isoforms: soluble and membrane bound. It is necessary to understand that a ligand is a substrate such as an activator, inhibitor or neurotransmitter that binds to a receptor found on a protein. Ligand binding to a receptor is generally very specific, as many non-covalent interactions must occur simultaneously. Once bound, the ligand can activate cell-signaling mechanisms, and in the case of Kit - Kit ligand binding, the Kit receptor becomes phosphorylated and initiates a complex signaling pathway. The Kit-ligand and

Kit receptor is a signaling pathway that plays a critical role in hematopoiesis, generation of melanocytes and the generation of germ cells. Most important for this thesis it also plays a significant role in the development of ICC in the GI tract. It is well established in humans and mice that signaling by kit receptor tyrosine kinase is mandatory for normal ICC development and maintenance in mature gastrointestinal tissues.

Soluble and membrane bound Kit ligand are encoded by human Kit Ligand *(KITLG)* gene. Initially, both the soluble and membrane bound isoforms of Kit ligand are synthesized and targeted to the plasma membrane. The soluble isoform of Kit ligand undergoes rapid proteolytic cleavage at exon 6 and is subsequently released from the cellular membrane in its biologically active conformation. The membrane bound isoform of Kit ligand is activated at a much slower rate because it lacks the proteolytic cleavage site of soluble Kit ligand. Soluble and membrane bound isoforms of Kit ligand are found in different ratios in various tissues. This is indicative that each isoform plays a definite physiological role in an assortment of tissue. For example, the Steel-Dickie mutant mouse lacks membrane bound Kit ligand and is also lacking ICC networks located in the myenteric plexus region of the GI tract (Maeda, et al., 1992). GI motility in the Steel Dickie mutant mouse is unorganized, uncoordinated and arrhythmic.

Zebrafish *kit ligand a (kitla)* and *kit ligand b (kitlb)* have been identified as co-orthologs to the mammalian *KIT* Ligand. The evolutionary linage can be

visualized using on a phylogenetic tree of well-known tetapod sequences. The two copies of zebrafish *kit ligand* appear more closely related to each other than the tetrapod clade. Evidence suggests that the two copies of the *kit ligand* gene in the zebrafish originated from a duplication event in the teleost lineage after the divergence from the tetrapod lineage, but before the teleost radiation (Hultman, Bahary, Zon, & Johnson, 2007). It is reasonable to infer that due to the resemblance of *kitla* and *kitlb* in zebrafish to the alternative splice forms of mammalian *KIT* Ligand, these genes would have similar functions and roles as the mouse isoforms.

This thesis uses *kitlb* morpholino oligonucleotide knockdown and examines its effect on gastrointestinal (GI) motility in zebrafish. ICC development was assayed by directly measuring GI motility patterns in 7 dpf transparent larvae. *Kitlb* MO treated larvae displayed uncoordinated motility patterns, had fewer contractions, and shorter contractions when compared to control larvae. These results show that *kitlb* is necessary for the development of normal motility patterns in the zebrafish GI tract

The Zebrafish Model

Model organisms are non-human species with extensively studied genomes. They are used to better understand biological events with the underlying ideology that understanding a model organism will help contribute to further insight of other organisms. Model organisms are commonly used to understand human diseases especially when experimentation on humans is unethical or unattainable. A model organism is selected for experimental use based primarily on its ability to be manipulated, but may also be chosen because of its accessibility, size, developmental rate or genetic conservation. The NIH has selected a small group of species that are accepted as good model organisms because of the wealth of data that has been collected for each organism. These models are divided into two categories; non-human mammalian models (rat and mouse) and non-mammalian models (budding yeast, roundworm, fruit fly and the zebrafish). Depending on the field of research a model organism may be more suitable over another. For example, genetics and cellular based biological experiments may migrate toward the use of more simple organisms such as budding yeast or toward organisms such as the fruit fly that can exhibit visible phenotypical traits. On the other hand, developmental biologist may want to choose the roundworm because of its fix number of cells making it easier to identify developmental patterns. Biologist choosing to study more complex physiological systems, development, disease, organ function, behavior or toxicology of vertebrates or mammalians may choose to work with the mouse or

zebrafish model. The mouse model (*Mus musculus*) is similar to mammals, has about the same size genome as humans and contains a well-conserved gene order that is helpful for studying human disease (Twyman, 2002). The zebrafish (*Dario rerio*) model shares many homologous genes with mammals and is used to understand vertebrate systems. The genome size of the zebrafish is smaller compared to the mouse, making it more manageable to work with (Twyman, 2002).

The zebrafish model organism is expanding as a system to study human disease. The presents of ICC in the zebrafish (Rich, et al., 2003) make it an appropriate model to study gastrointestinal (GI) motility in a high throughput fashion. Naturally, zebrafish flourish in the freshwaters of south Asia. However, for laboratory purposes the zebrafish thrive in temperature regulated and chemically balanced aquariums. Zebrafish tanks are kept in a facility that has a controlled 24-hour light/dark cycle simulating the length of an entire day. The light cycle is important for laboratory-raised zebrafish by establishing a regular feeding and breeding schedule. Male and female zebrafish reach sexual maturity by four months of age and a single pair of adults has the ability to produce 100-200 offspring. Zebrafish embryos develop outside of the female zebrafish . The embryos develop into optically transparent larvae twenty-four hours post fertilization and remain transparent through 10 days post fertilization. The transparency of the larvae make it possible for the observation of developmental processes such as the multi-chambered heart, brain, kidney, notochord and

eventually the contractions of the gastrointestinal tract all of which can be recorded using time lapse imaging.

Manipulations of the model systems genome using genetic engineering can alter cellular DNA causing change in traits or it can be used to produce biological products. In the case of the zebrafish model system, genetic manipulations can be made by RNA interference or by triple-helix forming molecules to reduce expression of a gene or interruption of transcription of a targeted gene respectively. For example, melanocyte pigment patterns in vertebrate systems have been long studied for pattern formation and morphogenesis. The pattern formations are used to identify genes, better understand of signal transduction as well as cell-to-cell communication (Hultman, Bahary, Zon, & Johnson, 2007). Observation of mRNA expression using *in situ* hybridization has identified one of the co-orthologs, *kitla* in zebrafish to be most similar to mouse KL-1. Both *kitla* and KL-1 retain the proteolytic site of exon 6, suggesting that the critical roles of the genes are conserved. Melanocyte migration and survival, one of the critical roles of KL-1 in mice was shown to maintain the same function as *kitla* in zebrafish. Experimental results using the zebrafish model system and a morpholino knockdown, revealed failure of melanocytes migration, while enhancement *kitla* morpholino caused hyperpigmentation (Hultman, Bahary, Zon, & Johnson, 2007). Further confirming the *kitla* gene identity and establishing that *kitla* plays all the necessary ligand roles for *kita*. Taken together, the results indicate

that *kit ligand* in zebrafish, just like in mouse and humans is responsible for the generation of melanocytes, hematopoiesis, the generation of germ cells. More over, in mice and humans it is well characterized that kit ligand has another critical role in the function of ICC. Careful analysis of previous experimental procedures using the zebrafish suggests that *kit ligand* may also play a role in ICC function.

The zebrafish sparse mutant phenotype is characterized by its absence of pigmentation and pigmentation migration. Careful analysis of the sparse mutant phenotype has identified the mutant of being null *kitla*. Literature demonstrates that along with pigmentation deficiencies, the sparse mutants also have distended GI tracts and unorganized GI muscular contractions (Rich, et al., 2003). These findings are coherent with *Kit* function compromised W/W^v mutant mice. Phenotypical characterization shows that W/W^v mutants also exhibit absences in melanocytes migration and display distended guts (Maeda, et al., 1992). Conservation of Kit function in the model systems of the mouse and zebrafish suggest that the zebrafish would be an excellent system to study human GI physiology.

Introduction

The gastrointestinal (GI) tract holds the responsibilities of digestion, absorption of nutrients and elimination of waste product. It may be best described as long and layered tube that extends a distance of 30 feet in adult humans. The long tube making up the GI tract is divided into different regions each with its own purpose. It starts at the mouth, duodenum, small intestine, large intestine and finally reaches the colon. All regions of the GI tract are comprised of four layers. The innermost layer is the mucosa, a mucous membrane made of smooth muscles that surrounds the lumen. The contractions of the mucosa enable the lumen to change in shape. Next, is a layer of dense irregular connective tissue known as submucosa. This layer is responsible for the secretion of enzymes and buffers into the lumen. Followed by the muscularis externa, which is comprised of smooth muscle cells that are arranged as circular and longitudinal cell layers and neurons. This layer plays a responsibility in the processing and movement of intestinal content. Finally, the serosa, a serous membrane is made up of loose connective tissues stabilizing the GI tract.

The epithelia lining of the GI tract is in close contact with lumen that connects to both internal and external environments. Therefore, a balance must be maintained in the GI tract to ensure there is an adequate absorption of water, electrolytes, nutrients and the appropriate elimination of waste all while instituting a barrier to separate the luminal cavity from the underlying tissues (Shen, 2009). The intestinal triad sustains regulation of this balance; a group of

cells working together to ensure that intestinal content is moved in an oral to colon direction. The triad is composed of enteric neurons, smooth muscle cells and interstitial cells of Cajal (ICC). Disruption in any one part of the intestinal triad may lead to GI motility disorders.

GI motility disorders affect a large percentage of the human population and are not limited to a specific demographic. Gastrointestinal disorders can greatly affect the quality of an individual's life. Symptoms of GI disorders can range from mild discomfort to severe pain, but are almost always embarrassing! It is estimated that around 10-20% of the human population suffer from dysmotility disorders including: Irritable Bowl Syndrome (IBS), Inflammatory Bowl Disease (IBD), Gastroparesis and related Diabetic Gastroparesis.

Diabetic Gastroparesis affects about 30-50% of the human population after 10 years of being diagnosed with Type 1 or Type 2 diabetes. Its symptoms can range from mild dyspepsia to severe abdominal pain and can eventually lead to malnutrition and imbalance of water and electrolytes. To better understand the pathophysiology of this GI disorder, non-obese (NOD) Type 1 diabetic mice were observed. Gastric emptying was measured, electrical activity of spontaneous and induced circular smooth muscles and presence of ICC was monitored (Ordog, Takayama, Cheung, Ward, & Sanders, 2000). Results concluded NOD mice have erratic loss of ICC and irregular electrical peacemaking further suggesting disruption in one part of the intestinal triad, in this case ICC may lead to GI motility disorders.

Currently, treatment for dysmotility is limited, leaving victims with embarrassing symptoms and discomfort. It is hopeful that novel drug treatments will come about with greater understanding of gastrointestinal physiology and the individual components of the intestinal triad. Knowledge of the development and maturation of ICC may contribute to further understanding of GI motility disorders and potential drug targets.

Kit Ligand

Kit-ligand, also known as steel factor, is a growth factor occurring in two physiological isoforms; soluble and membrane bound. A signaling cascade is initiated by the binding of steel factor to the Kit receptor tyrosine kinase. This growth factor plays critical roles in hematopoiesis, generation of melanocytes, and the generation of germ cells, which give rise to gametes (Linnekin D., 1999). A vast literature exists describing the molecular mechanisms involved in this signaling pathway and specific aspects of the signaling pathway that play an important role in leukemia (Linnekin D., 1999). The physiological roles for Kit-Kit ligand signaling are pleiotropic. Maeda and coworkers identified a specific role for Kit signaling in ICC development by injecting the neutralizing antibody ACK2 into the peritoneum of mice (Maeda, et al., 1992). Injected mice displayed grossly distended small intestines, and immunostaining revealed an absence of ICC. Kit ligand also plays a significant role in the development of ICC found in the gastrointestinal tract. The Steel Dickie mutant mouse that is lacking one form of Stem Cell factor demonstrates the role of Kit ligand. The Steel Dickie mouse displays a distended small intestine, and is therefore similar to the W/W^v mutant mouse that lacks functional Kit receptors (Maeda, et al., 1992). The mutant mouse models show that signaling cascades initiated by binding interactions between Kit ligand and the Kit receptor tyrosine kinase is mandatory for normal ICC development and maintenance in mature gastrointestinal tissues (Ward, Burns, Torihashi, & Sanders, 1994) (Huizinga,

Thuneberg, kluppel, Mikkelsen, & Berstein, 1995) (Kluppel, Huizinga, Malysz, & Berstein, 1998).

Soluble and membrane bound steel factor isoforms are encoded by the KITLG gene (Huang, Nocka, Buck, & Besmer, 1992). These isoforms are expressed as transmembrane proteins at surface of the cells. Initially both the soluble and membrane bound isoforms of steel factor (SF) are transcribed and targeted to the plasma membrane in an inactive conformation (Huang, Nocka, Buck, & Besmer, 1992) The soluble isoform of SF undergoes rapid proteolytic cleavage and is subsequently released from the cellular membrane in its biologically active conformation. The membrane bound isoform of SF is solubilized and activated at a much slower rate because it lacks the proteolytic cleavage site of soluble SF (Huang, Nocka, Buck, & Besmer, 1992). Soluble and membrane bound SF is found in assorted ratios in various tissues. This is indicative that each isoform plays a definite physiological role in an assortment of tissue. For example membrane-bound SF is essential for the development and maintenance of ICC networks located in the myenteric plexus, and in the Steel-Dickie mutant mouse that lacks membrane-bound-SF, networks of ICC in the myenteric plexus region are impaired (Broudy, 1997). The decrease in density of the ICC networks in the myenteric plexus region are correlated with unorganized, uncoordinated and arrhythmic patterns in the Steel-Dickie mutant mouse consistent with a role for ICC in the generation of coordinated motility patterns.

How the KIT Gene Works

KIT encodes a receptor tyrosine kinase that is expressed on the plasma membrane and is activated by the binding of Kit ligand. The natural receptor for Kit is Kit ligand, and when Kit ligand binds to the extracellular component of Kit a signaling cascade is triggered that initiates cell differentiation. Therefore KIT is considered to be a growth factor receptor. The Kit receptor is expressed on a variety of cell types including germ cells, mast cells, and hematopoietic stem cells. Kit plays an important role in the migration of melanocytes, development of sensory neurons of the peripheral nervous system, and in ICC development and maintenance of the ICC phenotype on mature tissue (Kluppel, Huizinga, Malysz, & Berstein, 1998).

The nomenclature and naming used for vertebrate genes and proteins can be confusing. It is important to understand the proper nomenclature early on to avoid confusion that may arise in the future. Below are charts that incorporated the important genes and proteins for this thesis.

Kit Ligand

The Kit Ligand gene works by encoding the ligand of the tyrosine- kinase receptor expressed by the gene *KIT*. Kit Ligand protein is classified as a cytokine, a signaling protein that binds to KIT to mediate cell communication of several cells types associated with cells differentiation, migration and survival

(NHI). Kit Ligand is referred to by several names including: Kit Ligand (KL),

Species	Gene Symbol	Protein Symbol
Homo sapiens (Human)	*KITLG*	KITLG
Mus musculus (Mouse)	*KL-1 and KL-2*	KL-1 and KL-2
Danio rerio (Zebrafish)	*kitla and kitlb*	Kitla and Kitlb

Mast Cell Growth Factor (MGF), Stem Cell Factor (SCF) and Steel Factor (SLF).

Kit

The Kit gene codes for the protein KIT, a cytokine receptor. Disruption in the signaling pathway of *KIT* may lead to some types of cancer. Again, the Kit receptor is known by several names, which include: Kit, c-kit, proto-oncogene c-Kit, Stem Cell growth receptor (SCGF), Mast cell growth factor (MCGF) and CD117.

Species	Gene Symbol	Protein Symbol
Homo sapiens (Human)	*KIT*	KIT
Mus musculus (Mouse)	*Kit-1 and Kit-2*	KIT-1 and KIT-2
Danio rerio (Zebrafish)	*kita and kitb*	Kita and Kitb

Mammalian development and maintenance throughout adult life requires complex mechanisms that regulate the effects of growth factors. Growth factors interact with receptors on cells surfaces and are responsible for proliferation, differentiation and survival of cells. For example the growth factor Kit Ligand

(KL) is the natural ligand for Kit. Kit, the transmembrane tyrosine kinase receptor that can be structurally classified the extracellular components of the receptor are five immunoglobulin- like domains. The first three extracellular domains bind Kit Ligand. The forth domain is believed to play a significant role in dimerization of the receptor. And, the fifth domain, closest to the cell surface has unknown function. Inside the cell the catalytic domains are divided into two separate domains; a Kinase insert serves to connect the domains (Linnekin D., 1999). KL structure can be briefly described as a ligand that can be expressed in two isoforms due to alternative splicing of mRNA. Proteolytic cleavage of the transmembrane protein results in the soluble isoform of KL, while membrane bound KL lacks the proteolytic cleavage site.

Kit Ligand works by binding to Kit inducing dimerization of the receptor. Dimerization of Kit results in autophosphorylation on a tyrosine residue. Catalytic activity of Kit is regulated due to phosphorylation of the kinase. Downstream of the Kit receptor many other signaling cascade components are activated, including: phosphatidylinositol – 3 – kinase, Src family members, JAK/STAT pathway and Ras – Raf – MAP kinase cascade (Yee, Langen, & Besmer, 1993).

In the mammalian mouse model the Kit receptor is coded for at the white spotting (W) loci while the steel (Sl) loci encodes for Kit Ligand. Previous work has shown that a mutation in the W or Sl loci can affect cellular targets in melanogensis, gemetogenesis, hematopoiesis of stem cells, growth and

development of mast cells and interstitial cells of Cajal. This suggests that Kit has a functional role in these cellular systems (Yee, Langen, & Besmer, 1993). Regulation of these cellular signaling cascades are maintained by the interactions of specific growth factors with receptors leading to various cellular responses, however, it too is important to control extracellular signals through down regulation of the receptors by means of a negative feedback loops.

Disruption in the regulation of cellular signaling cascades results from mutations in the receptor, KIT. These mutations are classified in two ways. Regulatory type mutations are a type of mutation that affects the regulation of the kinase molecule. And, enzymatic pocket type mutation caused by a substitution in the amino acid sequences at the enzymatic pocket. Both classes of mutations result in constitutive phosphorylation and activation of KIT (Longley, Reguera, & Ma, 2001). The most prevalent conditions associated with mutations in KIT include hematologic diseases, disruption in pigmentation patterns and well as formation of gastrointestinal Stromal tumors (GIST).

Mastocytosis is an increase in the number of mast cells and is a result of an enzymatic pocket mutation. This mutation occurs when the amino acid sequence for aspartate is substituted with valine at the site of the enzymatic pocket. This particular mutation can be characterized by mast cell hyperplasia in bone marrow and lymph nodes as well as organs including the liver, spleen, skin and gastrointestinal tract (Nagata, et al., 1995). There are four classes of Mastocytosis including: indolent mastocytosis, mastocytosis with associated

hematologic disorder, aggressive mastocytosis and mast cell leukemia (Nagata, et al., 1995).

Pigmentation patterns of the skin and hair may be disrupted as a result of a regulatory mutation that affects the kinase molecule in KIT. In the case of this mutation, there is an amino acid substitution of glycine for arginine within the tyrosine kinase domain (Giebel & Spritz, 1991). This mutation is referred to as Piebaldism. It is an autosomal dominant genetic disorder characterized by loss of pigmentation in the hair and skin of humans due to the absents of melanocytes (Giebel & Spritz, 1991). Similar phenotypes are observed in white spotting mice (W). These mice also have a mutation in *Kit,* which causes absents of melanocytes migration in turn making their fur appear white.

Gastrointestinal Stromal tumors (GIST) are the most prevalent type of mesenchymal tumor found in the gastrointestinal tract. This tumor arises from a regulatory type mutation, a deletion or point mutation of KIT within the juxtamembrane domain (Taniguchi, et al., 1999). It is a gain – of – function mutation causing constitutive activation of KIT signaling in the GI tract which can alter ICC development and maintenance leading to the formation of benign or malignant GISTs (Sanders & Ward, 2006) Most benign tumors are in located within the submucosa of the gastrointestinal tract. Malignant tumors are more commonly found in the liver and spread to the peritoneal cavity. Their exophtic growth patterns make them accountable for constipation, severe abdominal pain and discomfort cause by obstruction of the intestine. Drug treatment for GISTs

using Imatitab/Gleevec works by blocking the function of Kit (Sanders & Ward, 2006). It results in the disappearance of ICC and also causes arrhythmic contractions in the GI tract. It is important to mention that although GISTs represent the most common type of sarcoma occurring in the GI tract, they are still extremely rare. It has been estimated that only 1% of all cancers occurring within adults is a type of sarcoma. On the other had carcinomas, a class of cancer that derives from epithelia cells is much more prevalent. Stomach cancer and colon cancer, two cancers of the GI tract fit into the carcinoma category. Of the estimated 1.4 million cases of cancer every year, only about 15,000 are sarcomas (GIST Support International- What is GIST?, 2011).

Continuing on with the GI tract. KIT is expressed on two cell types, ICC and mast cell. These two cell types are easily distinguished by means of cell morphology. ICC appears larger in dimension when compared to the 20μm granule containing ovoid shaped mast cells (Stone, Prussin, & Metcalfe, 2011). Biochemical activation of KIT by Kit ligand promotes the signaling pathway in the ICC and is fundamental for ICC development and maintenance of the ICC phenotype in GI muscles (Sanders & Ward, 2006). Reduction in tyrosine kinase activity due to the partial loss of function of KIT signaling was studied at the University of Nevada using compound heterozygous mice mutants W/W^v and S/Sl^d. Staining of ICC-MY using methylene blue revealed the presence of 534 ± 47 mm $^{-2}$ ICC-MY in the wild type mouse compared to the 58 ± 8mm $^{-2}$ ICC-MY observed in the compound heterozygous mice (Ward, Burns, Torihashi, &

Sanders, 1994). Reduction in ICC-MY of the myenteric plexus region likely suggest the role KIT has on the development of ICC networks (Huizinga, Thuneberg, kluppel, Mikkelsen, & Berstein, 1995). Failure of ICC to develop will lead to abnormalities in the GI tract that result in uncoordinated motility patterns. It appears that point mutation affecting KIT only results in activity of the tyrosine kinase receptor and its effects on the development of ICC as smooth muscle cells and enteric neurons, the two other components of the intestinal triad, do not appear to have developmental disruption (Sanders & Ward, 2006).

It is important to note that GISTs were identified using KIT antibodies, but about 10-15% of GISTs did not react with KIT antibodies (Scherzer, 2007). Molecular advancements have lead to the identification of the Tmem16 gene. Tmem16 is found in an assortment of isoforms: Tmem16A-Tmem16H and Tmem16J. The gene is expressed on epithelial tissue and plays a contribution to the secretion of fluid by the epithelia cells (Yang, et al., 2008). Tmem16A, is calcium-activated chloride selective ion channel found in the plasma membrane of ICC, it has been identified in the GI tract of Humans, Mice and now Zebrafish (Chen, et al., 2007) (Gomez-Pinilla, et al., 2009) (Hwang S. J., et al., 2009) (Zhu, et al., 2009). In Humans and Mice, Tmem16A has proven to be novel in the identification of GISTs due to its ability to mark ICC while being unrelated to kit. Also in Humans and Mice, Tmem16a has been shown to play a functional role in the development of slow wave activity giving ICC their characteristic pacemaker trait (Hwang S. J., et al., 2009) (Zhu, et al., 2009). Although Tmem16A is present

in the GI tract of zebrafish, its function and exactly how it is involved with ICC if not yet well understood.

Anatomical and Functional Role of ICC

Interstitial cells of Cajal (ICC) were first observed by Ramon y Cajal in the early in the 18th century using non-specific histological staining. Techniques used for the identification of ICC have progressed as quickly as advancements in technology have allowed. ICC were later identified with electron microscopy a technique that allows for the ultrastructure of the cell to be observed in great detail, however, this technique is extremely demanding and subjected to error. Now, ICC can be observed using immunohistochemistry which is made possible by antibodies specific for Kit (Sanders & Ward, Interstitial cells of Cajal: a new perspective on smooth muscle function, 2006). Mature ICC can be identified specifically by appearance. The descriptive features of ICC include pronounced nucleus, large stellate shaped cells and appear to branch indicating that they play a role in mediating or transmitting signals to other cells. Single ICC are observed within the circular and longitudinal muscle layers of the GI tract and ICC to form interconnected networks found in the myenteric plexus region, the space between the circular muscle layer and the longitudinal muscle layer (Hwang S. J., et al., 2009). The anatomical position and the cellular features led to the hypothesis that ICC demonstrates three main functions: pacemaker activity, facilitating active propagation of electrical events, and mediating neurotransmission.

Distribution of ICC in GI tissues is complicated. There are several classes of ICC all of which are found in different regions of the GI tract and their function

is related to distribution and the morphology. Myenteric interstitial cells (ICC-MY) make up the largest density of ICC. They are located in highest density in the tunica muscularis of the small intestine, more specifically in the myenteric plexus a region between the circular muscle layer and the longitudinal muscle layer. ICC-MY are most commonly studied in the small intestine but this network of ICC is also found in the myenteric plexus region of the stomach and large intestine. ICC-MY are absent from small regions that separate organs in the GI tract such as the pyloric sphincter that separates the stomach from the duodenum, the first segment of the small intestine. ICC-MY are connected to each other and to smooth muscle with gap junctions. ICC-MY generate an electric pacemaker signal known and the slow wave that contributes a pacemaker function to GI motility and the electrical slow wave is transmitted from cell-to-cell via gap junctions.

Intramuscular ICC (ICC-IM) are another class of ICC and are most abundant in the esophagus, lesser curvature and pylorus of the stomach. They appear spindle/bipolar shaped and are found dispersed in and near the edges of circular and longitudinal muscle layers. ICC-IM do not form large networks like ICC-MY, but do develop gap junctions with the surrounding smooth muscle cells resulting in smaller groups of functionally coupled cells. ICC-IM are spontaneously active and produce unitary potentials which are small spontaneous depolarization's in membrane potential that are transmitted to nearby longitudinal and circular smooth muscles via gap junctions (Zhu, et al.,

2009). Propagating smooth muscle contractions result from unitary potentials when summation occurs and the smooth muscle resting membrane potential is sufficient (Hwang S. J., et al., 2009). ICC-IM are found in very close proximity to intramural neurons and play a critical role in mediating neural inputs. This was demonstrated with W/W^v hemizygous mutant mouse that lacks ICC-IM and shows a significant decline in their ability to generate typical motor reflexes (Ward, Burns, Torihashi, & Sanders, 1994).

Deep muscular plexus cells (ICC-DMP) are derived from undifferentiating cells along the submucosal surface of the circular muscle layer in the GI tract (Ward & Sanders, 2001). Mature ICC-DMP form a network in the large intestine. Previous work with mice has shown that ICC-DMP are not involved the initiation of slow wave activity, but instead could be mediators of neural inputs. Kit Immunoreactivity is used to identify the presence of ICC during developmental time points. It has been show that ICC-MY is established at developmental stage E-18 in mice and is responsible for the presence of slow waves. On the other hand, ICC-DMP proceed the development of ICC-MY and are not responsible for the slow wave. (Ward & Sanders, 2001).

Classes of ICC act collectively to generate a pacemaking signal or electrical slow wave that may be thought of as a slow oscillation in smooth muscle excitability, with muscular contractions likely to occur at the regularly occurring peaks. Contraction and relaxation of the GI tract smooth muscles result from depolarization and hyperpolarization of membrane potential that is

driven by the gap-junctioned ICC and the slow wave that originates in the ICC (Hwang S. J., et al., 2009). ICC-MY produce the electrical slow waves that are electrically transmitted to the smooth muscles cells through gap junctions. ICC-IM play a more regulatory role in GI excitability and synapse on both nerve and smooth muscle cells and enhance the relay of information from enteric neurons to smooth muscles (Streutker, Huizinga, Driman, & Riddell, 2007) It is also true that ICC-IM are spontaneously active, producing unitary potentials, which contribute to excitability of nearby longitudinal smooth muscles. The anatomically separate classes of ICC, as well as smooth muscle and enteric neurons, regulate complex GI motor patterns, responding to local mechanical stimuli such as stretch and also responding to external influences of the central nervous system and the endocrine system

The course of events leading to the production of the peacemaking function can be best outlined beginning with the formation of gap junctions by ICC-IM. They connect the bipolar shaped ICC to smooth muscles of the GI tract. The ICC-DMP act similar to smooth muscle cells. The electrical impulse created by ICC slow waves cause for oscillation in ICC as well as smooth muscle cells.

Zebrafish ICC

The anatomical, morphological and functional components of teleost GI tracts strongly resemble mammalian small intestine. Histological and immunohistochemical analysis has been done to establish the features

conserved by zebrafish (Wallace, Akhter, Smith, Lorent, & Pack, 2005). In the zebrafish, just like mammalian organism, the GI tract is a tube of concentric tissue layers. Moving inward through the layers of the GI tract are the serosa, muscularis externa, submucosa and mucosa. Cellular components that make up the intestinal triad (ICC, enteric neurons and smooth muscle cells) are responsible for the regulation of GI motility and are found organized within the layers in the same way they are in humans and all mammals. The muscularis externa layer is where longitudinal and circular smooth muscle cells are found. The longitudinal cells are smooth muscle cells that are found most externally with their long axis oriented parallel to the length of the GI tract, while circular smooth muscle cells are found closer to the submucosa with their long axis perpendicular to the long axis of the GI tract. Therefore, when longitudinal muscle contract the GI tract shortens, and when circular muscle cells contract the lumen of the GI tract is occluded or compressed. A region called the myenteric plexus divides layers of longitudinal smooth muscle cells and the circular smooth muscle cells. The myenteric plexus region is where ICC and enteric neurons are found in the highest density. Together smooth muscle cells, ICC and enteric neurons function to regulate spontaneous and coordinated muscular contractions in the GI tract.

Mammals and zebrafish alike have regionalized guts that occupy most of the abdominal cavity. However, zebrafish are stomachless. They lack a region containing acidic pH levels that is separated from other functional regions of the

GI tract by sphincters. Instead, in the anterior region of their intestine, they have an intestinal bulb, which is connected to a short muscular esophagus. The intestinal bulb is a section of the gut where the lumen is wider compared to the posterior portion of the intestine and contains epithelia folds and digestive enzymes, it purpose is apparently similar to the stomach of mammals (Wallace, Akhter, Smith, Lorent, & Pack, 2005). It functions to mix luminal content preparing the bolus to move by propagating contraction through the mid-intestine and out through the anus in an anterograde motion.

Cellular anatomy in zebrafish is highly conserved when compared to humans. Smooth muscle cells, and enteric neurons have been observed in zebrafish, but it was not until recently that ICC had been identified in the GI tract of zebrafish (Rich, et al., 2007). ICC serves as control or pacemaker elements for the mixing and propulsion of luminal contents by coordinating both the rhythmic and spontaneous muscular contractions of the GI tract. They derive from the mesoderm tissue layer and are differentiated from other cells produced in this layer by Kit expression. Zebrafish have two kit genes, *kita* and *kitb*, these genes are orthologous to human *KIT*. Zebrafish also have two kit ligand genes, *kitla* and *kitlb*, and these genes are orthologous to human Stem Cell Factor. Using primers specific for *kita*, *kitb*, *kitla* and *kitlb* and polymerase chain reaction our lab has shown mRNA expression of these genes in gastrointestinal tissue of zebrafish. Further analysis using Anti-kit antibodies has confirmed protein expression of *kita* and *kitb* on intact, fixed, zebrafish GI tissues. These

observations have led to the identification of two ICC types. Stellate ICC are found in the myenteric plexus region and bipolar ICC are found along the edges of the submucosa. The positioning of these two types of ICC are highly comparable to how it appears in both human and mouse (Rich, et al., 2007).

The presences of kit receptors are required for normal gastrointestinal function and ICC development, but regulation of ICC development, maturation and survivability is not well understood. Any alteration in ICC expression levels can result in uncoordinated GI muscular contractions (Rich, et al., 2003). Experiments performed for this thesis will help to determine if a single gene, *kitlb*, is necessary for the growth and maintenance of ICC, which will allow for the development of normal motility patterns in the zebrafish GI tract. These experiments are aimed at understanding ICC growth and development at a molecular level and could ultimately lead to GI dysmotility treatment options.

Morpholinos (MOs)

Morpholino oligonucleotides (MOs) were first developed by James Summerton, who used MOs to inhibit the translation of RNA transcripts *in vivo*. Now, MOs are the most common anti-sense "knockdown" technique used in zebrafish. MO work at a molecular level and are typically used to determine gene function *in vivo* as well as to verify mutant phenotypes, however, MOs can also function in zebrafish to reduce maternal and zygomatic gene function (Corey & Abrams, 2001). A morpholino oligonucleotide may be structurally

described as a neutrally charged phosphorodiamidate backbone containing 25 morpholino bases (Bill, Petzold, Clark, Schimmenti, & Ekker, 2009). The structure of the MO allows complimentary binding to RNA of interest and results in the disruption of transcriptional or translational processing due to steric hindrance.

There are two types of MOs that are used in the zebrafish. A splice blocking morpholino oligonucleotide is a MO that works by binding to pre-mRNA and prevents the assembly of splice components, therefore disrupting post - transcriptional modification and preventing the formation of mature RNA. Products of a splice blocking MO can be observed using reverse transcriptase polymerase chain reaction (RT-PCR) and gel electrophoresis. Translational blocking morpholino oligonucleotides are designed to bind mRNA within the 5' untranslated region located near the translational start site. Binding of the MO prevents the assembly of the ribosome blocking translation of mRNA. Antibodies that bind to the protein of interest are used to determine the level of knockdown that has occurred as a result of a translational blocking MO (Bill, Petzold, Clark, Schimmenti, & Ekker, 2009).

MOs are introduced into the yolk of a developing embryo by microinjection before the 4 - cell stage. Ubiquitous delivery of an MO to all dividing cells is a result of early introduction of the MO into the embryo. Also, rapid diffusion of a MO occurs within the dividing cell of an embryo due to presences of cytoplasmic bridges that serve to connect embryonic cells (Bill,

Petzold, Clark, Schimmenti, & Ekker, 2009). Currently, there are no known enzymes found in cells that work to eliminate MO expression. This is likely due to the nonionic backbone of MOs, which make it resistant to digestion (Corey & Abrams, 2001). However, the efficacy of an MO is directly related to binding affinity and protein kinetics, more specifically protein turnover, the effectiveness of an MO appears to be limited to 7 days post fertilization (dpf), with most phenotypes observable during the first three days of development (Bill, Petzold, Clark, Schimmenti, & Ekker, 2009). Observation of phenotypes resulting from introduction of a MO into a developing embryo require a rigorous set of controls that are used to screen for nonspecific effects of a morpholino.

Fish Disease

In general terms, zebrafish are hearty. However, they can be highly susceptible to contagious diseases such as velvet disease, fish tuberculosis and nematode infection as well as vegetative bacteria, especially when the zebrafish is stressed or injured (Brand, Granato, Nusslein-Volhard, & Christiane, Zebrafish, 2002). There are some treatments available for diseases such as velvet disease and nematode infection as well as antibiotics that can be used to treat bacterial infections. It is highly suggested that treatment of diseased fish is avoided; instead zebrafish that exhibit symptoms should be discarded immediately to help prevent transmission to other zebrafish within the colony. If the entire

system becomes contaminated the system should be shut down and cleaned properly with a chlorine dioxide-based high level disinfectant.

Outside venders such pet stores may not follow rigorous quarantine protocols when their zebrafish are diseased. It is important that proper measured are taken by a laboratory when outside fish are brought in. Disease and bacteria are not likely to spread through the air or dried material, but infectious agents thrive in moist environments (Brand, Granato, Nusslein-Volhard, & Christiane, Zebrafish, 2002). To avoid contamination it is necessary to keep outside zebrafish in quarantine tanks, to disinfect shared nets and filter between handling also bleach breeder boxes after use.

Objective and Experimental Plan

Aim of Experiment

The overall aim of this thesis is to better understand the role of *kitlb* on ICC development. It is known that stem cell factor, or kit ligand, is necessary for ICC development but the molecular mechanisms are poorly understood. There are two isoforms of mammalian Kit ligand, one is primarily soluble and the other is primarily membrane bound. The relative importance for each isoform on ICC development, ICC turnover, and ICC maintenance is unknown. Morpholino knockdown of *kitlb* expression will be used to test the hypothesis that *kitlb* is necessary for ICC development in zebrafish. We anticipate that development of normal motility patterns in the GI tract will be disrupted because ICC

development will be delayed when *kitlb*, similar to the membrane-bound isoform of mammalian Kit ligand, expression is reduced. A better understanding of the role of the membrane bound form of kit ligand may contribute to our overall understanding of ICC development and the regulation of GI motility, and thereby further understanding of GI motility disorders and drug target development.

Experimental Plan

The function of *kitlb* on maintenance and development of ICC will be examined by knocking down its expression. A morpholino (MO) will be used to specifically and selectively knockdown for *kitlb* gene expression. The MO is introduced into the embryo before the 4-cell stage. The MO was purchased with a fluorescent tag and MO injection is verified using fluorescence microscopy. MO-injected embryos are allowed to develop until 7 dpf when ICC networks are developed and when ICC regulation of spontaneous and propagating contractions occurs (Parichy, Elizondo, Mills, Gordon, & Engeszer, 2009). It is possibly the MO injection can delay or interfere with normal development. To test this possibility standard length is measured at 7dpf. Parichy et al showed that standard length is a reliable method to examine development of zebrafish, and is more reliable when compared to simple days post fertilization (Parichy, Elizondo, Mills, Gordon, & Engeszer, 2009). Standard length is measured by imaging the anterior and posterior portions of the larva and tiling images

because an entire larva is too large for a single image. Also at 7dpf, a GI motility assay will be completed for each larva. The GI motility assay consists of anaesthetizing larvae in MESAB, immobilizing in 1.9% agarose in a polyethylene capillary tube, and capturing time-lapse digital images at a rate of 1 per second. A total of 600 images are collected spanning 10 minutes. The sequential images are converted to a single spatial temporal maps (STMaps) using Volumetry, which are used to further analyze GI motility by quantifying the motility index (MI), total number of contractions, and contraction distance, velocity and frequency. Reverse transcriptase polymerase chain reaction (RT-PCR) is used to verify the effects of *kitlb* MO injection on *kitlb* mRNA production in the larvae.

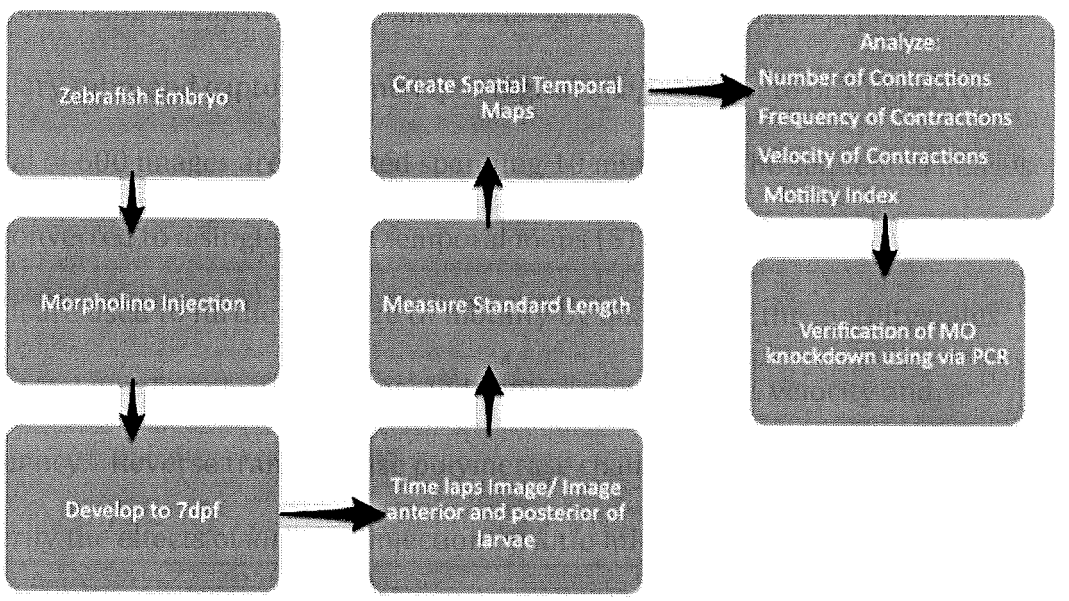

Experimental Procedures

The techniques used in this thesis are briefly described. A more detailed description of the protocols used can be found in the Appendix.

Aquaculture:

The Zebrafish International Resource Center (ZIRC) provides our lab with wild-type zebrafish. These zebrafish are maintained in full accordance with the IACUC guidelines. Our system is filled with water that has been processed through reverse osmosis and has been supplemented with 240mg/L of Instant Ocean Sea Salt and 75mg/L $NaHCO_3$. Reverse osmosis of the system water is established using a filter. The filter allows for water to overcome the natural tendency to flow from a region of high solute concentration to an area of low solute concentration by overcoming osmotic pressure. This process is advantageous due to its ability to take tap water and produce purified water that is free from the contaminants such as copper, lead, arsenic, chlorine, pesticides, etc. Water that has been filtered by reverse osmosis and added to the system is then carefully monitored for its pH, temperature, ammonia and nitrate levels to ensure the water chemistry is maintained within normal range. The pH level should range from 6.9 to 7.4, ideally around 7. Temperature of the system can range from 25°-29°, however, it had been found that the water temperature that is maintained around 28.5 is ideal for zebrafish breeding. Ammonia and nitrate levels should be 0ppm and conductivity can range from 800-1200μS.

Adult zebrafish are fed three times daily. They receive dry food for breakfast between the hours 8am-10am (aquaneering food), brine shrimp (dehydrated decapsulated irtenua cycts, which is cultured daily) between 12pm-2pm, and dry food for dinner (orange cysts) between the hours of 4pm-6pm.

The fish colony is maintained on a 14hr/10hr light/dark cycle. This helps to establish a circadian rhythm for the zebrafish. This cycle is most advantageous for establishing a normal feeding and breeding schedule.

Breeding/crossing of the adult zebrafish is designated to the early morning hours, right as the lights turn on in the fish room (7am). Breeding boxes are used to set up crosses containing as many as 3 Females X 2 Males or as few as 1 Female X 1 Male. Embryos gathered from these crosses are maintained in embryo medium called E2 (recipe can be found in the Zebrafish Handbook) are incubated at 28°.

Streamline Zebrafish Husbandry:

Small changes have been made to the maintenance of the zebrafish colony. The colony is still maintained in accordance with IACUC guidelines. The system is now filled with tap water that has been aged for around a day to allow for the release of chlorine. This replaces the more expensive process of reverse osmosis that was used to fill the system with water. The pH of the system water is now maintained within the 6.9 – 7.4 range with the ideal pH of 7. Change in conductivity, or the waters ability to conduct an electrical current is

now maintained around 300μS with addition of Instant Ocean Sea Salt added as needed. The shift to a more neutral pH level and lower conductivity level are hypothesized to benefit breeding results. All other components of the systems water and fish care have remained identical to what has been explained in the previous aquaculture paragraph.

Cleaning Larvae

After breeding has concluded, embryos are sorted and unfertilized embryos are removed. The fertilized embryos are then further divided into 25 embryos per petri dish, which helps maintain good health. Daily cleaning of the embryos / larvae is necessary for viability. Transfer pipettes are used to remove dead embryos as well as empty chorions, which would provide nutrients for the growth of bacteria and mold (Brand, Granato, Nusslein-Volhard, & Christiane, 2002). As much old E2 as possible is siphoned out of the petri dish and then replaced with fresh E2 medium. Establishment of good cleaning habits like those mentioned above result in greater viability by preventing the E2 in each petri dish from spoiling.

Bleaching of embryos before 28 hours post fertilization (hpf) is an additional step that may be taken to achieve better cleanliness of embryos. It is a multiple step process that is time sensitive that works by killing bacteria and other microorganisms decreasing the spread of disease. The embryos are rinsed in a diluted bleach solution, than rinsed twice in E2 medium. It is

necessary that bleaching is completed before 28 hpf. After 28 hpf hatching enzymes are released from the embryo in preparation of the larvae to break free of its chorion (Brand, Granato, Nusslein-Volhard, & Christiane, 2002). The enzymes work by degrading the chorion. Therefore, the weak chorion does not provide suitable protection to the young larvae and the introduction of a detergent such as bleach would put the viability of the larvae at immediate risk.

Embryos used in the experiments for this thesis were not bleach. The experiments required embryos to undergo microinjections in order to deliver a morpholino into the dividing cells. Piercing of the choiron for morpholino delivery makes the chorion weak and cleaning with bleach may have been detrimental.

Counting / Logging Larvae Viability

Viability and good health of developing larvae is important. Counting and logging of larvae viability is done daily at the same time E2 media is changed. The total number of surviving embryos / larvae are counted and recorded in a laboratory notebook. It is important that the log of larvae viability is well organized and easy to reference. The daily log should include the parent line, day post fertilization, experimental indication (ex: *kitlb* injected or control injected) and total number of healthy surviving embryos / larvae. This log is started at 0dpf and is continued through 7dpf when the larvae are used for time - lapse imaging. Daily records of embryos / larvae survivability allow for easy

identification of healthy breeding lines or breeding pairs. It is extremely important to have healthy embryos / larvae for experimental purposes.

Morpholino

In a eukaryotic cell, pre – mRNA is processed into mature mRNA. Small nuclear ribonuclear proteins (snurps) direct a splicesome to make cuts in the pre – mRNA at splice junctions to remove introns and splice together exons, resulting in mature mRNA. A Morpholino (MO), an antisense oligonucleotides is designed to redirect splicing. The MO will complementarily bind to pre – mRNA at an internal splice junction, blocking the splice junction of an internal exon causing the removal of the exon as well as both flanking introns. For this project a splice blocking MO for *kitlb* was used. Splice blocking MOs works by binding to an intron- exon pre-mRNA target. The MO binds to the pre-mRNA target and works by sterically disrupting the molecules that direct the spliceosome to splice sites. The end result is a new splice pattern of mature mRNA, different from the mature mRNA that would have been produced in the absence of the MO (Mouton & Jiang, 2009). Therefore an effective MO results in a different mRNA product compared to a non-injected control. For this project the splice blocking MO *(kitlb)* was modeled after work previously done by Keith Hultman and colleagues (Hultman, Bahary, Zon, & Johnson, 2007). The MO binds to target pre-mRNA at the intron 2 - exon 3 boundary resulting in the excision of target exon 3. This causes an in- frame shift and splicing of exon 2 to exon 4. This

exon excision will result in production of an ineffective protein, effectively knocking out *kitlb* and helping better understand the function of the *kitlb* gene in vivo.

MO Design

Kitlb MO that was created and designed based off Keith Hultman's work as well as assistance from Gene Tools, LLC. A splice blocking MO was chosen so that the efficacy of the MO could be tested using reverse transcriptase polymerase chain reaction (RT-PCR). Characterization of the MO using RT-PCR was observed using Gel electrophoreses as a shifted band due to the new splice pattern in mature mRNA.

When placing the order it is necessary to know the pre-mRNA sequence including all exon – intron and intron – exon boundaries so the MO can be designed to reach its optimal target and have the greatest efficacy. *Kitlb* MO sequence was designed as (5' – CACATGTATACTTACCACATCCTTT – 3') to block processing at the splice donor site of exon 3. A negative control was also designed in accordance to Hultman's work and with assistance from Gene Tools, LLC to control for any nonspecific effects of a MO. The Negative control MO sequence was designed as (5' – CCTCTTACCTCAGTTACAATTTATA – 3').

Preparation/Storage of Stock Solution

The MO is delivered as a prequantitated, sterile, salt-free, lyophilized powder. Gene Tools, LLC recommends that the solid is solubalized into a 1mM stock solution in distilled water or Danieau buffer.

The 300nmole *kitlb* and control MOs were made into 1mM stock solution by adding 0.30mL of distilled water. Stock solutions were stored at room temperature, as directed by Gene Tools LLC. MOs can be stored in the refrigerator or freezer, but the cold temperatures can cause the MO to come out of solution.

Working Solution

Stock solutions of *kitlb* and control MOs were made into a 20μM working solution by a 1:50 dilution using Daneau buffer. Since the control MO was not ordered with a 3' Flurescein tag 0.5% phenol red was added into the working solution as a visual indicator.

1:50 Dilution: *to prepare 100μl of injectable MO solution*

$$C_1V_1 = C_2V_2$$

$$(1000\mu M)\ (X\mu L) = (20\mu M)\ (100\mu L)$$

$$X = 2\mu L$$

Add 98 μl Daniau buffer and 2μl of stock MO solution

0.5% Phenol Red:

0.5μL per 100μL

Testing Efficacy of MO

MO knockdown is extremely effective during early development but MO concentration declines during embryonic development as the MO concentration continuously declines with cell division. When looking at later developmental time points it is important to directly measure MO efficacy. Expression of the *kitlb* gene was tested using RT-PCR on cDNA prepared from total RNA that was isolated from 5dpf and 7dpf *kitlb* MO injected zebrafish larvae. Identical experiments were performed on age-matched control MO injected, or wild type non-injected larvae. Primer sets for *kitlb* gene were designed to span exon 3 resulting in a shorter amplicon when the kitlb MO is effective, and longer amplicon (containing exon 3) for wild type or for ineffective MO injection. The primers also span intron – exon boundaries to eliminate (or lesson) the effects of potential genomic contamination. *Kitlb* primer set was used to test the efficacy of both *kitlb* MO injected and control MO injected larvae. *Kitlb* forward primer 5' – ACCTGCTCAGGTGTTTTTGG – 3', binds upstream to the 5' region of *kitlb* gene and *kitlb* reverse primer 5' – CATTCTGTCCTCCAGGTCGT – 3', identifies the downstream 3' end of *kitlb* gene. *Kitlb* forward and reverse primers anneal to complementary DNA surrounding the gene of interest, which is followed by amplification of the gene of interest.

PCR products of *kitlb* MO injected larvae and control MO injected larvae should appear as different lengths in the gel. The presence of *kitlb* MO is expected to splice the mature mRNA resulting in an in-frame deletion of exon 3. PCR conformation of the exon excision would result in the presence of a 241 base pair band, which is shorter than 288 base pairs, the expected size of wild type zebrafish PCR products of control MO injected larvae should reveal a band at the expected length of 288 base pairs since the control MO would not have disrupted the normal splicing patterns on pre-mRNA into mature mRNA.

It is important to mention that β-actin is always used as a positive control in PCR reactions to help with trouble shooting. The control shows that the reaction is working as predicted and that there is not contamination. More specifically, β-actin is used to make sure the cDNA template is good and the enzymes in the reaction are working.

GI Motility Assay

Observation of gastrointestinal motility using time-lapse imaging is possible in the optically transparent larvae. Larvae are transparent until approximately 10 days post fertilization, and even longer if pigmentation is inhibited. In this thesis zebrafish at the developmental stage of 7dpf were used. Visual data collection provides additional significance to molecular and morphological information surrounding the development of the gastrointestinal tract (Holberg, Schwerte, Pelster, & Holmgren, 2004).

Fertilization and MO injection:

Embryos were collected from the laboratory breeding stock. The developmental stages of the zebrafish were tracked by days post fertilization and by measuring from snout to tail. The first day of fertilization is termed 0dpf. Within an hour after birth, and before the 4-cell stage, embryos were microinjected with *kitla / kitlb, kitlb* and control morpholino (Gene -Tools LLC.). Embryos were subsequently placed in petri dishes containing E2 and held in the incubator at 28°C. It is important to limit embryo density to 25 per dish. Viability of the embryos was counted each day when E2 was changed. Zebrafish larvae were not fed during the experimental period. Larvae that developed to 7dpf were used for visual data collection.

Screening of Embryos:

Morpholino-injected embryos were screened 5 hours post injection. Screening was completed to ensure the presence of morpholino in each injected embryo as well as ubiquitous delivery among the diving cells. The experimental morpholino used (*kitla / kitlb* and *kitlb*) were purchased from Gene -Tools LLC with a 3' flourecein tag. This tag allowed visualization of the injected MO within embryos using a fluorescent microscope. Phenol Red was added to control morpholino because it was not purchased with a 3' fluorescent tag.

Transmitted light is sufficient to identify phenol red injected embryos. Embryos were discarded if morpholino was not observed in dividing cells.

Mounting 7dpf Larvae and Digital Imaging

Larvae surviving to 7dpf were used to test the effects of morpholino knockdown of *kitlb* in GI motility. Zebrafish were removed from the incubator and anesthetized in .75% MESAB, transferred into .9% agar containing MESAB and E2, maintained at 42°C using a water bath. A pipette pump was used to draw 0 .9% agar and the zebrafish larvae into a fluorinated ethylene propylene (FEP) tube (1/32" diameter, Cole Parmer). Agar was drawn up in the FEP tube to keep the zebrafish larvae stabilized and immobile while imaging. At this concentration agar gels, or solidifies at room temperature. The FEP tube containing the larvae was placed onto a homemade foam holder, which helps to position the FEP tube to enable lateral imaging of the larvae. The foam channel had edges higher than the outer diameter of the tube creating a chamber. Both ends of the tube extend beyond the channel to allow for rotational adjustment of the tube to gain the optimal lateral view of the GI tract. Water was used to fill the chamber, surrounding the FEP tube. Water is an ideal optical correction solution and reduces image distortion (Petzold, et al., 2010). Under 4X magnification on a Nikon Diaphot inverted microscope with an attached Spot Insight video camera images of the 7dpf zebrafish were collected using Spot software (Diagnostics Instruments, Inc.). At the start of each experiment an

image of the posterior half and a second image of the anterior half was collected so that the length of the entire larva could be determined. Sequential images of the entire length of the GI tract were taken every second for ten minutes. Spot software (Diagnostics Instruments, Inc.) complied all 600 images as a sequence file that could be played back as a movie. Each movie was reviewed for analysis of the contractions occurring in the GI tract.

Tiling Images:

Images collected of the anterior and posterior regions from each 7dpf zebrafish larva were tiled together to form one image of the entire length of the larva using Image Pro Plus (software version 5.0; Media Cybernetics). Tiled images were used to measure the standard length of the 7dpf zebrafish larvae. Standard length is defined as the total distance from snout to the posterior tip of caudal fin. Parichy and coworkers showed that standard length is an accurate method to gauge development, and is the most accurate method to assess post-embryonic fish developmental stage (Parichy, Elizondo, Mills, Gordon, & Engeszer, 2009). A normally developing zebrafish should have a standard length measurement just under 4mm at 7dpf. All zebrafish larvae used for thesis experiments were assessed using standard length to validate developmental stage of the zebrafish was not altered by the delivery of the morpholino.

Digital Image Analysis:

The sequence files of the experimental larvae that were collected using Spot software (Diagnostics Instruments, Inc.) were analyzed using Volumetry, a custom written program (Volumetry G6a, Grant Hennig). A rectangular region of interest was manually drawn over the image sequence files, which only included the GI tract. Using the region of interested, a spatio temporal map (STMap) is created by calculating the average brightness, or pixel intensity along columns of pixels from the region of interest. Each image results in a single row in the spatiotemporal map. Changes in average intensity along the GI tract appear as dark bands. The intensity change results from occlusion of the intestinal lumen and represents contractions. The STMap therefore reduces 600 time-lapse images into a single image enabling visualization of propagating contractions as dark bands. Furthermore, patterns or the lack of patterns is readily apparent and quantification of each contraction is possible. More specifically, STMaps provide the ability to identify the site of initiation for each contraction, allow the propagating distance of each contraction to be measured and also provide the means to calculate velocity and frequency of the contractions occurring in the GI tract. The distance and velocity of contractions was calculated by manually drawing a line over the entire length each dark band that represents a propagating contraction on the STMap. The total number of contractions that occurred over the 10-minute period of recorded time was used to calculate frequency of contractions. The spaces in between peak contractions

were measured and reported as intervals. It is important to know that frequency and interval are not always the same because contractions can occur at irregular intervals. Qualitative analysis of the STMaps was quantified a motility index resulting in a binary score or 'coordinated' or uncoordinated. Coordinated motility patterns refers to a series of propagating muscular contractions that cause the lumen to narrow and result in propulsion of intestinal content moving in an aboral direction.

Motility Index (MI):

When analyzing STMpas we realized that the majority of maps show about 1 propagating contraction per second, but some maps showed none, or just 2 or 3, while other maps had periods of inactivity. Contractile behavior was ignored by merely measuring contraction distance, velocity, and interval. We therefore developed the Motility index (MI) as a technique to rapidly assess STMaps as coordinated or uncoordinated. This method scores GI motility as 1 (coordinated) or 0 (uncoordinated) by analyzing the contractions appearing on the STMaps. STMaps receiving a score of 1 have shown propagating contractions moving in the anterograde direction (mouth to colon) for at least 75% of the contractions with no more than one irregular/skipped contraction during the 10 minute recorded period. It is anticipated that zebrafish with fully developed gastrointestinal tract should have fully propagating anterograde contractions about 75% of the time since this is reported in humans.

Statistical Analysis

The averages of the data were reported ± the standard error of the mean (SEM). A two – tailed distribution, two – sample equal variance t – Test was performed to determine statistical significance with data scoring equal to or greater than the 95th percentile considered significant.

RNA Isolation

Total RNA extraction was possible using intact zebrafish. RNA was extracted from morpholino injected zebrafish, control injected and wild-type zebrafish at 5dpf and 7dpf developmental time points. The intact zebrafish were first placed in RNAlater, a solution that works to stablalize and protect cellular RNA by quickly penetrating the tissue of the fish. The zebrafish in RNAlater were stored for up to one week at room temperature or four weeks when refrigerated. The procedure of RNA isolation was done using an RNeasy Plus Mini Kit (Qiagen, Chatsworth, CA). iSCript cDNA synthesis kit (Bio – Rad Laboratories, Hercules, CA) was used for first strand synthesis.

Quantifying RNA by Spectral Absorption

Purity of RNA directly influences RT-PCR results. The purity of total RNA isolated from morpholino and control injected zebrafish at developmental time points, 5dpf and 7dpf was measured using the Nano Drop. The Nano Drop analyzes the RNA sample by spectrophotometric quantification. Absorption of a total RNA sample is expressed as an absorbance ratio at 260 and 280nm (A260/280). This ratio is used to determine the purity of a RNA sample by measuring the amount of ultraviolet (UV) light that passes through the nucleic acids of the sample at a wavelength of 260nm. A pure RNA sample has greater absorption levels as a result of increased number of nucleic acids within the sample. The absorbance ratio of a pure RNA sample will be measured around 2.

cDNA Synthesis

RNA was isolated from morpholino and control injected larvae at 5dpf and 7dpf. Total RNA was used with iScript cDNA Synthesis Kit (Bio-Rad Laboratories, Hercules, CA) for first strand synthesis. Mature mRNA serves as the template in this catalytic reaction that utilizes reverse transcriptase (RT), random primers, oligo (dT) and nucleasue free water to synthesize cDNA. DNA complements are synthesized from mature mRNA when RT enzyme binds and complementary base pairing occurs.

Reverse Transcriptase Polymerase Chain Reaction (RT-PCR)

Primers to test the MO efficacy for the *kitlb* gene were designed using Primer 3 software that is freely available on the internet (http://primer3plus.com/web_3.0.0/primer3web_input.htm). Primers were ordered from IDT (San Diego, California). Forward and reverse primers for *kitlb* were created to span intron – exon boundaries to prevent PCR amplification of genomic contamination and to enhance the quality of expected PCR product. More specifically, the *kitlb* primer set was designed to span the entire length of exon 3, the targeted exon as well as bind upstream to exon 2 and downstream to exon 4 so that different PCR products would result from control versus MO injected larvae.

The length of PCR product using these primers is expected just under 300 base pairs for control, and 241 base pairs for MO injected larvae. Reverse transcriptase PCR was performed using a kit, PCR – EZ D – PCR Master Mix (Bio Basic Inc, Markham Ontario L3R 1G6 Canada). The PCR – EZ D – PCR Master Mix kit contains a 2X master mix consisting of Taq Polymerase, KCL, $(NH_4)_2SO_4$, Tris HCL, Triton X – 100, BSA, $MgCl_2$ and dNTPs. To this I added 1μL of forward and reverse primers (20μM each), 1μL of cDNA, and 10.5μL of water. Control cDNA template was prepared from total RNA isolated from adult GI tissues, or from intact non-injected larvae. The PCR program denatured at 92° C, annealed primers at 54° C and elongated cDNA at 72°. The PCR reactions were run for 35 cycles. PCR products were then analyzed using a 2% agarose gel.

Pitfalls

Morpholino oligonucleotides are used as a powerful molecular technique to inhibit the translation of RNA transcripts *in vivo.* MOs are used to identify specific gene function or to verify a mutant phenotype. However, there are potential pitfalls associated with the use of MOs. Most importantly, an MO can cause off target effects, which may lead to false conclusions associated with genetic relationships and developmental mechanisms. An off target effect may result in the observed phenotype which is not due to the intended knockdown, but instead is a result of the MO interacting with an off target sequence of RNA. There are several potential approached to determine if the MO had off target effects. One possibility would be rescuing of the observed phenotype by injecting a rescue mRNA. One other possibility would be the comparison of the observed phenotype with the mutant strain. It is also possible that knockdown of a target gene by an MO will lead to gene compensation. More specifically, the MO used in this project was designed to knockdown expression of *kitlb*, one of the two co - orthologos for the human *KIT* gene. Knocking down expression of *kitlb* may result in and increased expression of *kita* and *kitb*, or even *kitla*, and this may minimize the effects of gene knockdown resulting in a less severe phenotype. A potential approach to solve this problem would be co-injection of *kitla* and *kitlb* morpholino. Co-injection of *kitla* and *kitlb* morpholino would knock down both co –orthologs for the human *KIT* gene possibly leading to more definitive results.

The Role of Kitlb on Development of Coordinated Muscular Contractions in the Zebrafish Gastrointestinal Tract

By
Brittany A. Heatherington

To
Graduate School in Partial Fulfillment of the Requirements
for the Degree of Master if Sciences in Biological Sciences

The College at Brockport

The College at
BROCKPORT
STATE UNIVERSITY OF NEW YORK
DEPARTMENT OF BIOLOGY

August 22, 2012 **Thesis Defense**

ittee Members	Approved	Not Approved	Comment
_____ Major Advisor	✓	____	
_____ Committee Member	✓	____	
_____ Committee Member	X	____	

ate Director: _____

tment Chair: _____

Abstract

Gastrointestinal (GI) motility is the spontaneous rhythmic contractions of smooth muscles that mix and propel the contents of the GI tract. Regulation of the complex muscular contractions is controlled by smooth muscles, interstitial cells of the Cajal (ICC) and enteric neurons. ICC act as pacemaker cells in the GI tract and set the frequency of spontaneous contractions. Altering ICC density results in uncoordinated GI muscular contractions. Our lab examines the role of ICC in GI motility and is focused on mechanisms that regulate ICC growth and development. Expression of the Kit receptor tyrosine kinase is used to identify ICC. Kit is stimulated by Kit ligand and stimulation is necessary for the growth and development of ICC. This project specifically examines the role of Kit - Kit ligand signaling on ICC development using the zebrafish model system. The zebrafish has two Kit genes (*kita* and *kitb*) that are orthologous to human *KIT*, and two Kit Ligand genes (*kitla* and *kitlb*). I will examine the role of *kitlb* on the development and maturation of ICC using morpholino oligonucleotides knockdown in zebrafish. Gene expression was quantified using reverse transcriptase PCR analysis. Digital imaging techniques was used to examine morphology of the GI tract. It is anticipated that continued stimulation of *kitb* by *kitlb* is necessary for development of the ICC network, and maintenance of the ICC network in adult animals.

Table of Contents

Abstract	2
Acknowledgments	8
Specific Goals of the Research	9
Introduction	16
KIT Ligand	19
How the KIT Gene Works	21
Anatomical and Functional Role of ICC	29
The Zebrafish Model	12
Zebrafish ICC	32
Morpholinos (MOs)	35
Fish Disease	37
Objective and Experimental Plan	38
Experimental Procedure	41
Aquaculture	41
Streamline Zebrafish Husbandry	42
Cleaning Larvae	43
Counting / Logging Larvae Viability	44
Morpholino	45
MO Design	46
Preparation / Storage of Stock Solution	47
Working Solution	47

Testing Efficacy of MO 48

GI Motility Assay 49

Fertilization and MO Injection 50

Screening of Embryos 50

Mounting 7dpf Larvae and Digital Imaging 51

Tiling Images 52

Digital Image Analysis 53

Motility Index 54

Statistical Analysis 55

RNA Isolation 55

Quantifying RNA by Spectral Absorption 56

cDNA Synthesis 56

Reverse Transcriptase Polymerase Chain Reaction (RT-PCR) 57

Potential Pitfalls 58

Results 59

Discussion/Conclusion 82

References 88

Appendix

1. Breeding Zebrafish Appendix 1

2. Larvae Care / Larvae Counting Appendix 2

3. Solutions Appendix 2

4. Micropipette Appendix 3

4.1: Pulling of Micropipette Appendix 3

4.2: Cutting Micropipette Appendix 4

4.3: Loading Micropipette for Injection Appendix 4

4.4: Attaching Micropipette in Pressure Injector Appendix 4

4.5: Prepping and Injection of Embryos Appendix 4

5. Primers Appendix 5

6. Mounting Agar / Standard Length Appendix 6

7. Standard Length Appendix 7

8. RNA Isolation (Qiagen Kit) Appendix 7

9. Synthesis of cDNA Appendix 8

9.1: Verification of RNA isolation and cDNA synthesis Appendix 8

10. Maintenance of the NanoDrop Appendix 11

10.1: Cleaning NanoDrop Appendix 11

10.2: Testing the NanoDrop Appendix 11

11. GI Motility Data Appendix 12

12. Motility Index Data Appendix 18

List of Figures

Figure 1, Genomic structure of zebrafish *kitla* and *kitlb* 61

Figure 2, Protein sequence comparison of zebrafish *kitla* and *kitlb* to mouse KL-1 and KL-2 62

Figure 3, Zebrafish *kitlb* amino acid sequence 63

Figure 4, Mouse KL-2 amino acid sequence 63

Figure 5, *kitlb* MO knockdown of *kitlb* expression 64

Figure 6, Verification of MO injection in embryos 66

Figure 7, Gel electrophoresis confirms *kitla / kitlb* MO knockdown in 5dpf larvae 67

Figure 8, Gel electrophoresis confirms *kitla / kitlb* MO knockdown in 7dpf larvae 69

Figure 9, Standard length of *kitla / kitlb* MO knockdown 5dpf larvae 71

Figure 10, Standard length of *kitla / kitlb* MO knockdown 7dpf larvae 72

Figure 11, Standard length of *kitlb* MO knockdown 7dpf larvae 73

Figure 12, Coordinated GI motor patterns inhibited with *kitla* and *kitlb* MO knockdown 75

Figure 13, Coordinated GI motor patterns in anterior GI region of 5dpf larvae inhibited with *kitla / kitlb* MO 76

Figure 14, Coordinated GI motor patterns in posterior GI region of 5dpf larvae inhibited with *kitla / kitlb* MO 77

Figure 15, Coordinated GI motor patterns in anterior GI region of 7dpf larvae inhibited with *kitla / kitlb* M0 78

Figure 16, Coordinated GI motor patterns inhibited in posterior GI region of 7dpf larvae by *kitla / kitlb* MO 79

Figure 17, Motility Index of 7dpf *kitlb* injected larvae 80

Figure 18, Motility Index of co – injected *kitla / kitlb* 5dpf and 7dpf MO injected larvae 81

Acknowledgments

I thank Dr. Rich, my advisor for giving me the opportunity to work in his laboratory, for his guidance, support and advice throughout my time at Brockport and with this project. I would like to express a special thanks to my committee members Dr. Tsubota and Dr. Pelletier for their assistance. I would also like to thank my fellow lab members for help caring for the zebrafish.

Specific Goals of the Research

The purpose of this study is to understand the role *kit ligand b (kitlb)* has on maturation and development of interstitial cells of Cajal (ICC) in the zebrafish. This is important because activation of Kit receptor by Kit ligand is necessary for growth and development of ICC in both humans and in mice (Hurst and Edwards 2004). ICC play an essential role in the regulation of complex motor patterns in the Gastrointestinal (GI) tract, a process called motility. Pathophysiological disturbances in motility, such as constipation and irritable bowel syndrome, are associated with decreased density of ICC. The zebrafish model system is used for experiments in this thesis because it is transparent during early developmental stages and GI motility can be directly observed in the intact animal.

Kit ligand is expressed in the GI tract by multiple cell types, including enteric neurons and smooth muscle cells (Ordog, Takayama, Cheung, Ward, & Sanders, 2000). Kit ligand functions as a growth factor and is expressed in two physiological isoforms: soluble and membrane bound. It is necessary to understand that a ligand is a substrate such as an activator, inhibitor or neurotransmitter that binds to a receptor found on a protein. Ligand binding to a receptor is generally very specific, as many non-covalent interactions must occur simultaneously. Once bound, the ligand can activate cell-signaling mechanisms, and in the case of Kit - Kit ligand binding, the Kit receptor becomes phosphorylated and initiates a complex signaling pathway. The Kit-ligand and

Kit receptor is a signaling pathway that plays a critical role in hematopoiesis, generation of melanocytes and the generation of germ cells. Most important for this thesis it also plays a significant role in the development of ICC in the GI tract. It is well established in humans and mice that signaling by kit receptor tyrosine kinase is mandatory for normal ICC development and maintenance in mature gastrointestinal tissues.

Soluble and membrane bound Kit ligand are encoded by human Kit Ligand *(KITLG)* gene. Initially, both the soluble and membrane bound isoforms of Kit ligand are synthesized and targeted to the plasma membrane. The soluble isoform of Kit ligand undergoes rapid proteolytic cleavage at exon 6 and is subsequently released from the cellular membrane in its biologically active conformation. The membrane bound isoform of Kit ligand is activated at a much slower rate because it lacks the proteolytic cleavage site of soluble Kit ligand. Soluble and membrane bound isoforms of Kit ligand are found in different ratios in various tissues. This is indicative that each isoform plays a definite physiological role in an assortment of tissue. For example, the Steel-Dickie mutant mouse lacks membrane bound Kit ligand and is also lacking ICC networks located in the myenteric plexus region of the GI tract (Maeda, et al., 1992). GI motility in the Steel Dickie mutant mouse is unorganized, uncoordinated and arrhythmic.

Zebrafish *kit ligand a (kitla)* and *kit ligand b (kitlb)* have been identified as co-orthologs to the mammalian *KIT* Ligand. The evolutionary linage can be

visualized using on a phylogenetic tree of well-known tetapod sequences. The two copies of zebrafish *kit ligand* appear more closely related to each other than the tetrapod clade. Evidence suggests that the two copies of the *kit ligand* gene in the zebrafish originated from a duplication event in the teleost lineage after the divergence from the tetrapod lineage, but before the teleost radiation (Hultman, Bahary, Zon, & Johnson, 2007). It is reasonable to infer that due to the resemblance of *kitla* and *kitlb* in zebrafish to the alternative splice forms of mammalian *KIT* Ligand, these genes would have similar functions and roles as the mouse isoforms.

This thesis uses *kitlb* morpholino oligonucleotide knockdown and examines its effect on gastrointestinal (GI) motility in zebrafish. ICC development was assayed by directly measuring GI motility patterns in 7 dpf transparent larvae. *Kitlb* MO treated larvae displayed uncoordinated motility patterns, had fewer contractions, and shorter contractions when compared to control larvae. These results show that *kitlb* is necessary for the development of normal motility patterns in the zebrafish GI tract

The Zebrafish Model

Model organisms are non-human species with extensively studied genomes. They are used to better understand biological events with the underlying ideology that understanding a model organism will help contribute to further insight of other organisms. Model organisms are commonly used to understand human diseases especially when experimentation on humans is unethical or unattainable. A model organism is selected for experimental use based primarily on its ability to be manipulated, but may also be chosen because of its accessibility, size, developmental rate or genetic conservation. The NIH has selected a small group of species that are accepted as good model organisms because of the wealth of data that has been collected for each organism. These models are divided into two categories; non-human mammalian models (rat and mouse) and non-mammalian models (budding yeast, roundworm, fruit fly and the zebrafish). Depending on the field of research a model organism may be more suitable over another. For example, genetics and cellular based biological experiments may migrate toward the use of more simple organisms such as budding yeast or toward organisms such as the fruit fly that can exhibit visible phenotypical traits. On the other hand, developmental biologist may want to choose the roundworm because of its fix number of cells making it easier to identify developmental patterns. Biologist choosing to study more complex physiological systems, development, disease, organ function, behavior or toxicology of vertebrates or mammalians may choose to work with the mouse or

zebrafish model. The mouse model (*Mus musculus*) is similar to mammals, has about the same size genome as humans and contains a well-conserved gene order that is helpful for studying human disease (Twyman, 2002). The zebrafish (*Dario rerio*) model shares many homologous genes with mammals and is used to understand vertebrate systems. The genome size of the zebrafish is smaller compared to the mouse, making it more manageable to work with (Twyman, 2002).

The zebrafish model organism is expanding as a system to study human disease. The presents of ICC in the zebrafish (Rich, et al., 2003) make it an appropriate model to study gastrointestinal (GI) motility in a high throughput fashion. Naturally, zebrafish flourish in the freshwaters of south Asia. However, for laboratory purposes the zebrafish thrive in temperature regulated and chemically balanced aquariums. Zebrafish tanks are kept in a facility that has a controlled 24-hour light/dark cycle simulating the length of an entire day. The light cycle is important for laboratory-raised zebrafish by establishing a regular feeding and breeding schedule. Male and female zebrafish reach sexual maturity by four months of age and a single pair of adults has the ability to produce 100-200 offspring. Zebrafish embryos develop outside of the female zebrafish . The embryos develop into optically transparent larvae twenty-four hours post fertilization and remain transparent through 10 days post fertilization. The transparency of the larvae make it possible for the observation of developmental processes such as the multi-chambered heart, brain, kidney, notochord and

eventually the contractions of the gastrointestinal tract all of which can be recorded using time lapse imaging.

Manipulations of the model systems genome using genetic engineering can alter cellular DNA causing change in traits or it can be used to produce biological products. In the case of the zebrafish model system, genetic manipulations can be made by RNA interference or by triple-helix forming molecules to reduce expression of a gene or interruption of transcription of a targeted gene respectively. For example, melanocyte pigment patterns in vertebrate systems have been long studied for pattern formation and morphogenesis. The pattern formations are used to identify genes, better understand of signal transduction as well as cell-to-cell communication (Hultman, Bahary, Zon, & Johnson, 2007). Observation of mRNA expression using *in situ* hybridization has identified one of the co-orthologs, *kitla* in zebrafish to be most similar to mouse KL-1. Both *kitla* and KL-1 retain the proteolytic site of exon 6, suggesting that the critical roles of the genes are conserved. Melanocyte migration and survival, one of the critical roles of KL-1 in mice was shown to maintain the same function as *kitla* in zebrafish. Experimental results using the zebrafish model system and a morpholino knockdown, revealed failure of melanocytes migration, while enhancement *kitla* morpholino caused hyperpigmentation (Hultman, Bahary, Zon, & Johnson, 2007). Further confirming the *kitla* gene identity and establishing that *kitla* plays all the necessary ligand roles for *kita*. Taken together, the results indicate

that *kit ligand* in zebrafish, just like in mouse and humans is responsible for the generation of melanocytes, hematopoiesis, the generation of germ cells. More over, in mice and humans it is well characterized that kit ligand has another critical role in the function of ICC. Careful analysis of previous experimental procedures using the zebrafish suggests that *kit ligand* may also play a role in ICC function.

The zebrafish sparse mutant phenotype is characterized by its absence of pigmentation and pigmentation migration. Careful analysis of the sparse mutant phenotype has identified the mutant of being null *kitla*. Literature demonstrates that along with pigmentation deficiencies, the sparse mutants also have distended GI tracts and unorganized GI muscular contractions (Rich, et al., 2003). These findings are coherent with *Kit* function compromised W/W^v mutant mice. Phenotypical characterization shows that W/W^v mutants also exhibit absences in melanocytes migration and display distended guts (Maeda, et al., 1992). Conservation of Kit function in the model systems of the mouse and zebrafish suggest that the zebrafish would be an excellent system to study human GI physiology.

Introduction

The gastrointestinal (GI) tract holds the responsibilities of digestion, absorption of nutrients and elimination of waste product. It may be best described as long and layered tube that extends a distance of 30 feet in adult humans. The long tube making up the GI tract is divided into different regions each with its own purpose. It starts at the mouth, duodenum, small intestine, large intestine and finally reaches the colon. All regions of the GI tract are comprised of four layers. The innermost layer is the mucosa, a mucous membrane made of smooth muscles that surrounds the lumen. The contractions of the mucosa enable the lumen to change in shape. Next, is a layer of dense irregular connective tissue known as submucosa. This layer is responsible for the secretion of enzymes and buffers into the lumen. Followed by the muscularis externa, which is comprised of smooth muscle cells that are arranged as circular and longitudinal cell layers and neurons. This layer plays a responsibility in the processing and movement of intestinal content. Finally, the serosa, a serous membrane is made up of loose connective tissues stabilizing the GI tract.

The epithelia lining of the GI tract is in close contact with lumen that connects to both internal and external environments. Therefore, a balance must be maintained in the GI tract to ensure there is an adequate absorption of water, electrolytes, nutrients and the appropriate elimination of waste all while instituting a barrier to separate the luminal cavity from the underlying tissues (Shen, 2009). The intestinal triad sustains regulation of this balance; a group of

cells working together to ensure that intestinal content is moved in an oral to colon direction. The triad is composed of enteric neurons, smooth muscle cells and interstitial cells of Cajal (ICC). Disruption in any one part of the intestinal triad may lead to GI motility disorders.

GI motility disorders affect a large percentage of the human population and are not limited to a specific demographic. Gastrointestinal disorders can greatly affect the quality of an individual's life. Symptoms of GI disorders can range from mild discomfort to severe pain, but are almost always embarrassing! It is estimated that around 10-20% of the human population suffer from dysmotility disorders including: Irritable Bowl Syndrome (IBS), Inflammatory Bowl Disease (IBD), Gastroparesis and related Diabetic Gastroparesis.

Diabetic Gastroparesis affects about 30-50% of the human population after 10 years of being diagnosed with Type 1 or Type 2 diabetes. Its symptoms can range from mild dyspepsia to severe abdominal pain and can eventually lead to malnutrition and imbalance of water and electrolytes. To better understand the pathophysiology of this GI disorder, non-obese (NOD) Type 1 diabetic mice were observed. Gastric emptying was measured, electrical activity of spontaneous and induced circular smooth muscles and presence of ICC was monitored (Ordog, Takayama, Cheung, Ward, & Sanders, 2000). Results concluded NOD mice have erratic loss of ICC and irregular electrical peacemaking further suggesting disruption in one part of the intestinal triad, in this case ICC may lead to GI motility disorders.

Currently, treatment for dysmotility is limited, leaving victims with embarrassing symptoms and discomfort. It is hopeful that novel drug treatments will come about with greater understanding of gastrointestinal physiology and the individual components of the intestinal triad. Knowledge of the development and maturation of ICC may contribute to further understanding of GI motility disorders and potential drug targets.

Kit Ligand

Kit-ligand, also known as steel factor, is a growth factor occurring in two physiological isoforms; soluble and membrane bound. A signaling cascade is initiated by the binding of steel factor to the Kit receptor tyrosine kinase. This growth factor plays critical roles in hematopoiesis, generation of melanocytes, and the generation of germ cells, which give rise to gametes (Linnekin D., 1999). A vast literature exists describing the molecular mechanisms involved in this signaling pathway and specific aspects of the signaling pathway that play an important role in leukemia (Linnekin D., 1999). The physiological roles for Kit-Kit ligand signaling are pleiotropic. Maeda and coworkers identified a specific role for Kit signaling in ICC development by injecting the neutralizing antibody ACK2 into the peritoneum of mice (Maeda, et al., 1992). Injected mice displayed grossly distended small intestines, and immunostaining revealed an absence of ICC. Kit ligand also plays a significant role in the development of ICC found in the gastrointestinal tract. The Steel Dickie mutant mouse that is lacking one form of Stem Cell factor demonstrates the role of Kit ligand. The Steel Dickie mouse displays a distended small intestine, and is therefore similar to the W/W^v mutant mouse that lacks functional Kit receptors (Maeda, et al., 1992). The mutant mouse models show that signaling cascades initiated by binding interactions between Kit ligand and the Kit receptor tyrosine kinase is mandatory for normal ICC development and maintenance in mature gastrointestinal tissues (Ward, Burns, Torihashi, & Sanders, 1994) (Huizinga,

Thuneberg, kluppel, Mikkelsen, & Berstein, 1995) (Kluppel, Huizinga, Malysz, & Berstein, 1998).

Soluble and membrane bound steel factor isoforms are encoded by the KITLG gene (Huang, Nocka, Buck, & Besmer, 1992). These isoforms are expressed as transmembrane proteins at surface of the cells. Initially both the soluble and membrane bound isoforms of steel factor (SF) are transcribed and targeted to the plasma membrane in an inactive conformation (Huang, Nocka, Buck, & Besmer, 1992) The soluble isoform of SF undergoes rapid proteolytic cleavage and is subsequently released from the cellular membrane in its biologically active conformation. The membrane bound isoform of SF is solubilized and activated at a much slower rate because it lacks the proteolytic cleavage site of soluble SF (Huang, Nocka, Buck, & Besmer, 1992). Soluble and membrane bound SF is found in assorted ratios in various tissues. This is indicative that each isoform plays a definite physiological role in an assortment of tissue. For example membrane-bound SF is essential for the development and maintenance of ICC networks located in the myenteric plexus, and in the Steel-Dickie mutant mouse that lacks membrane-bound-SF, networks of ICC in the myenteric plexus region are impaired (Broudy, 1997). The decrease in density of the ICC networks in the myenteric plexus region are correlated with unorganized, uncoordinated and arrhythmic patterns in the Steel-Dickie mutant mouse consistent with a role for ICC in the generation of coordinated motility patterns.

How the KIT Gene Works

KIT encodes a receptor tyrosine kinase that is expressed on the plasma membrane and is activated by the binding of Kit ligand. The natural receptor for Kit is Kit ligand, and when Kit ligand binds to the extracellular component of Kit a signaling cascade is triggered that initiates cell differentiation. Therefore KIT is considered to be a growth factor receptor. The Kit receptor is expressed on a variety of cell types including germ cells, mast cells, and hematopoietic stem cells. Kit plays an important role in the migration of melanocytes, development of sensory neurons of the peripheral nervous system, and in ICC development and maintenance of the ICC phenotype on mature tissue (Kluppel, Huizinga, Malysz, & Berstein, 1998).

The nomenclature and naming used for vertebrate genes and proteins can be confusing. It is important to understand the proper nomenclature early on to avoid confusion that may arise in the future. Below are charts that incorporated the important genes and proteins for this thesis.

Kit Ligand

The Kit Ligand gene works by encoding the ligand of the tyrosine- kinase receptor expressed by the gene *KIT*. Kit Ligand protein is classified as a cytokine, a signaling protein that binds to KIT to mediate cell communication of several cells types associated with cells differentiation, migration and survival

(NHI). Kit Ligand is referred to by several names including: Kit Ligand (KL),

Species	Gene Symbol	Protein Symbol
Homo sapiens (Human)	*KITLG*	KITLG
Mus musculus (Mouse)	*KL-1 and KL-2*	KL-1 and KL-2
Danio rerio (Zebrafish)	*kitla and kitlb*	Kitla and Kitlb

Mast Cell Growth Factor (MGF), Stem Cell Factor (SCF) and Steel Factor (SLF).

Kit

The Kit gene codes for the protein KIT, a cytokine receptor. Disruption in the signaling pathway of *KIT* may lead to some types of cancer. Again, the Kit receptor is known by several names, which include: Kit, c-kit, proto-oncogene c-Kit, Stem Cell growth receptor (SCGF), Mast cell growth factor (MCGF) and CD117.

Species	Gene Symbol	Protein Symbol
Homo sapiens (Human)	*KIT*	KIT
Mus musculus (Mouse)	*Kit-1 and Kit-2*	KIT-1 and KIT-2
Danio rerio (Zebrafish)	*kita and kitb*	Kita and Kitb

Mammalian development and maintenance throughout adult life requires complex mechanisms that regulate the effects of growth factors. Growth factors interact with receptors on cells surfaces and are responsible for proliferation, differentiation and survival of cells. For example the growth factor Kit Ligand

(KL) is the natural ligand for Kit. Kit, the transmembrane tyrosine kinase receptor that can be structurally classified the extracellular components of the receptor are five immunoglobulin- like domains. The first three extracellular domains bind Kit Ligand. The forth domain is believed to play a significant role in dimerization of the receptor. And, the fifth domain, closest to the cell surface has unknown function. Inside the cell the catalytic domains are divided into two separate domains; a Kinase insert serves to connect the domains (Linnekin D., 1999). KL structure can be briefly described as a ligand that can be expressed in two isoforms due to alternative splicing of mRNA. Proteolytic cleavage of the transmembrane protein results in the soluble isoform of KL, while membrane bound KL lacks the proteolytic cleavage site.

Kit Ligand works by binding to Kit inducing dimerization of the receptor. Dimerization of Kit results in autophosphorylation on a tyrosine residue. Catalytic activity of Kit is regulated due to phosphorylation of the kinase. Downstream of the Kit receptor many other signaling cascade components are activated, including: phosphatidylinositol – 3 – kinase, Src family members, JAK/STAT pathway and Ras – Raf – MAP kinase cascade (Yee, Langen, & Besmer, 1993).

In the mammalian mouse model the Kit receptor is coded for at the white spotting (W) loci while the steel (Sl) loci encodes for Kit Ligand. Previous work has shown that a mutation in the W or Sl loci can affect cellular targets in melanogensis, gemetogenesis, hematopoiesis of stem cells, growth and

development of mast cells and interstitial cells of Cajal. This suggests that Kit has a functional role in these cellular systems (Yee, Langen, & Besmer, 1993). Regulation of these cellular signaling cascades are maintained by the interactions of specific growth factors with receptors leading to various cellular responses, however, it too is important to control extracellular signals through down regulation of the receptors by means of a negative feedback loops.

Disruption in the regulation of cellular signaling cascades results from mutations in the receptor, KIT. These mutations are classified in two ways. Regulatory type mutations are a type of mutation that affects the regulation of the kinase molecule. And, enzymatic pocket type mutation caused by a substitution in the amino acid sequences at the enzymatic pocket. Both classes of mutations result in constitutive phosphorylation and activation of KIT (Longley, Reguera, & Ma, 2001). The most prevalent conditions associated with mutations in KIT include hematologic diseases, disruption in pigmentation patterns and well as formation of gastrointestinal Stromal tumors (GIST).

Mastocytosis is an increase in the number of mast cells and is a result of an enzymatic pocket mutation. This mutation occurs when the amino acid sequence for aspartate is substituted with valine at the site of the enzymatic pocket. This particular mutation can be characterized by mast cell hyperplasia in bone marrow and lymph nodes as well as organs including the liver, spleen, skin and gastrointestinal tract (Nagata, et al., 1995). There are four classes of Mastocytosis including: indolent mastocytosis, mastocytosis with associated

hematologic disorder, aggressive mastocytosis and mast cell leukemia (Nagata, et al., 1995).

Pigmentation patterns of the skin and hair may be disrupted as a result of a regulatory mutation that affects the kinase molecule in KIT. In the case of this mutation, there is an amino acid substitution of glycine for arginine within the tyrosine kinase domain (Giebel & Spritz, 1991). This mutation is referred to as Piebaldism. It is an autosomal dominant genetic disorder characterized by loss of pigmentation in the hair and skin of humans due to the absents of melanocytes (Giebel & Spritz, 1991). Similar phenotypes are observed in white spotting mice (W). These mice also have a mutation in *Kit*, which causes absents of melanocytes migration in turn making their fur appear white.

Gastrointestinal Stromal tumors (GIST) are the most prevalent type of mesenchymal tumor found in the gastrointestinal tract. This tumor arises from a regulatory type mutation, a deletion or point mutation of KIT within the juxtamembrane domain (Taniguchi, et al., 1999). It is a gain – of – function mutation causing constitutive activation of KIT signaling in the GI tract which can alter ICC development and maintenance leading to the formation of benign or malignant GISTs (Sanders & Ward, 2006) Most benign tumors are in located within the submucosa of the gastrointestinal tract. Malignant tumors are more commonly found in the liver and spread to the peritoneal cavity. Their exophtic growth patterns make them accountable for constipation, severe abdominal pain and discomfort cause by obstruction of the intestine. Drug treatment for GISTs

using Imatitab/Gleevec works by blocking the function of Kit (Sanders & Ward, 2006). It results in the disappearance of ICC and also causes arrhythmic contractions in the GI tract. It is important to mention that although GISTs represent the most common type of sarcoma occurring in the GI tract, they are still extremely rare. It has been estimated that only 1% of all cancers occurring within adults is a type of sarcoma. On the other had carcinomas, a class of cancer that derives from epithelia cells is much more prevalent. Stomach cancer and colon cancer, two cancers of the GI tract fit into the carcinoma category. Of the estimated 1.4 million cases of cancer every year, only about 15,000 are sarcomas (GIST Support International- What is GIST?, 2011).

Continuing on with the GI tract. KIT is expressed on two cell types, ICC and mast cell. These two cell types are easily distinguished by means of cell morphology. ICC appears larger in dimension when compared to the 20μm granule containing ovoid shaped mast cells (Stone, Prussin, & Metcalfe, 2011). Biochemical activation of KIT by Kit ligand promotes the signaling pathway in the ICC and is fundamental for ICC development and maintenance of the ICC phenotype in GI muscles (Sanders & Ward, 2006). Reduction in tyrosine kinase activity due to the partial loss of function of KIT signaling was studied at the University of Nevada using compound heterozygous mice mutants W/W^v and S/Sl^d. Staining of ICC-MY using methylene blue revealed the presence of 534 ± 47 mm $^{-2}$ ICC-MY in the wild type mouse compared to the 58 ± 8mm $^{-2}$ ICC-MY observed in the compound heterozygous mice (Ward, Burns, Torihashi, &

Sanders, 1994). Reduction in ICC-MY of the myenteric plexus region likely suggest the role KIT has on the development of ICC networks (Huizinga, Thuneberg, kluppel, Mikkelsen, & Berstein, 1995). Failure of ICC to develop will lead to abnormalities in the GI tract that result in uncoordinated motility patterns. It appears that point mutation affecting KIT only results in activity of the tyrosine kinase receptor and its effects on the development of ICC as smooth muscle cells and enteric neurons, the two other components of the intestinal triad, do not appear to have developmental disruption (Sanders & Ward, 2006).

It is important to note that GISTs were identified using KIT antibodies, but about 10-15% of GISTs did not react with KIT antibodies (Scherzer, 2007). Molecular advancements have lead to the identification of the Tmem16 gene. Tmem16 is found in an assortment of isoforms: Tmem16A-Tmem16H and Tmem16J. The gene is expressed on epithelial tissue and plays a contribution to the secretion of fluid by the epithelia cells (Yang, et al., 2008). Tmem16A, is calcium-activated chloride selective ion channel found in the plasma membrane of ICC, it has been identified in the GI tract of Humans, Mice and now Zebrafish (Chen, et al., 2007) (Gomez-Pinilla, et al., 2009) (Hwang S. J., et al., 2009) (Zhu, et al., 2009). In Humans and Mice, Tmem16A has proven to be novel in the identification of GISTs due to its ability to mark ICC while being unrelated to kit. Also in Humans and Mice, Tmem16a has been shown to play a functional role in the development of slow wave activity giving ICC their characteristic pacemaker trait (Hwang S. J., et al., 2009) (Zhu, et al., 2009). Although Tmem16A is present

in the GI tract of zebrafish, its function and exactly how it is involved with ICC if not yet well understood.

Anatomical and Functional Role of ICC

Interstitial cells of Cajal (ICC) were first observed by Ramon y Cajal in the early in the 18th century using non-specific histological staining. Techniques used for the identification of ICC have progressed as quickly as advancements in technology have allowed. ICC were later identified with electron microscopy a technique that allows for the ultrastructure of the cell to be observed in great detail, however, this technique is extremely demanding and subjected to error. Now, ICC can be observed using immunohistochemistry which is made possible by antibodies specific for Kit (Sanders & Ward, Interstitial cells of Cajal: a new perspective on smooth muscle function, 2006). Mature ICC can be identified specifically by appearance. The descriptive features of ICC include pronounced nucleus, large stellate shaped cells and appear to branch indicating that they play a role in mediating or transmitting signals to other cells. Single ICC are observed within the circular and longitudinal muscle layers of the GI tract and ICC to form interconnected networks found in the myenteric plexus region, the space between the circular muscle layer and the longitudinal muscle layer (Hwang S. J., et al., 2009). The anatomical position and the cellular features led to the hypothesis that ICC demonstrates three main functions: pacemaker activity, facilitating active propagation of electrical events, and mediating neurotransmission.

Distribution of ICC in GI tissues is complicated. There are several classes of ICC all of which are found in different regions of the GI tract and their function

is related to distribution and the morphology. Myenteric interstitial cells (ICC-MY) make up the largest density of ICC. They are located in highest density in the tunica muscularis of the small intestine, more specifically in the myenteric plexus a region between the circular muscle layer and the longitudinal muscle layer. ICC-MY are most commonly studied in the small intestine but this network of ICC is also found in the myenteric plexus region of the stomach and large intestine. ICC-MY are absent from small regions that separate organs in the GI tract such as the pyloric sphincter that separates the stomach from the duodenum, the first segment of the small intestine. ICC-MY are connected to each other and to smooth muscle with gap junctions. ICC-MY generate an electric pacemaker signal known and the slow wave that contributes a pacemaker function to GI motility and the electrical slow wave is transmitted from cell-to-cell via gap junctions.

Intramuscular ICC (ICC-IM) are another class of ICC and are most abundant in the esophagus, lesser curvature and pylorus of the stomach. They appear spindle/bipolar shaped and are found dispersed in and near the edges of circular and longitudinal muscle layers. ICC-IM do not form large networks like ICC-MY, but do develop gap junctions with the surrounding smooth muscle cells resulting in smaller groups of functionally coupled cells. ICC-IM are spontaneously active and produce unitary potentials which are small spontaneous depolarization's in membrane potential that are transmitted to nearby longitudinal and circular smooth muscles via gap junctions (Zhu, et al.,

2009). Propagating smooth muscle contractions result from unitary potentials when summation occurs and the smooth muscle resting membrane potential is sufficient (Hwang S. J., et al., 2009). ICC-IM are found in very close proximity to intramural neurons and play a critical role in mediating neural inputs. This was demonstrated with W/W^v hemizygous mutant mouse that lacks ICC-IM and shows a significant decline in their ability to generate typical motor reflexes (Ward, Burns, Torihashi, & Sanders, 1994).

Deep muscular plexus cells (ICC-DMP) are derived from undifferentiating cells along the submucosal surface of the circular muscle layer in the GI tract (Ward & Sanders, 2001). Mature ICC-DMP form a network in the large intestine. Previous work with mice has shown that ICC-DMP are not involved the initiation of slow wave activity, but instead could be mediators of neural inputs. Kit Immunoreactivity is used to identify the presence of ICC during developmental time points. It has been show that ICC-MY is established at developmental stage E-18 in mice and is responsible for the presence of slow waves. On the other hand, ICC-DMP proceed the development of ICC-MY and are not responsible for the slow wave. (Ward & Sanders, 2001).

Classes of ICC act collectively to generate a pacemaking signal or electrical slow wave that may be thought of as a slow oscillation in smooth muscle excitability, with muscular contractions likely to occur at the regularly occurring peaks. Contraction and relaxation of the GI tract smooth muscles result from depolarization and hyperpolarization of membrane potential that is

driven by the gap-junctioned ICC and the slow wave that originates in the ICC (Hwang S. J., et al., 2009). ICC-MY produce the electrical slow waves that are electrically transmitted to the smooth muscles cells through gap junctions. ICC-IM play a more regulatory role in GI excitability and synapse on both nerve and smooth muscle cells and enhance the relay of information from enteric neurons to smooth muscles (Streutker, Huizinga, Driman, & Riddell, 2007) It is also true that ICC-IM are spontaneously active, producing unitary potentials, which contribute to excitability of nearby longitudinal smooth muscles. The anatomically separate classes of ICC, as well as smooth muscle and enteric neurons, regulate complex GI motor patterns, responding to local mechanical stimuli such as stretch and also responding to external influences of the central nervous system and the endocrine system

The course of events leading to the production of the peacemaking function can be best outlined beginning with the formation of gap junctions by ICC-IM. They connect the bipolar shaped ICC to smooth muscles of the GI tract. The ICC-DMP act similar to smooth muscle cells. The electrical impulse created by ICC slow waves cause for oscillation in ICC as well as smooth muscle cells.

Zebrafish ICC

The anatomical, morphological and functional components of teleost GI tracts strongly resemble mammalian small intestine. Histological and immunohistochemical analysis has been done to establish the features

conserved by zebrafish (Wallace, Akhter, Smith, Lorent, & Pack, 2005). In the zebrafish, just like mammalian organism, the GI tract is a tube of concentric tissue layers. Moving inward through the layers of the GI tract are the serosa, muscularis externa, submucosa and mucosa. Cellular components that make up the intestinal triad (ICC, enteric neurons and smooth muscle cells) are responsible for the regulation of GI motility and are found organized within the layers in the same way they are in humans and all mammals. The muscularis externa layer is where longitudinal and circular smooth muscle cells are found. The longitudinal cells are smooth muscle cells that are found most externally with their long axis oriented parallel to the length of the GI tract, while circular smooth muscle cells are found closer to the submucosa with their long axis perpendicular to the long axis of the GI tract. Therefore, when longitudinal muscle contract the GI tract shortens, and when circular muscle cells contract the lumen of the GI tract is occluded or compressed. A region called the myenteric plexus divides layers of longitudinal smooth muscle cells and the circular smooth muscle cells. The myenteric plexus region is where ICC and enteric neurons are found in the highest density. Together smooth muscle cells, ICC and enteric neurons function to regulate spontaneous and coordinated muscular contractions in the GI tract.

Mammals and zebrafish alike have regionalized guts that occupy most of the abdominal cavity. However, zebrafish are stomachless. They lack a region containing acidic pH levels that is separated from other functional regions of the

GI tract by sphincters. Instead, in the anterior region of their intestine, they have an intestinal bulb, which is connected to a short muscular esophagus. The intestinal bulb is a section of the gut where the lumen is wider compared to the posterior portion of the intestine and contains epithelia folds and digestive enzymes, it purpose is apparently similar to the stomach of mammals (Wallace, Akhter, Smith, Lorent, & Pack, 2005). It functions to mix luminal content preparing the bolus to move by propagating contraction through the mid-intestine and out through the anus in an anterograde motion.

Cellular anatomy in zebrafish is highly conserved when compared to humans. Smooth muscle cells, and enteric neurons have been observed in zebrafish, but it was not until recently that ICC had been identified in the GI tract of zebrafish (Rich, et al., 2007). ICC serves as control or pacemaker elements for the mixing and propulsion of luminal contents by coordinating both the rhythmic and spontaneous muscular contractions of the GI tract. They derive from the mesoderm tissue layer and are differentiated from other cells produced in this layer by Kit expression. Zebrafish have two kit genes, *kita* and *kitb*, these genes are orthologous to human *KIT*. Zebrafish also have two kit ligand genes, *kitla* and *kitlb*, and these genes are orthologous to human Stem Cell Factor. Using primers specific for *kita*, *kitb*, *kitla* and *kitlb* and polymerase chain reaction our lab has shown mRNA expression of these genes in gastrointestinal tissue of zebrafish. Further analysis using Anti-kit antibodies has confirmed protein expression of *kita* and *kitb* on intact, fixed, zebrafish GI tissues. These

observations have led to the identification of two ICC types. Stellate ICC are found in the myenteric plexus region and bipolar ICC are found along the edges of the submucosa. The positioning of these two types of ICC are highly comparable to how it appears in both human and mouse (Rich, et al., 2007).

The presences of kit receptors are required for normal gastrointestinal function and ICC development, but regulation of ICC development, maturation and survivability is not well understood. Any alteration in ICC expression levels can result in uncoordinated GI muscular contractions (Rich, et al., 2003). Experiments performed for this thesis will help to determine if a single gene, *kitlb*, is necessary for the growth and maintenance of ICC, which will allow for the development of normal motility patterns in the zebrafish GI tract. These experiments are aimed at understanding ICC growth and development at a molecular level and could ultimately lead to GI dysmotility treatment options.

Morpholinos (MOs)

Morpholino oligonucleotides (MOs) were first developed by James Summerton, who used MOs to inhibit the translation of RNA transcripts *in vivo*. Now, MOs are the most common anti-sense "knockdown" technique used in zebrafish. MO work at a molecular level and are typically used to determine gene function *in vivo* as well as to verify mutant phenotypes, however, MOs can also function in zebrafish to reduce maternal and zygomatic gene function (Corey & Abrams, 2001). A morpholino oligonucleotide may be structurally

described as a neutrally charged phosphorodiamidate backbone containing 25 morpholino bases (Bill, Petzold, Clark, Schimmenti, & Ekker, 2009). The structure of the MO allows complimentary binding to RNA of interest and results in the disruption of transcriptional or translational processing due to steric hindrance.

There are two types of MOs that are used in the zebrafish. A splice blocking morpholino oligonucleotide is a MO that works by binding to pre-mRNA and prevents the assembly of splice components, therefore disrupting post - transcriptional modification and preventing the formation of mature RNA. Products of a splice blocking MO can be observed using reverse transcriptase polymerase chain reaction (RT-PCR) and gel electrophoresis. Translational blocking morpholino oligonucleotides are designed to bind mRNA within the 5' untranslated region located near the translational start site. Binding of the MO prevents the assembly of the ribosome blocking translation of mRNA. Antibodies that bind to the protein of interest are used to determine the level of knockdown that has occurred as a result of a translational blocking MO (Bill, Petzold, Clark, Schimmenti, & Ekker, 2009).

MOs are introduced into the yolk of a developing embryo by microinjection before the 4 - cell stage. Ubiquitous delivery of an MO to all dividing cells is a result of early introduction of the MO into the embryo. Also, rapid diffusion of a MO occurs within the dividing cell of an embryo due to presences of cytoplasmic bridges that serve to connect embryonic cells (Bill,

Petzold, Clark, Schimmenti, & Ekker, 2009). Currently, there are no known enzymes found in cells that work to eliminate MO expression. This is likely due to the nonionic backbone of MOs, which make it resistant to digestion (Corey & Abrams, 2001). However, the efficacy of an MO is directly related to binding affinity and protein kinetics, more specifically protein turnover, the effectiveness of an MO appears to be limited to 7 days post fertilization (dpf), with most phenotypes observable during the first three days of development (Bill, Petzold, Clark, Schimmenti, & Ekker, 2009). Observation of phenotypes resulting from introduction of a MO into a developing embryo require a rigorous set of controls that are used to screen for nonspecific effects of a morpholino.

Fish Disease

In general terms, zebrafish are hearty. However, they can be highly susceptible to contagious diseases such as velvet disease, fish tuberculosis and nematode infection as well as vegetative bacteria, especially when the zebrafish is stressed or injured (Brand, Granato, Nusslein-Volhard, & Christiane, Zebrafish, 2002). There are some treatments available for diseases such as velvet disease and nematode infection as well as antibiotics that can be used to treat bacterial infections. It is highly suggested that treatment of diseased fish is avoided; instead zebrafish that exhibit symptoms should be discarded immediately to help prevent transmission to other zebrafish within the colony. If the entire

system becomes contaminated the system should be shut down and cleaned properly with a chlorine dioxide-based high level disinfectant.

Outside venders such pet stores may not follow rigorous quarantine protocols when their zebrafish are diseased. It is important that proper measured are taken by a laboratory when outside fish are brought in. Disease and bacteria are not likely to spread through the air or dried material, but infectious agents thrive in moist environments (Brand, Granato, Nusslein-Volhard, & Christiane, Zebrafish, 2002). To avoid contamination it is necessary to keep outside zebrafish in quarantine tanks, to disinfect shared nets and filter between handling also bleach breeder boxes after use.

Objective and Experimental Plan

Aim of Experiment

The overall aim of this thesis is to better understand the role of *kitlb* on ICC development. It is known that stem cell factor, or kit ligand, is necessary for ICC development but the molecular mechanisms are poorly understood. There are two isoforms of mammalian Kit ligand, one is primarily soluble and the other is primarily membrane bound. The relative importance for each isoform on ICC development, ICC turnover, and ICC maintenance is unknown. Morpholino knockdown of *kitlb* expression will be used to test the hypothesis that *kitlb* is necessary for ICC development in zebrafish. We anticipate that development of normal motility patterns in the GI tract will be disrupted because ICC

development will be delayed when *kitlb*, similar to the membrane-bound isoform of mammalian Kit ligand, expression is reduced. A better understanding of the role of the membrane bound form of kit ligand may contribute to our overall understanding of ICC development and the regulation of GI motility, and thereby further understanding of GI motility disorders and drug target development.

Experimental Plan

The function of *kitlb* on maintenance and development of ICC will be examined by knocking down its expression. A morpholino (MO) will be used to specifically and selectively knockdown for *kitlb* gene expression. The MO is introduced into the embryo before the 4-cell stage. The MO was purchased with a fluorescent tag and MO injection is verified using fluorescence microscopy. MO-injected embryos are allowed to develop until 7 dpf when ICC networks are developed and when ICC regulation of spontaneous and propagating contractions occurs (Parichy, Elizondo, Mills, Gordon, & Engeszer, 2009). It is possibly the MO injection can delay or interfere with normal development. To test this possibility standard length is measured at 7dpf. Parichy et al showed that standard length is a reliable method to examine development of zebrafish, and is more reliable when compared to simple days post fertilization (Parichy, Elizondo, Mills, Gordon, & Engeszer, 2009). Standard length is measured by imaging the anterior and posterior portions of the larva and tiling images

because an entire larva is too large for a single image. Also at 7dpf, a GI motility assay will be completed for each larva. The GI motility assay consists of anaesthetizing larvae in MESAB, immobilizing in 1.9% agarose in a polyethylene capillary tube, and capturing time-lapse digital images at a rate of 1 per second. A total of 600 images are collected spanning 10 minutes. The sequential images are converted to a single spatial temporal maps (STMaps) using Volumetry, which are used to further analyze GI motility by quantifying the motility index (MI), total number of contractions, and contraction distance, velocity and frequency. Reverse transcriptase polymerase chain reaction (RT-PCR) is used to verify the effects of *kitlb* MO injection on *kitlb* mRNA production in the larvae.

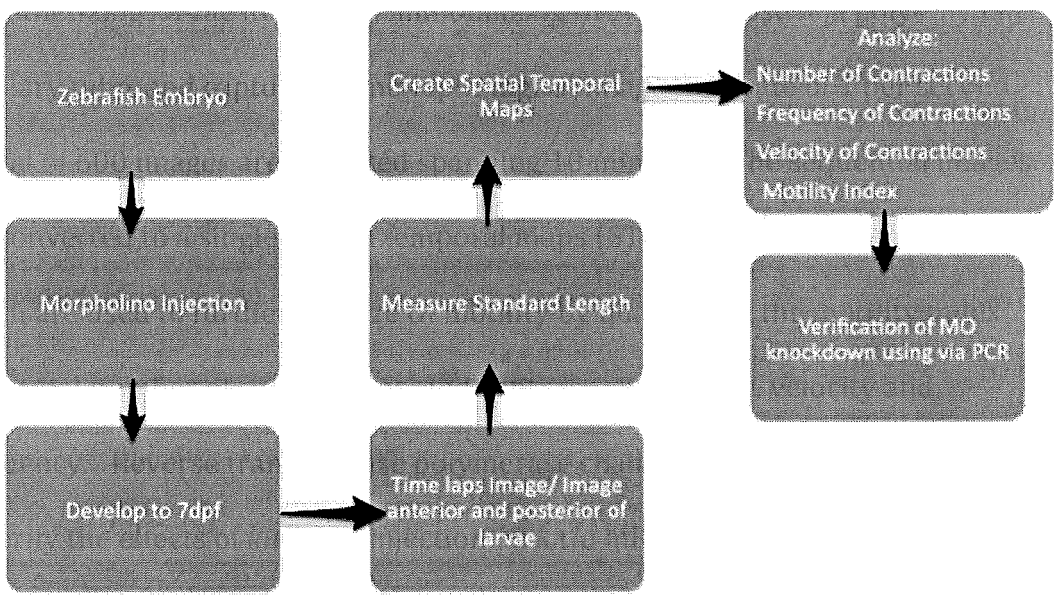

Experimental Procedures

The techniques used in this thesis are briefly described. A more detailed description of the protocols used can be found in the Appendix.

Aquaculture:

The Zebrafish International Resource Center (ZIRC) provides our lab with wild-type zebrafish. These zebrafish are maintained in full accordance with the IACUC guidelines. Our system is filled with water that has been processed through reverse osmosis and has been supplemented with 240mg/L of Instant Ocean Sea Salt and 75mg/L $NaHCO_3$. Reverse osmosis of the system water is established using a filter. The filter allows for water to overcome the natural tendency to flow from a region of high solute concentration to an area of low solute concentration by overcoming osmotic pressure. This process is advantageous due to its ability to take tap water and produce purified water that is free from the contaminants such as copper, lead, arsenic, chlorine, pesticides, etc. Water that has been filtered by reverse osmosis and added to the system is then carefully monitored for its pH, temperature, ammonia and nitrate levels to ensure the water chemistry is maintained within normal range. The pH level should range from 6.9 to 7.4, ideally around 7. Temperature of the system can range from 25°-29°, however, it had been found that the water temperature that is maintained around 28.5 is ideal for zebrafish breeding. Ammonia and nitrate levels should be 0ppm and conductivity can range from 800-1200μS.

Adult zebrafish are fed three times daily. They receive dry food for breakfast between the hours 8am-10am (aquaneering food), brine shrimp (dehydrated decapsulated irtenua cycts, which is cultured daily) between 12pm-2pm, and dry food for dinner (orange cysts) between the hours of 4pm-6pm.

The fish colony is maintained on a 14hr/10hr light/dark cycle. This helps to establish a circadian rhythm for the zebrafish. This cycle is most advantageous for establishing a normal feeding and breeding schedule.

Breeding/crossing of the adult zebrafish is designated to the early morning hours, right as the lights turn on in the fish room (7am). Breeding boxes are used to set up crosses containing as many as 3 Females X 2 Males or as few as 1 Female X 1 Male. Embryos gathered from these crosses are maintained in embryo medium called E2 (recipe can be found in the Zebrafish Handbook) are incubated at 28°.

Streamline Zebrafish Husbandry:

Small changes have been made to the maintenance of the zebrafish colony. The colony is still maintained in accordance with IACUC guidelines. The system is now filled with tap water that has been aged for around a day to allow for the release of chlorine. This replaces the more expensive process of reverse osmosis that was used to fill the system with water. The pH of the system water is now maintained within the 6.9 – 7.4 range with the ideal pH of 7. Change in conductivity, or the waters ability to conduct an electrical current is

now maintained around 300μS with addition of Instant Ocean Sea Salt added as needed. The shift to a more neutral pH level and lower conductivity level are hypothesized to benefit breeding results. All other components of the systems water and fish care have remained identical to what has been explained in the previous aquaculture paragraph.

Cleaning Larvae

After breeding has concluded, embryos are sorted and unfertilized embryos are removed. The fertilized embryos are then further divided into 25 embryos per petri dish, which helps maintain good health. Daily cleaning of the embryos / larvae is necessary for viability. Transfer pipettes are used to remove dead embryos as well as empty chorions, which would provide nutrients for the growth of bacteria and mold (Brand, Granato, Nusslein-Volhard, & Christiane, 2002). As much old E2 as possible is siphoned out of the petri dish and then replaced with fresh E2 medium. Establishment of good cleaning habits like those mentioned above result in greater viability by preventing the E2 in each petri dish from spoiling.

Bleaching of embryos before 28 hours post fertilization (hpf) is an additional step that may be taken to achieve better cleanliness of embryos. It is a multiple step process that is time sensitive that works by killing bacteria and other microorganisms decreasing the spread of disease. The embryos are rinsed in a diluted bleach solution, than rinsed twice in E2 medium. It is

necessary that bleaching is completed before 28 hpf. After 28 hpf hatching enzymes are released from the embryo in preparation of the larvae to break free of its chorion (Brand, Granato, Nusslein-Volhard, & Christiane, 2002). The enzymes work by degrading the chorion. Therefore, the weak chorion does not provide suitable protection to the young larvae and the introduction of a detergent such as bleach would put the viability of the larvae at immediate risk.

Embryos used in the experiments for this thesis were not bleach. The experiments required embryos to undergo microinjections in order to deliver a morpholino into the dividing cells. Piercing of the choiron for morpholino delivery makes the chorion weak and cleaning with bleach may have been detrimental.

Counting / Logging Larvae Viability

Viability and good health of developing larvae is important. Counting and logging of larvae viability is done daily at the same time E2 media is changed. The total number of surviving embryos / larvae are counted and recorded in a laboratory notebook. It is important that the log of larvae viability is well organized and easy to reference. The daily log should include the parent line, day post fertilization, experimental indication (ex: *kitlb* injected or control injected) and total number of healthy surviving embryos / larvae. This log is started at 0dpf and is continued through 7dpf when the larvae are used for time - lapse imaging. Daily records of embryos / larvae survivability allow for easy

identification of healthy breeding lines or breeding pairs. It is extremely important to have healthy embryos / larvae for experimental purposes.

Morpholino

In a eukaryotic cell, pre – mRNA is processed into mature mRNA. Small nuclear ribonuclear proteins (snurps) direct a splicesome to make cuts in the pre – mRNA at splice junctions to remove introns and splice together exons, resulting in mature mRNA. A Morpholino (MO), an antisense oligonucleotides is designed to redirect splicing. The MO will complementarily bind to pre – mRNA at an internal splice junction, blocking the splice junction of an internal exon causing the removal of the exon as well as both flanking introns. For this project a splice blocking MO for *kitlb* was used. Splice blocking MOs works by binding to an intron- exon pre-mRNA target. The MO binds to the pre-mRNA target and works by sterically disrupting the molecules that direct the spliceosome to splice sites. The end result is a new splice pattern of mature mRNA, different from the mature mRNA that would have been produced in the absence of the MO (Mouton & Jiang, 2009). Therefore an effective MO results in a different mRNA product compared to a non-injected control. For this project the splice blocking MO *(kitlb)* was modeled after work previously done by Keith Hultman and colleagues (Hultman, Bahary, Zon, & Johnson, 2007). The MO binds to target pre-mRNA at the intron 2 - exon 3 boundary resulting in the excision of target exon 3. This causes an in- frame shift and splicing of exon 2 to exon 4. This

exon excision will result in production of an ineffective protein, effectively knocking out *kitlb* and helping better understand the function of the *kitlb* gene in vivo.

MO Design

Kitlb MO that was created and designed based off Keith Hultman's work as well as assistance from Gene Tools, LLC. A splice blocking MO was chosen so that the efficacy of the MO could be tested using reverse transcriptase polymerase chain reaction (RT-PCR). Characterization of the MO using RT-PCR was observed using Gel electrophoreses as a shifted band due to the new splice pattern in mature mRNA.

When placing the order it is necessary to know the pre-mRNA sequence including all exon – intron and intron – exon boundaries so the MO can be designed to reach its optimal target and have the greatest efficacy. *Kitlb* MO sequence was designed as (5' – CACATGTATACTTACCACATCCTTT – 3') to block processing at the splice donor site of exon 3. A negative control was also designed in accordance to Hultman's work and with assistance from Gene Tools, LLC to control for any nonspecific effects of a MO. The Negative control MO sequence was designed as (5' – CCTCTTACCTCAGTTACAATTTATA – 3').

Preparation/Storage of Stock Solution

The MO is delivered as a prequantitated, sterile, salt-free, lyophilized powder. Gene Tools, LLC recommends that the solid is solubalized into a 1mM stock solution in distilled water or Danieau buffer.

The 300nmole *kitlb* and control MOs were made into 1mM stock solution by adding 0.30mL of distilled water. Stock solutions were stored at room temperature, as directed by Gene Tools LLC. MOs can be stored in the refrigerator or freezer, but the cold temperatures can cause the MO to come out of solution.

Working Solution

Stock solutions of *kitlb* and control MOs were made into a 20μM working solution by a 1:50 dilution using Daneau buffer. Since the control MO was not ordered with a 3' Flurescein tag 0.5% phenol red was added into the working solution as a visual indicator.

1:50 Dilution: *to prepare 100μl of injectable MO solution*

$$C_1V_1 = C_2V_2$$

$$(1000\mu M)\ (X\mu L) = (20\mu M)\ (100\mu L)$$

$$X = 2\mu L$$

Add 98 μl Daniau buffer and 2μl of stock MO solution

0.5% Phenol Red:

0.5μL per 100μL

Testing Efficacy of MO

MO knockdown is extremely effective during early development but MO concentration declines during embryonic development as the MO concentration continuously declines with cell division. When looking at later developmental time points it is important to directly measure MO efficacy. Expression of the *kitlb* gene was tested using RT-PCR on cDNA prepared from total RNA that was isolated from 5dpf and 7dpf *kitlb* MO injected zebrafish larvae. Identical experiments were performed on age-matched control MO injected, or wild type non-injected larvae. Primer sets for *kitlb* gene were designed to span exon 3 resulting in a shorter amplicon when the kitlb MO is effective, and longer amplicon (containing exon 3) for wild type or for ineffective MO injection. The primers also span intron – exon boundaries to eliminate (or lesson) the effects of potential genomic contamination. *Kitlb* primer set was used to test the efficacy of both *kitlb* MO injected and control MO injected larvae. *Kitlb* forward primer 5' – ACCTGCTCAGGTGTTTTTGG – 3', binds upstream to the 5' region of *kitlb* gene and *kitlb* reverse primer 5' – CATTCTGTCCTCCAGGTCGT – 3', identifies the downstream 3' end of *kitlb* gene. *Kitlb* forward and reverse primers anneal to complementary DNA surrounding the gene of interest, which is followed by amplification of the gene of interest.

PCR products of *kitlb* MO injected larvae and control MO injected larvae should appear as different lengths in the gel. The presence of *kitlb* MO is expected to splice the mature mRNA resulting in an in-frame deletion of exon 3. PCR conformation of the exon excision would result in the presence of a 241 base pair band, which is shorter than 288 base pairs, the expected size of wild type zebrafish PCR products of control MO injected larvae should reveal a band at the expected length of 288 base pairs since the control MO would not have disrupted the normal splicing patterns on pre-mRNA into mature mRNA.

It is important to mention that β-actin is always used as a positive control in PCR reactions to help with trouble shooting. The control shows that the reaction is working as predicted and that there is not contamination. More specifically, β-actin is used to make sure the cDNA template is good and the enzymes in the reaction are working.

GI Motility Assay

Observation of gastrointestinal motility using time-lapse imaging is possible in the optically transparent larvae. Larvae are transparent until approximately 10 days post fertilization, and even longer if pigmentation is inhibited. In this thesis zebrafish at the developmental stage of 7dpf were used. Visual data collection provides additional significance to molecular and morphological information surrounding the development of the gastrointestinal tract (Holberg, Schwerte, Pelster, & Holmgren, 2004).

Fertilization and MO injection:

Embryos were collected from the laboratory breeding stock. The developmental stages of the zebrafish were tracked by days post fertilization and by measuring from snout to tail. The first day of fertilization is termed 0dpf. Within an hour after birth, and before the 4-cell stage, embryos were microinjected with *kitla / kitlb, kitlb* and control morpholino (Gene –Tools LLC.). Embryos were subsequently placed in petri dishes containing E2 and held in the incubator at 28°C. It is important to limit embryo density to 25 per dish. Viability of the embryos was counted each day when E2 was changed. Zebrafish larvae were not fed during the experimental period. Larvae that developed to 7dpf were used for visual data collection.

Screening of Embryos:

Morpholino-injected embryos were screened 5 hours post injection. Screening was completed to ensure the presence of morpholino in each injected embryo as well as ubiquitous delivery among the diving cells. The experimental morpholino used (*kitla / kitlb* and *kitlb*) were purchased from Gene –Tools LLC with a 3' flourecein tag. This tag allowed visualization of the injected MO within embryos using a fluorescent microscope. Phenol Red was added to control morpholino because it was not purchased with a 3' fluorescent tag.

Transmitted light is sufficient to identify phenol red injected embryos. Embryos were discarded if morpholino was not observed in dividing cells.

Mounting 7dpf Larvae and Digital Imaging

Larvae surviving to 7dpf were used to test the effects of morpholino knockdown of *kitlb* in GI motility. Zebrafish were removed from the incubator and anesthetized in .75% MESAB, transferred into .9% agar containing MESAB and E2, maintained at 42°C using a water bath. A pipette pump was used to draw 0 .9% agar and the zebrafish larvae into a fluorinated ethylene propylene (FEP) tube (1/32" diameter, Cole Parmer). Agar was drawn up in the FEP tube to keep the zebrafish larvae stabilized and immobile while imaging. At this concentration agar gels, or solidifies at room temperature. The FEP tube containing the larvae was placed onto a homemade foam holder, which helps to position the FEP tube to enable lateral imaging of the larvae. The foam channel had edges higher than the outer diameter of the tube creating a chamber. Both ends of the tube extend beyond the channel to allow for rotational adjustment of the tube to gain the optimal lateral view of the GI tract. Water was used to fill the chamber, surrounding the FEP tube. Water is an ideal optical correction solution and reduces image distortion (Petzold, et al., 2010). Under 4X magnification on a Nikon Diaphot inverted microscope with an attached Spot Insight video camera images of the 7dpf zebrafish were collected using Spot software (Diagnostics Instruments, Inc.). At the start of each experiment an

image of the posterior half and a second image of the anterior half was collected so that the length of the entire larva could be determined. Sequential images of the entire length of the GI tract were taken every second for ten minutes. Spot software (Diagnostics Instruments, Inc.) complied all 600 images as a sequence file that could be played back as a movie. Each movie was reviewed for analysis of the contractions occurring in the GI tract.

Tiling Images:

Images collected of the anterior and posterior regions from each 7dpf zebrafish larva were tiled together to form one image of the entire length of the larva using Image Pro Plus (software version 5.0; Media Cybernetics). Tiled images were used to measure the standard length of the 7dpf zebrafish larvae. Standard length is defined as the total distance from snout to the posterior tip of caudal fin. Parichy and coworkers showed that standard length is an accurate method to gauge development, and is the most accurate method to assess post-embryonic fish developmental stage (Parichy, Elizondo, Mills, Gordon, & Engeszer, 2009). A normally developing zebrafish should have a standard length measurement just under 4mm at 7dpf. All zebrafish larvae used for thesis experiments were assessed using standard length to validate developmental stage of the zebrafish was not altered by the delivery of the morpholino.

Digital Image Analysis:

The sequence files of the experimental larvae that were collected using Spot software (Diagnostics Instruments, Inc.) were analyzed using Volumetry, a custom written program (Volumetry G6a, Grant Hennig). A rectangular region of interest was manually drawn over the image sequence files, which only included the GI tract. Using the region of interested, a spatio temporal map (STMap) is created by calculating the average brightness, or pixel intensity along columns of pixels from the region of interest. Each image results in a single row in the spatiotemporal map. Changes in average intensity along the GI tract appear as dark bands. The intensity change results from occlusion of the intestinal lumen and represents contractions. The STMap therefore reduces 600 time-lapse images into a single image enabling visualization of propagating contractions as dark bands. Furthermore, patterns or the lack of patterns is readily apparent and quantification of each contraction is possible. More specifically, STMaps provide the ability to identify the site of initiation for each contraction, allow the propagating distance of each contraction to be measured and also provide the means to calculate velocity and frequency of the contractions occurring in the GI tract. The distance and velocity of contractions was calculated by manually drawing a line over the entire length each dark band that represents a propagating contraction on the STMap. The total number of contractions that occurred over the 10-minute period of recorded time was used to calculate frequency of contractions. The spaces in between peak contractions

were measured and reported as intervals. It is important to know that frequency and interval are not always the same because contractions can occur at irregular intervals. Qualitative analysis of the STMaps was quantified a motility index resulting in a binary score or 'coordinated' or uncoordinated. Coordinated motility patterns refers to a series of propagating muscular contractions that cause the lumen to narrow and result in propulsion of intestinal content moving in an aboral direction.

Motility Index (MI):

When analyzing STMpas we realized that the majority of maps show about 1 propagating contraction per second, but some maps showed none, or just 2 or 3, while other maps had periods of inactivity. Contractile behavior was ignored by merely measuring contraction distance, velocity, and interval. We therefore developed the Motility index (MI) as a technique to rapidly assess STMaps as coordinated or uncoordinated. This method scores GI motility as 1 (coordinated) or 0 (uncoordinated) by analyzing the contractions appearing on the STMaps. STMaps receiving a score of 1 have shown propagating contractions moving in the anterograde direction (mouth to colon) for at least 75% of the contractions with no more than one irregular/skipped contraction during the 10 minute recorded period. It is anticipated that zebrafish with fully developed gastrointestinal tract should have fully propagating anterograde contractions about 75% of the time since this is reported in humans.

Statistical Analysis

The averages of the data were reported ± the standard error of the mean (SEM). A two – tailed distribution, two – sample equal variance t – Test was performed to determine statistical significance with data scoring equal to or greater than the 95th percentile considered significant.

RNA Isolation

Total RNA extraction was possible using intact zebrafish. RNA was extracted from morpholino injected zebrafish, control injected and wild-type zebrafish at 5dpf and 7dpf developmental time points. The intact zebrafish were first placed in RNAlater, a solution that works to stablalize and protect cellular RNA by quickly penetrating the tissue of the fish. The zebrafish in RNAlater were stored for up to one week at room temperature or four weeks when refrigerated. The procedure of RNA isolation was done using an RNeasy Plus Mini Kit (Qiagen, Chatsworth, CA). iSCript cDNA synthesis kit (Bio – Rad Laboratories, Hercules, CA) was used for first strand synthesis.

Quantifying RNA by Spectral Absorption

Purity of RNA directly influences RT-PCR results. The purity of total RNA isolated from morpholino and control injected zebrafish at developmental time points, 5dpf and 7dpf was measured using the Nano Drop. The Nano Drop analyzes the RNA sample by spectrophotometric quantification. Absorption of a total RNA sample is expressed as an absorbance ratio at 260 and 280nm (A260/280). This ratio is used to determine the purity of a RNA sample by measuring the amount of ultraviolet (UV) light that passes through the nucleic acids of the sample at a wavelength of 260nm. A pure RNA sample has greater absorption levels as a result of increased number of nucleic acids within the sample. The absorbance ratio of a pure RNA sample will be measured around 2.

cDNA Synthesis

RNA was isolated from morpholino and control injected larvae at 5dpf and 7dpf. Total RNA was used with iScript cDNA Synthesis Kit (Bio-Rad Laboratories, Hercules, CA) for first strand synthesis. Mature mRNA serves as the template in this catalytic reaction that utilizes reverse transcriptase (RT), random primers, oligo (dT) and nucleasue free water to synthesize cDNA. DNA complements are synthesized from mature mRNA when RT enzyme binds and complementary base pairing occurs.

Reverse Transcriptase Polymerase Chain Reaction (RT-PCR)

Primers to test the MO efficacy for the *kitlb* gene were designed using Primer 3 software that is freely available on the internet (http://primer3plus.com/web_3.0.0/primer3web_input.htm). Primers were ordered from IDT (San Diego, California). Forward and reverse primers for *kitlb* were created to span intron – exon boundaries to prevent PCR amplification of genomic contamination and to enhance the quality of expected PCR product. More specifically, the *kitlb* primer set was designed to span the entire length of exon 3, the targeted exon as well as bind upstream to exon 2 and downstream to exon 4 so that different PCR products would result from control versus MO injected larvae.

The length of PCR product using these primers is expected just under 300 base pairs for control, and 241 base pairs for MO injected larvae. Reverse transcriptase PCR was performed using a kit, PCR – EZ D – PCR Master Mix (Bio Basic Inc, Markham Ontario L3R 1G6 Canada). The PCR – EZ D – PCR Master Mix kit contains a 2X master mix consisting of Taq Polymerase, KCL, $(NH_4)_2SO_4$, Tris HCL, Triton X – 100, BSA, $MgCl_2$ and dNTPs. To this I added 1μL of forward and reverse primers (20μM each), 1μL of cDNA, and 10.5μL of water. Control cDNA template was prepared from total RNA isolated from adult GI tissues, or from intact non-injected larvae. The PCR program denatured at 92° C, annealed primers at 54° C and elongated cDNA at 72°. The PCR reactions were run for 35 cycles. PCR products were then analyzed using a 2% agarose gel.

Pitfalls

Morpholino oligonucleotides are used as a powerful molecular technique to inhibit the translation of RNA transcripts *in vivo.* MOs are used to identify specific gene function or to verify a mutant phenotype. However, there are potential pitfalls associated with the use of MOs. Most importantly, an MO can cause off target effects, which may lead to false conclusions associated with genetic relationships and developmental mechanisms. An off target effect may result in the observed phenotype which is not due to the intended knockdown, but instead is a result of the MO interacting with an off target sequence of RNA. There are several potential approached to determine if the MO had off target effects. One possibility would be rescuing of the observed phenotype by injecting a rescue mRNA. One other possibility would be the comparison of the observed phenotype with the mutant strain. It is also possible that knockdown of a target gene by an MO will lead to gene compensation. More specifically, the MO used in this project was designed to knockdown expression of *kitlb*, one of the two co - orthologos for the human *KIT* gene. Knocking down expression of *kitlb* may result in and increased expression of *kita* and *kitb*, or even *kitla*, and this may minimize the effects of gene knockdown resulting in a less severe phenotype. A potential approach to solve this problem would be co-injection of *kitla* and *kitlb* morpholino. Co-injection of *kitla* and *kitlb* morpholino would knock down both co –orthologs for the human *KIT* gene possibly leading to more definitive results.

Spatio temporal maps (STMaps) are created through digital imaging. STMaps provide the ability to identify the site of initiation for each contraction, allowing the propagating distance of each contraction to be measured and also provide the means to calculate velocity and frequency of the contractions occurring in the GI tract over a 10 – minute period of time. It is possible that the 10 – minute period of recorded time is not a long enough recording period to accurately measure the frequency of contractions since GI motility is highly variable. Complexity of GI transit is a result of several tissue types and external influences such as circadian rhythm working together. Pitfalls may skew the results of the statistical data and falsely calculate a value as statistically insignificant when a change does occur, type 1 error. A more realistic representation of GI motility could be visualized using a GI transit assay. A transit assay could help evaluate the motility throughout the entire length of the GI tract over a 24 - hour period of time and help aid in the identification and severity of transit dysfunction.

RESULTS

Searching the zebrafish genome using Ensemble and the latest assembly of the zebrafish genome (Zv9, completed in February 2011) for kit ligand returns 2 genes, *kitla* (ENSDARG00000070917) and *kitlb* (ENSDARG00000058042), which are located on chromosomes 4 and 25, respectively. The gene structure was accessed by clicking on the gene name resulting in a transcript summary

and the intron-exon structure. The length and specific coding sequence for each intron and each exon was accessed by clicking on the 'Exons' command under 'Transcript based displays'. The genomic structure for *kitla* and *kitlb* was determined in this manner and is summarized in Figure 1. Using an identical approach the genomic structure for human and mouse kit ligand was determined, and compared with the 2 kit ligand orthologues that are present in the zebrafish genome. Human *Kit* Ligand, like zebrafish *kitla*, is comprised of 9 exons. Careful sequence comparisons using NCBI Blast revel close similarity and show that *kitla* expressed exon 6 that contains a putative proteolytic cleavage sight allowing release of soluble kit ligand (Hultman, Bahary, Zon, & Johnson, 2007). The second kit ligand orthologue, *kitlb*, lacks exon 6 and therefore lacks the proteolytic cleavage site and is therefore a putative form of membrane-bound kit ligand.

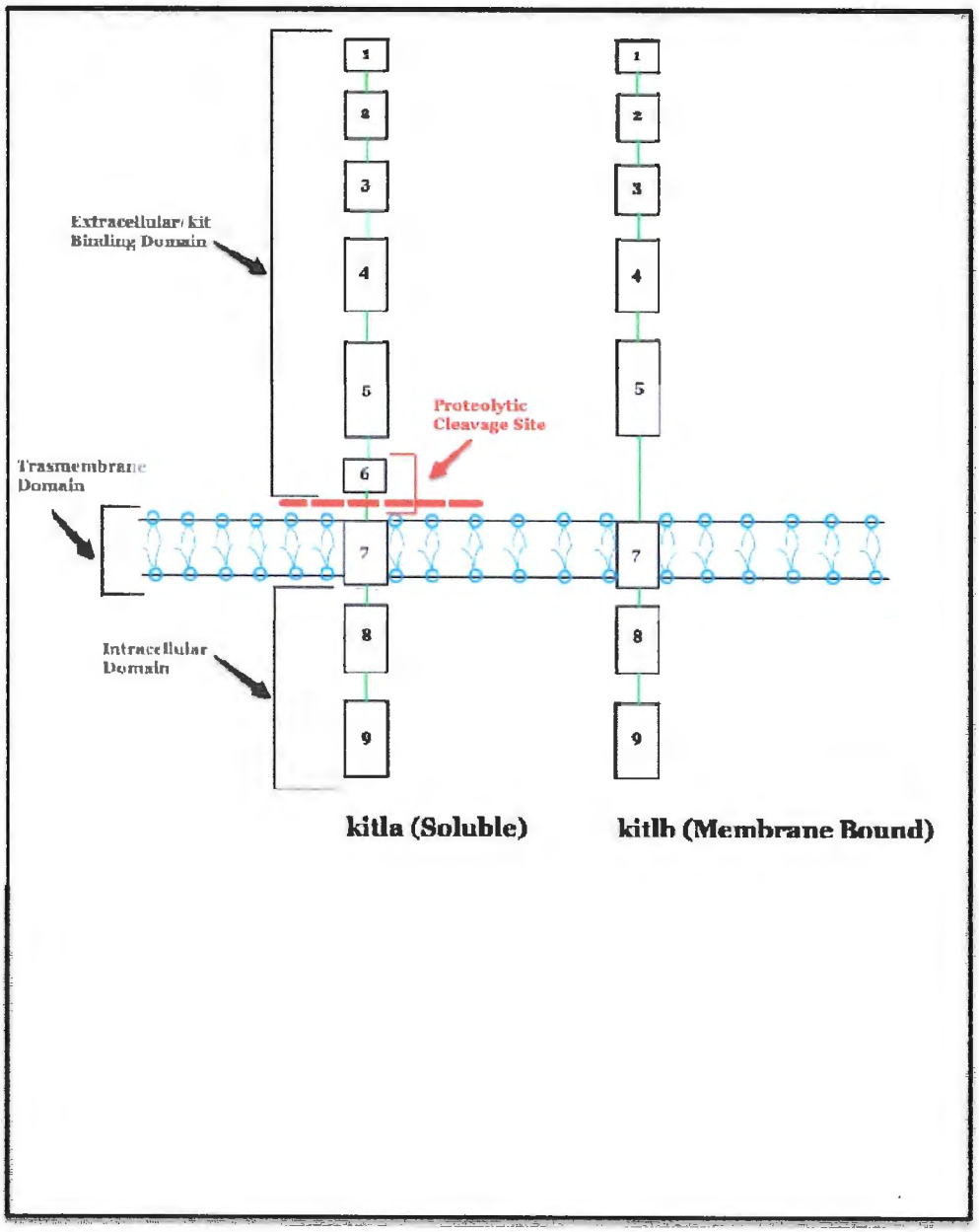

Figure 1. Genomic structure of zebrafish *kitla* and *kitlb*.
Exons (boxes) are labeled according to sequence homology with mouse and human KITL sequence. Coding sequences corresponding to extracellular, intracellular, and transmembrane protein domains are indicated. The two zebrafish Kit Ligand (*kitla* and *kitlb*) genes are homologous to the mouse soluble isoform and the membrane bound isoform. A conserved proteolytic site on *kitla* (left panel) allows extracellular release of kit ligand. *kitlb* lacks the proteolytic cleavage site and is therefore released at a much slower rate

Membrane bound and soluble Kit ligand result from alternative splicing in humans and in mice. The protein sequence of *kitla* and *kitlb* were compared to the membrane-bound and soluble kit ligand isoforms to better understand if the genes are orthologous (Figure 2). *Kitla* was most similar to soluble kit ligand of the mouse (41%).

Protein	Accession Number	Species	Amino Acid Length	Max Id	E-value	Form
kitlb	NP_001018137	ZF	267	n/a	n/a	MB
KL-1	P20826	Mouse	273	34%	1E-11	Soluble
KL-2	AAB22555	Mouse	245	34%	1E-11	MB
kitla	AAX76926	ZF	272	n/a	n/a	Soluble
KL-1	P20826	Mouse	273	41%	2E-19	Soluble
KL-2	AAB22555	Mouse	245	31%	3E-40	MB

Figure 2. Protein sequence comparison of zebrafish *kitla and kitlb* to mouse KL-1 and KL-2. BLAST results show the highest similarity (41%) between *kitla* and KL-1.

The amino acid sequence for each gene was determined using Ensemble and clicking the gene name, then the transcript summary, and selecting protein.

The linear amino acid sequence with individual exons in alternating colors are shown for zebrafish *kitlb* (Figure 3) and mouse KL – 2 (Figure 4).

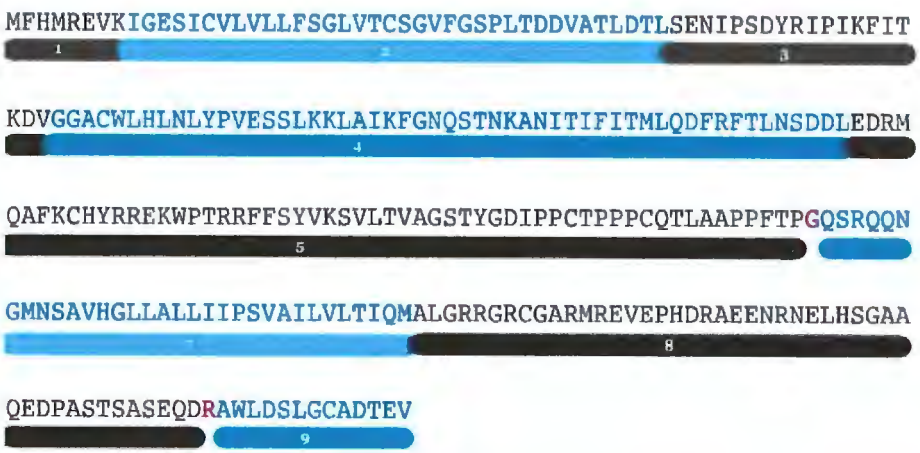

Figure 3. Zebrafish *kitlb* amino acid sequence.
Alternating exons (predicted) are highlighted in black and blue. Red amino acids show residue overlap splice sites.

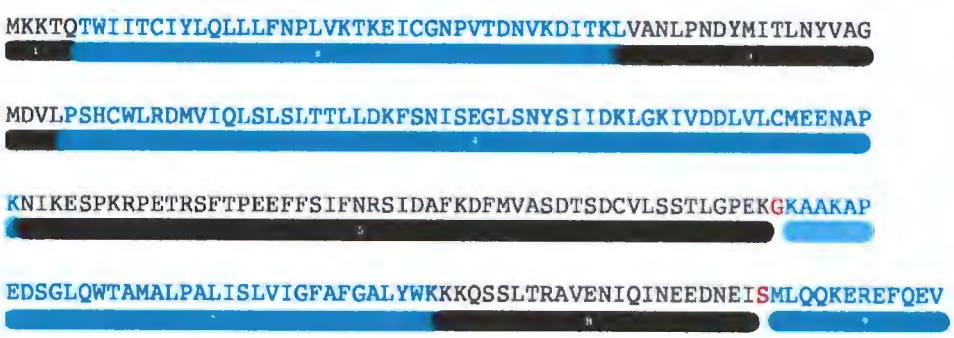

Figure 4. Mouse KL-2 amino acid sequence.
Alternating exons (predicted) are highlighted in black and blue. Red amino acids show residue overlap splice sites

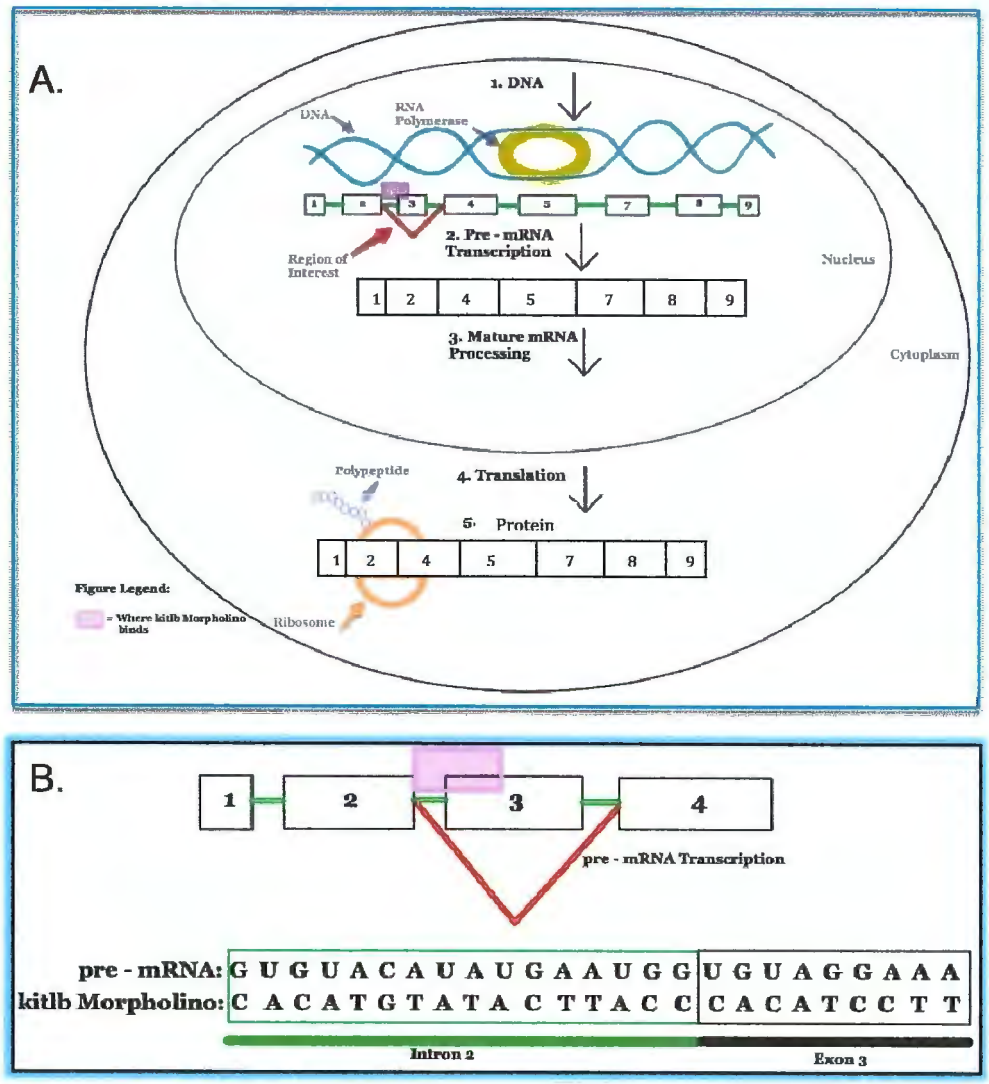

Figure 5. *Kitlb* morpholino (MO) knockdown of *kitlb* expression.
A. Overview of the Central Dogma and mechanism of action of MO knockdown. DNA is transcribed into RNA in the cell nucleus. The *kitlb* MO is designed to be a splice blocker, and hybridizes at the intron 2 – exon 3 border (pink box), preventing assembly of splice components and disrupting excision of exon 3 and introns 2 and 3. Mature mRNA is translated into a protein lacking exon 3.
B. Detailed schematic showing *kiltb* MO, a 25-nucleotide complimentary sequence, hybridizing to the intron 2 – exon 3 border within the nucleus on pre-mRNA. *Kitlb* MO results in a shorter mRNA and smaller protein product.

Splice altering MOs were used to reduce gene expression. MOs are designed to complementarily bind to pre-mRNA at intron-exon borders

effectively hiding splice junctions from the splicesosomes resutling in alternative splicing (Figure 5a). For these experiments MOs were designed to complementarily bind to the pre – mRNA at an internal splice junction at the exon 3 – intron 2 boundaries resulting in the excision of exon 3 in the mature mRNA (Figure 5a). Excision of exon 3 causes an in-frame shift and splicing of exon 2 to exon 4 resulting in the production of a protein lacking amino acids encoded by exon 3 which is assumed to be non functioning. One example for *kitlb* is shown in Figure 5b.

Zebrafish embryos were collected immediately after fertilization. *Kitla / kitlb, kitlb* and control morpholinos (Gene – Tools LLC.) were introduced by microinjection into the yolk of the developing embryo before the 4 – cell stage. Early delivery enables ubiquitous delivery of the MO to all of the diving cells. MO injected embryos were screened about 5 to 6 hours post injection to ensure presence and ubiquitous distribution of MO among the dividing cells. It is not possible to visualize a MO and therefore a maker must be included. The phenol red dye was added to the control MO solution. Phenol red is a commonly used dye that is inert. *Kitlb* MOs were purchased with a 3' fluorescent tag. Phenol Red injected embryos were identified using brightfield illumination and *kitlb* were identified using fluorescence microscopy (Figure 6a and d). Phenol red injected embryos do not fluoresce and the *kitlb* injected embryos appear as normal under brightfield illumination (Figure 6b and c).

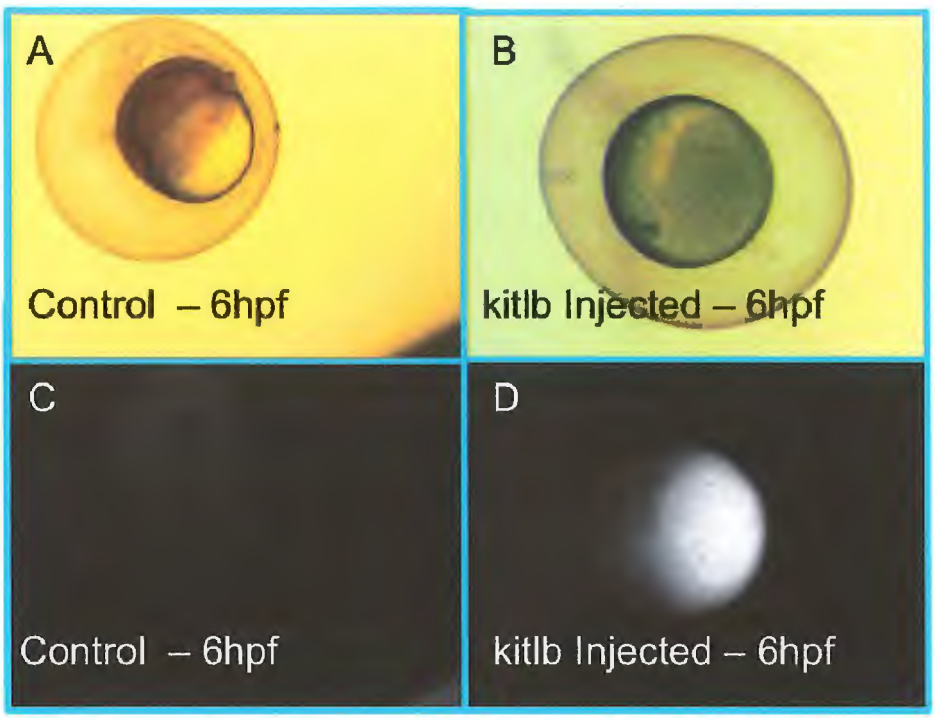

Figure 6. MO injection is verified in control injections using phenol red marker that can be seen in the yolk of injected embryos and by fluorescence in *kitlb* injected larvae.
Panel A - Control MO injected embryo at 6hpf. Presence of phenol red indicates delivery of MO into embryo.
Panel B – *Kitlb* MO injected embryo at 6hpf. Brightfeild illumination shows that MO injected embryos appear healthy.
Panel C – Fluorescence micrograph of control MO injected 6hpf embryo showing that embryos do not autofluoresce.
Panel D – Fluorescence micrograph of *kitlb* MO injected embryo at 6hpf. Fluorescence indicates delivery of of *kitlb* MO into embryo.

MO efficacy was tested in 5 and 7dpf larvae. MO knockdown is most effective at earlier developmental stages because MO concentration decreases as cells grow and divide. MO knockdown is used most commonly to knock down gene expression during early embryogenesis, before 2 dpf. Therefore it is essential to examine gene expression and MO efficacy at reducing gene

expression at later developmental stages. In these experiments expression of *kitla* and *kitlb* in 5dpf larvae was compared in control MO injected and experimental MO injected larvae. Reverse transcriptase PCR was performed using cDNA template prepared from total RNA isolated from 5dpf MO injected zebrafish larvae and age – matched control MO injected, or wildtype non – injected larvae (Figure 7).

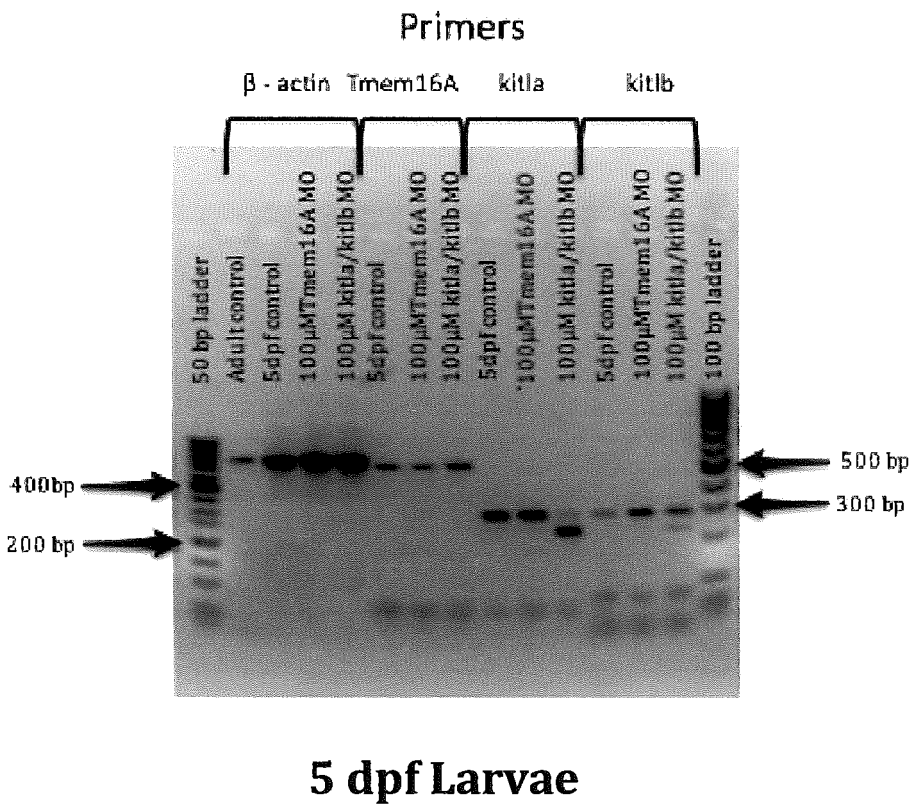

Figure 7: Gel electrophoresis confirms *kitla / kitlb* MO knockdown in 5dpf larvae.
cDNA template from 5dpf *kitla / kitlb* MO injected larvae used with βactin, Tmem16A, kitla, or kitlb primers in PCR reaction. Results revealed double banding for both *kitla* and *kitlb*. Presence of MO and partial knockdown of kitla or kitlb is indicated by bands at 300bp and 250bp. B-actin was used as a positive control.

Two ladders were used (50bp and 100bp) as a DNA standard. A β-actin primer was also used for a positive control on adult, 5dpf control, Tmem16A MO injected and *kitla / kitlb* MO injected cDNA. A single band at 500 bp, the β-actin positive control, verified that both template and PCR enzymes were functional. Two bands were observed for both *kitla* and *kitlb* primers when using template prepared form *kitla* MO and the *kitlb* MO cDNA. The double bands were predicted for MO injected larvae at later developmental stages and result from expression of wild type mRNA (longer band) and the alternatively spliced mRNA lacking exon 3 and resulting from MO knockdown (shorter band). The bands were observed near 250bp and about 300bp confirming knockdown of *kitla* and *kitlb* by morpholino injection at 5dpf (Figure 7). A third gene, TMEM16A, was also assayed because it is expressed on ICC. The TMEM16A MO did not appear to be effective at 5 dpf.

At 7dpf the efficacy of the *kitla / kitlb* MO was also tested. cDNA was prepared from total RNA isolated from 7dpf MO injected zebrafish larvae and age – matched control MO injected or wildtype non – injected larvae. Gel electrophoresis revealed a band at 500 bp when using β - actin primers confirming that the template was intact and enzymes were functional. *Kitla* primers were used to examine *kitla* efficacy and *kitlb* primers were used to examine *kitlb* MO efficacy. *Kitla* primers are predicted to amplify a 300 bp product in wildtype mRNA and a 250 bp product from alternatively spliced *kitla* induced by *kitla* MO. For *kitlb* MO injected cDNA a single band was observed

with *kitla* primers, as expected. For the cDNA template prepared from dual injected *kitla / kitlb* MOs a strong wildtype band was observed near 300 bp and a second faint band at 250 bp. *Kitlb* primers resulted in two bands for cDNa templates prepared from *kitlb* MO and for dual injected *kitla / kitlb* MO samples. These results show that the *kitlb* MO partially knocked down *kitlb* mRNA expression at 5 and at 7 dpf. (Figure 8).

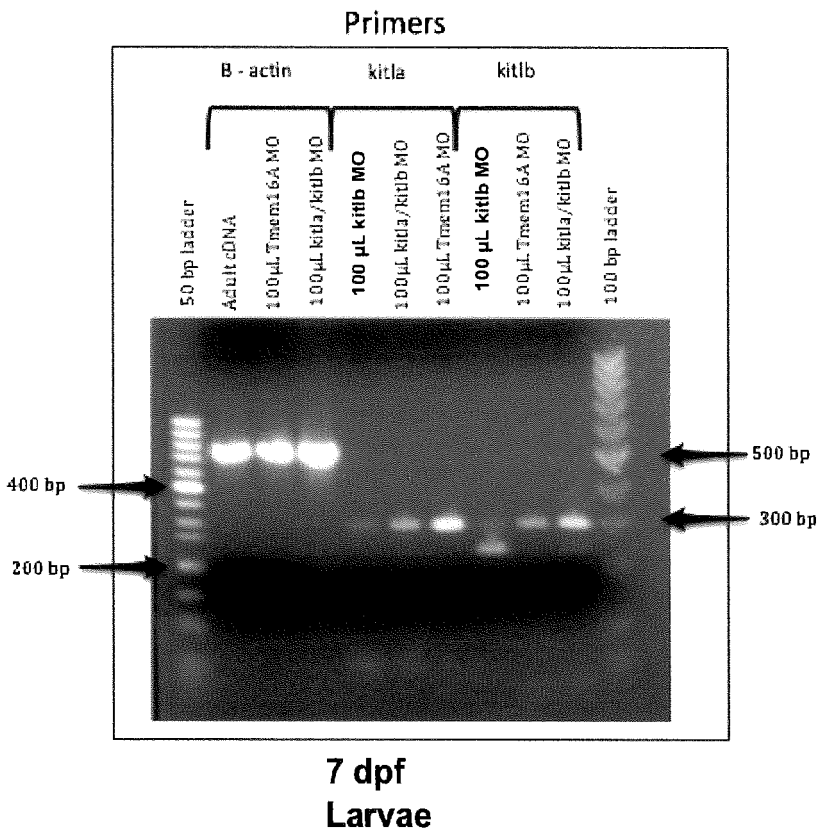

Figure 8: Gel electrophoresis confirms *kitla / kitlb* MO knockdown in 7dpf larvae.
cDNA template from 7dpf *kitla / kitlb* MO injected larvae used with βactin, *kitla*, or *kitlb* primers in PCR reaction. Results revealed double banding for *kitla* and for *kitlb* indicating partial knockdown of *kitla* and *kitlb* at 7 dpf. β-actin was used as a positive control.

The developmental progress of experimental and control zebrafish larvae are essential to confirm that the developmental stages of the larvae were not distorted by the delivery of MO. Parichy and coworkers developed standard length, an accurate method used to access post – embryonic fish developmental stages by measuring the total distance from snout to the posterior tip of the caudal fin (Figure 9a, Figure 9b, Figure 10a, Figure 10b, Figure 11a and Figure 11b) (Parichy, Elizondo, Mills, Gordon, & Engeszer, 2009). Images were collected of the anterior and posterior region from each 5dpf and 7dpf zebrafish larvae and tiled together to form one imagine of the entire length of the larva. Normally developing zebrafish larvae should have a standard length of just below 2mm at 5dpf (Figure 9c) and a standard length of just less than 4mm at 7dpf (Figure 10c and Figure 11c).

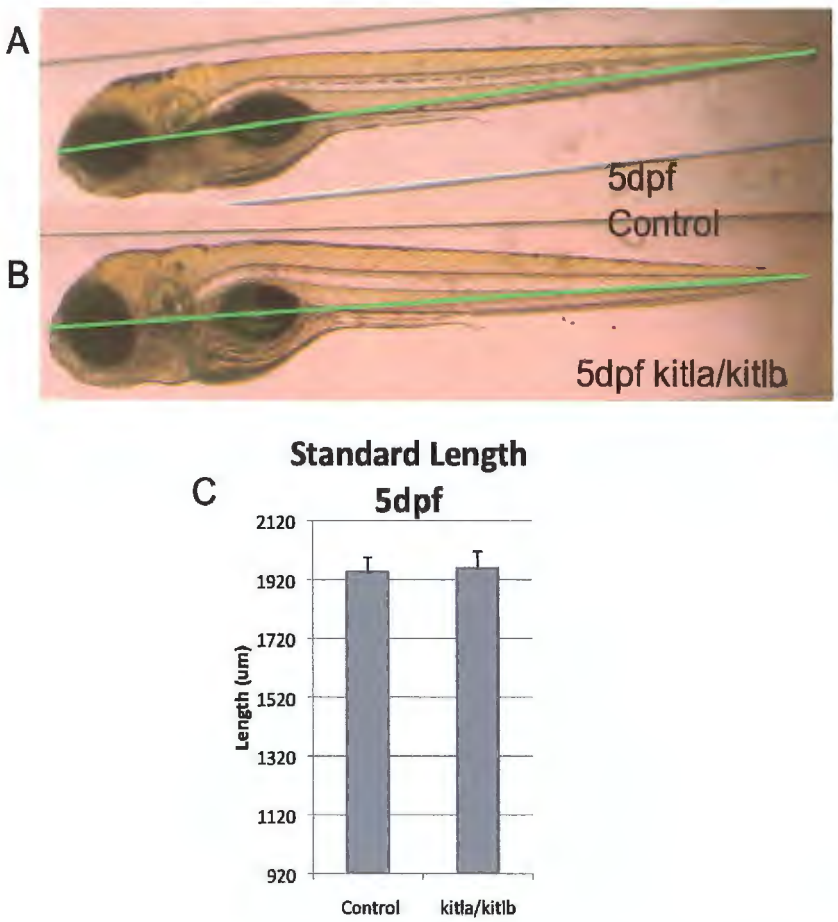

Figure 9: Standard length of co – injected *kitla / kitlb* MO knockdown 5dpf larvae.
The standard length of MO injected larvae was measured to determine if MO injection affects overall development.
Panel A - 5dpf control larvae. Green line indicates standard length measurement.
Panel B - 5dpf *kitla / kitlb* MO injected larvae. Green line indicates standard length measurement.
Panel C - Quantitative comparison of Standard Length of 5dpf control larvae and 5dpf *kitla / kitlb* MO injected larvae.

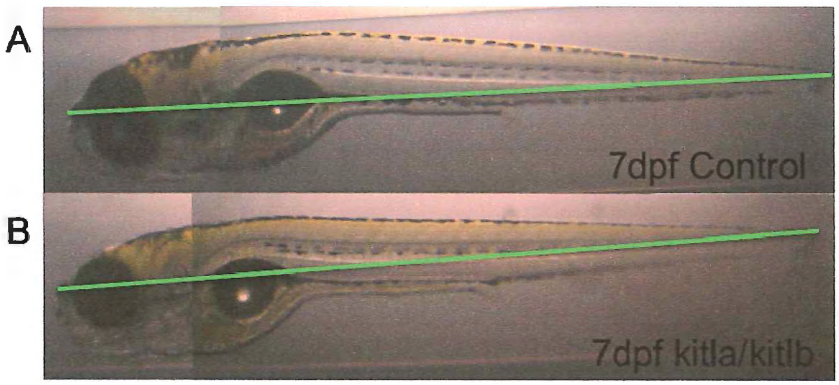

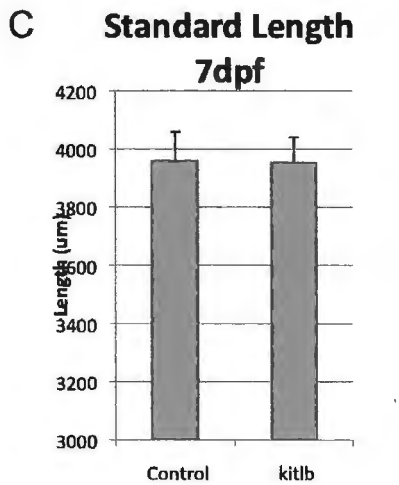

Figure 10: Standard length of co – injected *kitla / kitlb* MO knockdown 7dpf larvae.
The standard length of MO injected larvae was measured to determine if MO injection affects overall development.
Panel A – 7dpf control larvae. Green line indicates standard length measurement.
Panel B – 7dpf *kitla / kitlb* MO injected larvae. Green line indicates standard length measurement.
Panel C – Quantitative comparison of 7dpf control larvae and 7dpf *kitla / kitlb* MO injected larvae.

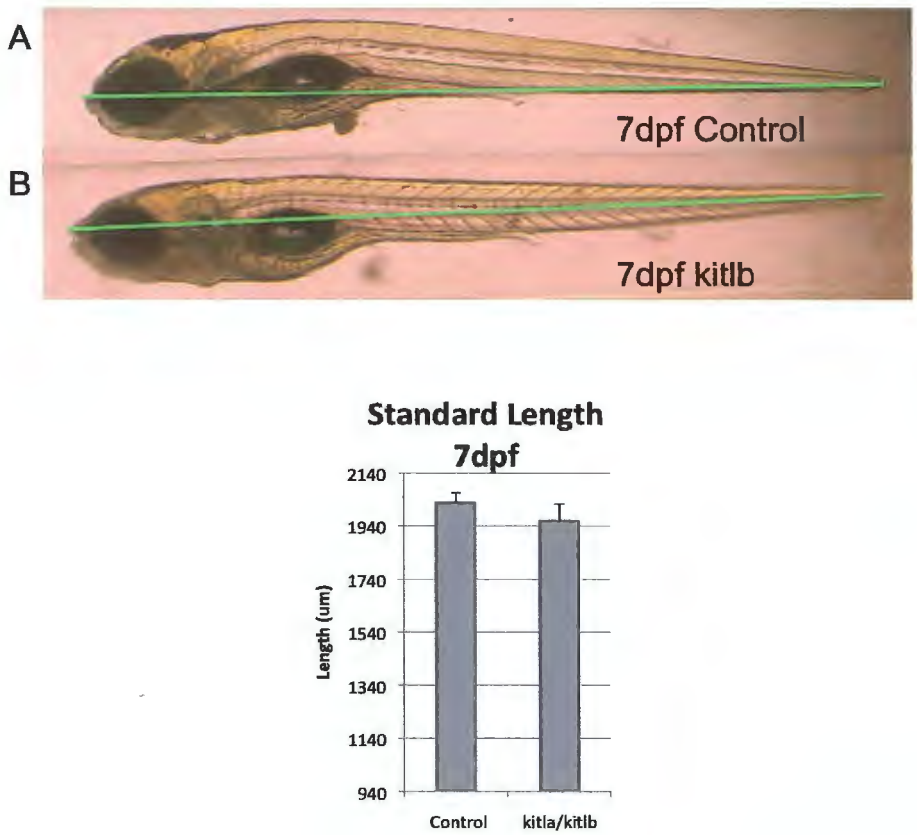

Figure 11: Standard length of *kitlb* MO knockdown 7dpf larvae.
The standard length of MO injected larvae was measured to determine if MO injection affects overall development.
Panel A – 7dpf control larvae. Green line indicates standard length measurement.
Panel B – 7dpf *kitlb* MO injected larvae. Green line indicates standard length measurement.
Panel C – Quantitative comparison of 7dpf control larvae and 7dpf *kitlb* MO injected larvae.

The effects on GI motility of *kitlb* and *kitla / kitlb* MO knockdown were examined on larvae and compared to their age – matched control injected or wildtype non – injected larvae. STMaps were created and used to identify the site of initiation for each contraction, measure the distance of each propagating contraction and also provides the means to calculate velocity and frequency occurring in the GI tract.

Analysis of all STMaps revealed MO knockdown of *kitla*, *kitlb* or dual *kitla / kitlb* at 5dpf and 7dpf display aberrant GI motor patterns compared to the age – matched controls (Figure 12a, Figure 13a, Figure 15a). Quantitative analysis of the data suggests that 7dpf *kitla* MO and *kitlb* MO injected larvae have reduced coordination of contractions as well as a decrease in total number of contractions. Further analysis suggest that *kitla* MO and *kitlb* MO injected larvae have reduced contraction distance, while *kitla* MO injected larvae appear to have a reduction in contraction velocity (Figure 12b).

The effects on GI motility as a result of dual *kitla / kitlb* MO injections was further analyzed on larvae surviving to 5dpf and 7dpf. At 5dpf the anterior region of the GI tract in dual injected larvae showed a reduction in the total number of contractions as well as the interval between each contraction (Figure 13b). The posterior GI region of the 5dpf co – *kitla / kitlb* MO injected larvae showed reduction in contraction interval as well as distance and velocity compared to control larvae (Figure 14a). At 7dpf the effects of the co – *kitla / kitlb* MO on GI motility was again analyzed. The anterior GI region of the 7dpf co – injected larvae revealed a decrease in the total number of contractions as well as a reduction in the frequency of contractions (Figure 15b). As for the posterior GI region of the 7dpf co – injected larvae, the GI motility seemed to be affected by a reduction in the total number of contractions and a decrease in frequency and interval of each contraction (Figure 16a).

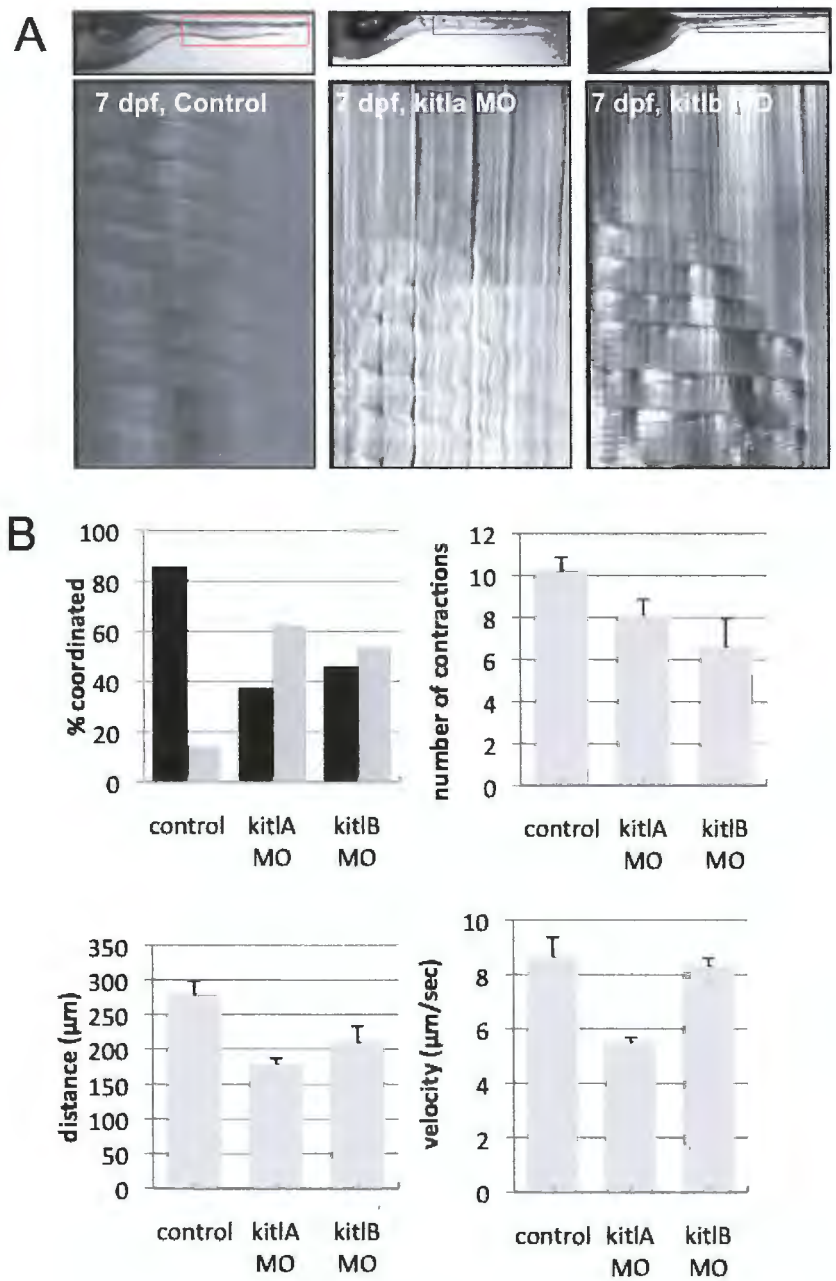

Figure 12. Development of coordinated GI motor patterns is inhibited with *kitla* and *kitlb* MO knockdown. A. STMaps show that *kitla* and *kitlb* MO injected embryos display aberrant GI motor patterns when compared to controls. B. Black bars indicate coordinated contractions, grey bars uncoordinated. *kitla* or *kitlb* MO injection reduced the reduced coordination and the number of contractions. *kitla* or *kitlb* MO injection reduced contraction distance, and *kitla* only reduced contraction velocity. •Sattora, J. (2009). Analysis of kit ligand a.

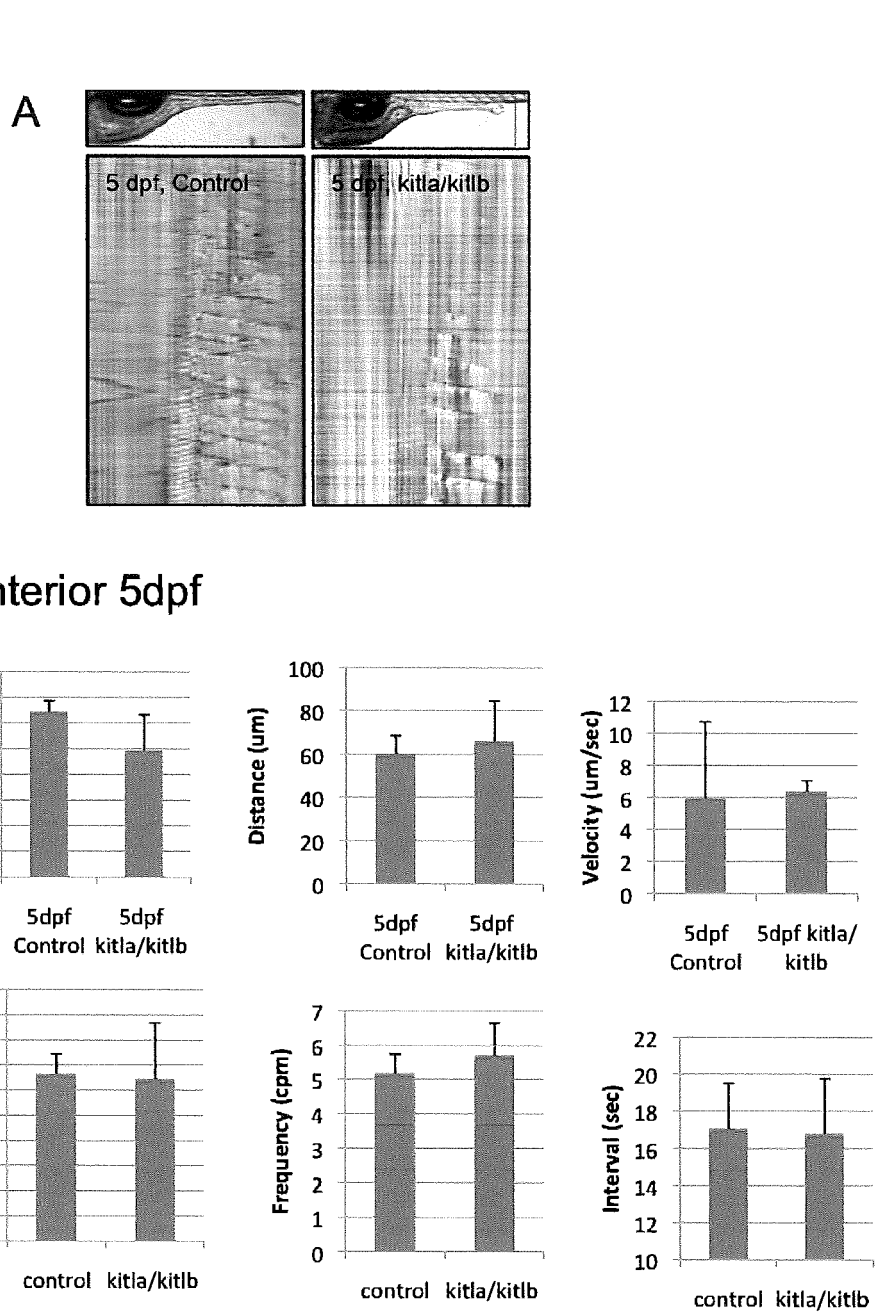

Figure 13. Development of coordinated GI motor patterns appear to be inhibited in the anterior GI region of 5dpf larvae co – injectioned with *kitla / kitlb* MO. A. STMaps show that co – injectioned *kitla / kitlb* MO larvae display aberrant GI motor patterns when compared to controls in the anterior (left hand side) region of the GI tract. B. Co – injected *kitla / kitlb* larvae show reduction in total number of contractions and interval between contractions.

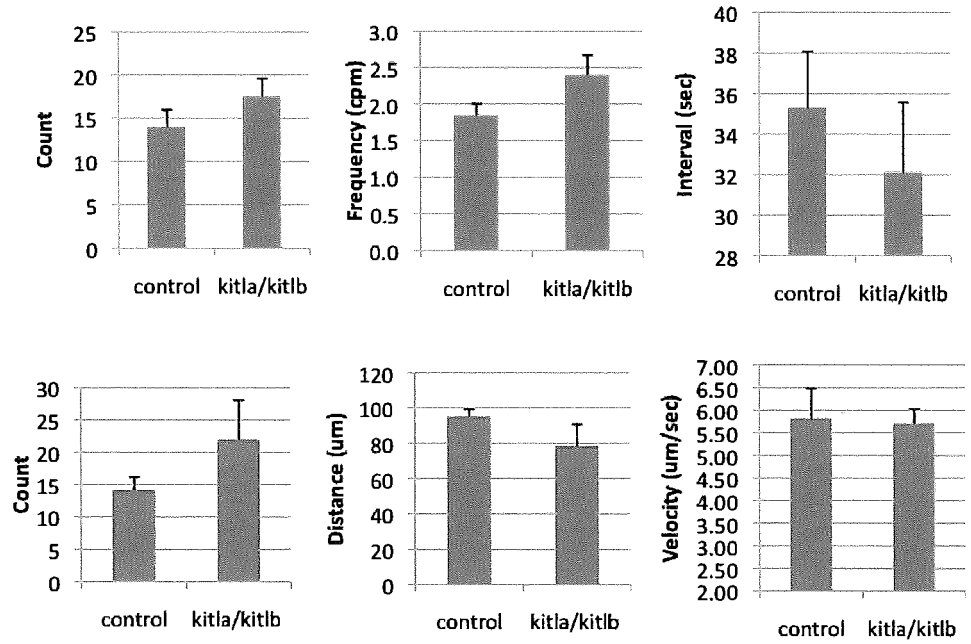

Figure 14. Development of coordinated GI motor patterns appears to be inhibited in the posterior GI region of 5dpf larvae by co - *kitla / kitlb* MO knockdown (STMaps, shown in Figure 13, posterior region corresponds to the right hand side). Co – injected *kitla / kitlb* larvae showed reduced contraction interval, distance and velocity.

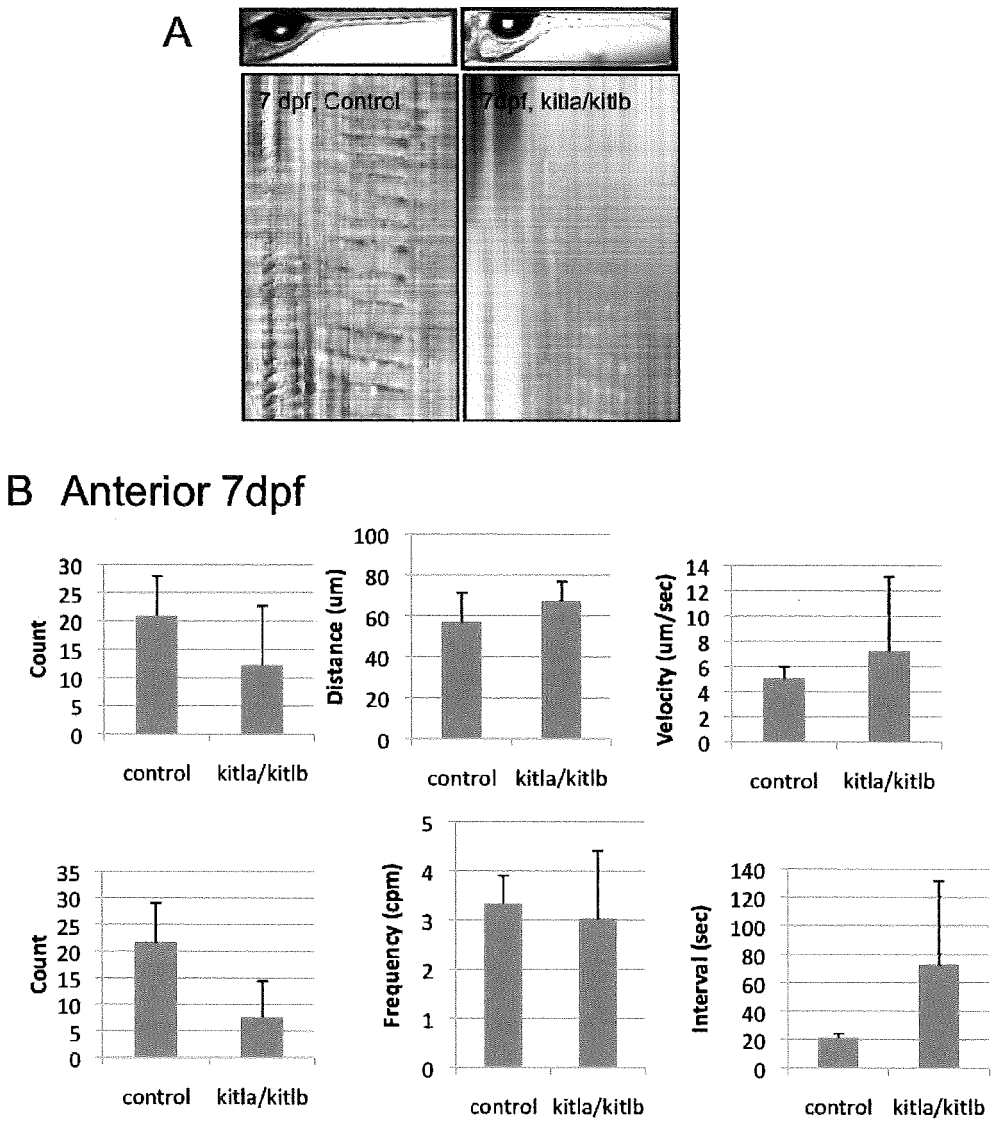

Figure 15. Development of coordinated GI motor patterns appears to be inhibited at 7dpf in the anterior region of co-injected *kitla / kitlb* M0. A. STMaps show that co – injected *kitla / kitlb* MO larvae display aberrant GI motor patterns when compared to controls. B. *Kitla / kitlb* co – injected larvae have fewer contractions and reduced contraction frequency.

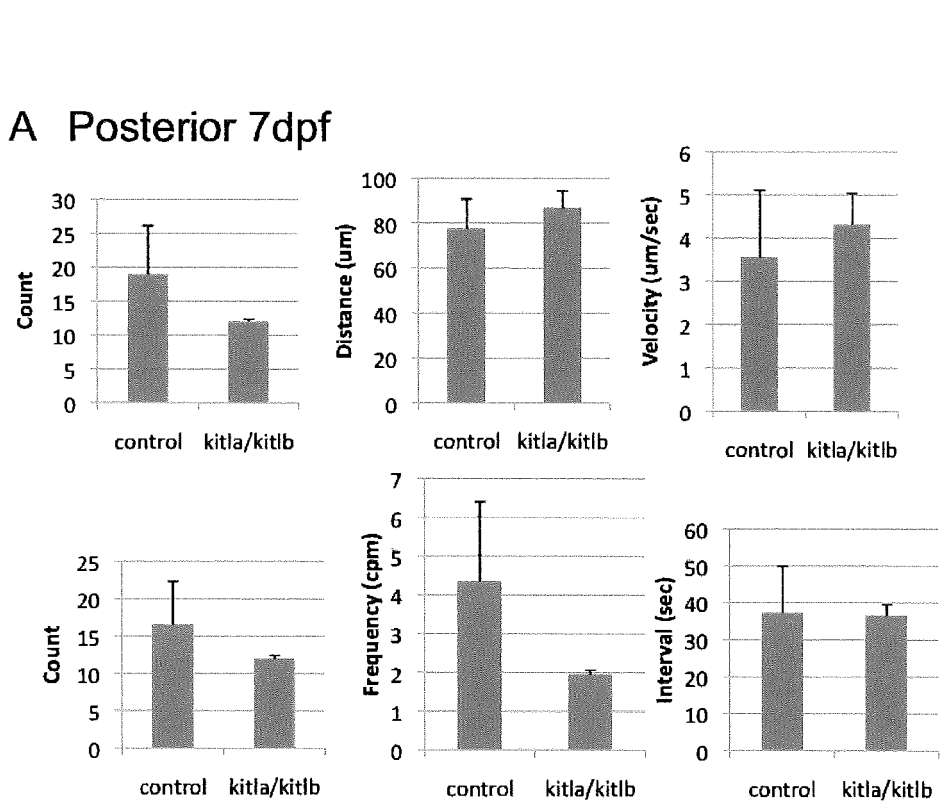

Figure 16. Development of coordinated GI motor patterns appears to be inhibited in the posterior GI region of 7dpf larvae by co – *kitla / kitlb* MO knockdown (STMaps, shown in Figure 15, posterior region corresponds to the right hand side). Co – injected *kitla / kitlb* larvae showed reduced number of contractions and reduced contraction frequency and interval.

Motility Index (MI) is qualitative analysis that was developed to quickly assess coordinated or uncoordinated GI motility patterns utilizing STMaps. This form of analysis scores GI motility as 1 (coordinated) or 0 (uncoordinated) by analyzing the contractions that appears on the STMaps. STMaps receiving a score of 1 have shown propagating contractions moving in the mouth to colon direction for at least 75% of the contractions with no more than one irregular / skipped contraction.

It was anticipated that control zebrafish would have fully developed GI tracts and therefore have propagating contractions moving in the anterograde

directions about 75% of the time since this is what is reported in humans. Results have indicated that the MI of 7dpf *kitlb* MO injected larvae had a reduced number of contractions compared to their age – matched controls (Figure 17).

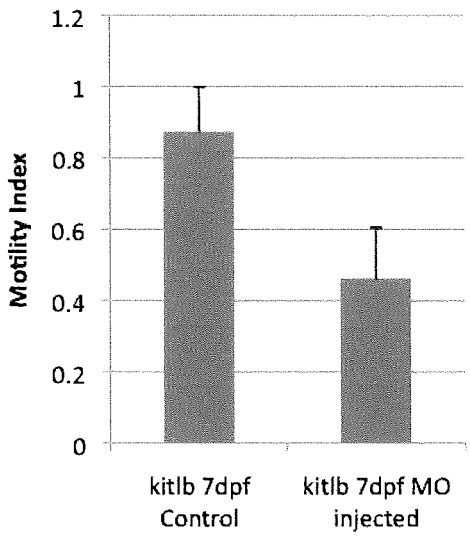

Figure 17. Motility Index of 7dpf *kitlb* injected larvae. MO injection reduced the number of STMaps with a normal motility index compared to control 7dpf larvae.

Experiments involving the co – *kitla / kitlb* MO injected larvae showed reduced MI of the anterior GI region of 7dpf co – injected larvae compared to control larvae (Figure 18a and Figure 18c). MI of the posterior GI region in 5dpf experimental larvae and control larvae remained the same (Figure 18b). And the MI in the posterior GI region of *kitla / kitlb* injected larvae was greater than the control (Figure 18d).

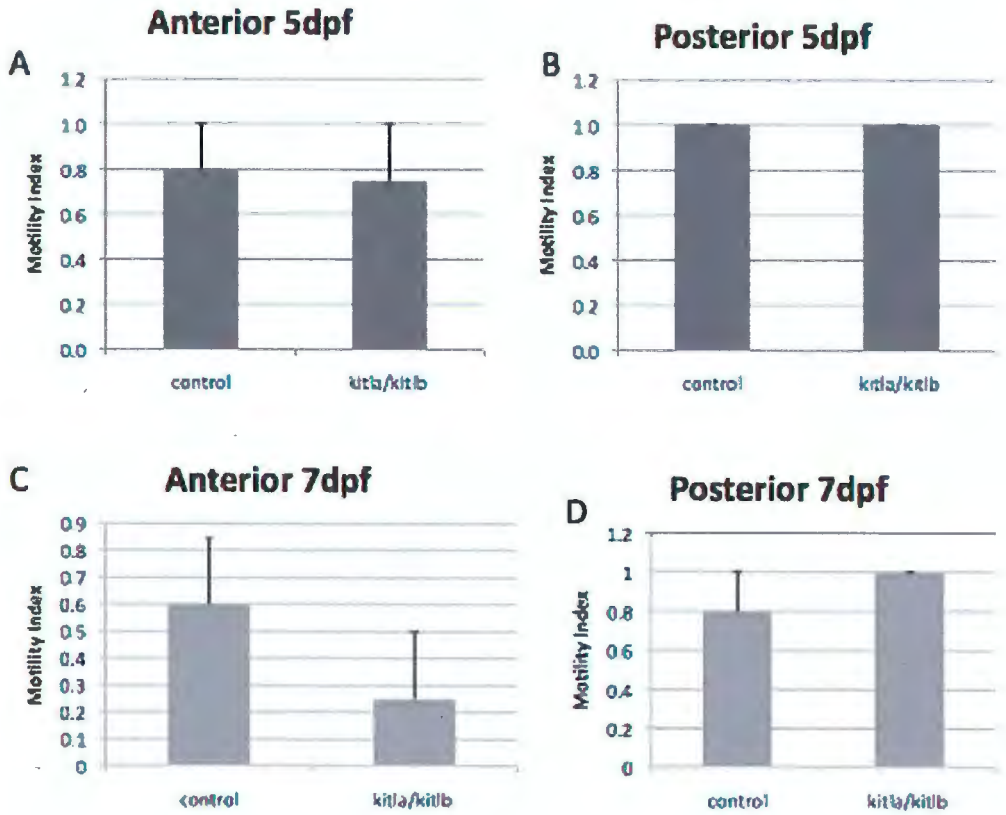

Figure 18. Motility Index (MI) of co – injected *kitla / kitlb* 5dpf and 7dpf MO injected larvae. *Kitla / kitlb* MO injection reduced the number of STMaps with a normal motility index compared to control in 5dpf and 7dpf anterior GI region (A) and (C). Motility Index appears the same in the 5dpf MO *kitla / kitlb* injected posterior GI region and 5dpf control larvae (B). 7dpf MO *kitla / kitlb* injected posterior GI region had greater Motility Index compared to 7dpf posterior region of control larvae (D).

Discussion

Experiments were performed to test the hypothesis that Kit - *kit ligand b* signaling plays a significant role in the maturation and development of interstitial cells of Cajal (ICC) in the zebrafish model system. Activation of Kit receptor by Kit Ligand is crucial for the growth and development of ICC in humans and in mice (Hirst & Edwards, 2004). In combination with smooth muscle cells and enteric neurons, ICC play a key role in the regulation of GI motility, or the complex muscular contractions of the GI tract. More specifically, ICC are involved with regulation and orchestration of the smooth muscle contractions leading to the mechanical processing of food, peristalsis and waste excretion (Izbeki, et al., 2010). Pathophysiological disturbances in motility, such as constipation and irritable bowel syndrome, are associated with a decreased density of ICC (Ward & Sanders, 2001) (Izbeki, et al., 2010)

Recently, work has been completed showing gastric dysfunction in progenic mice, deficient in the anti-aging peptide Klotho. Klotho (KL) is a protein associated with premature ageing. KL expression declines with age in mice, rats and monkeys, while in humans, the variation of the gene or allele of the gene affects life span. Mice deficient in KL present the pre-mature ageing phenotype, while mice over expressing the protein live 20 – 30% longer than their wildtype litter mates (Kurosu et al 2005). Cryosectioning revealed expression of KL in the mouse stomach. ICC density dramatically declined when expression of KL was decreased. These findings are consistent with the phenotype of gastric human

ageing, which includes changes in the GI tract such as increased gastroesphophageal reflux, silent aspiration, irritable bowel syndrome or constipation. These conditions suggest that weakened slow wave activity presented in elderly human subjects 85 years or older is a result of ICC loss. The decreased density of ICC in ageing humans is similar to the decreased density in KL deficient mice. This infers that ICC loss may reduce the ability of the GI tract to accurately adapt to various homeostatic challenges like gas, bloating or abdominal pain (Izbeki, et al., 2010).

This thesis project examined the role of *kitlb* on the development and maturation of ICC and its effect on gastrointestinal motility using morpholino oligonucleotide knockdown. Results presented here show that MO knockdown of *Kitlb* did not alter GI motility. Count, frequency, interval, distance, velocity and motility index were measured and no change was measured. These experiments suggest that knockdown of *Kitlb* has no significant affect of the development and maturation of ICC in the zebrafish GI tract.

These results are not consistent with previous work done with Steel Dickie mutant mice. Steel Dickie mice lack the membrane bound form of Kit ligand and exhibit distended small intestines. This is similar to W/W^v mutant mice, which lack functional Kit receptors preventing Kit signaling and have diminished ICC networks (Maeda, et al., 1992). Steel Dickie mutant mice have impaired networks of ICC as well as decreased ICC density in the myenteric plexus region. It has been established that membrane bound Kit ligand is

essential for the development and maintenance of ICC networks located in the myenteric plexus in mice (Maeda, et al., 1992). A decreased density of ICC in the myenteric plexus region are correlated with unorganized, uncoordinated and arrhythmic motility patterns (Broudy, 1997).

The zebrafish expresses two orthologues for mammalian *KIT*, *kitla* and *kitlb*, Experiments performed for this thesis used an MO to knock down the expression of *kitlb*. It is possible that knocking down *kitlb* expression may have resulted in an increased expression of *kitla*. Increased expression of *kitla* may minimize the effects of gene knockdown resulting in a less server phenotype. With this possibility in mind future experiments are planned that will co – inject *kitla* and *kitlb* MO. In addition, iut will be important to assess MO efficacy using reverse transcriptase PCR to determine if the MO results in alternative splicing, and quantitative PCR to measure MO efficacy. Preliminary experiments co injecting *kitla* and *kitlb* MO did not inhibit development of coordinated motility patterns. The simplest interpretation of these results is that ICC development in the zebrafish GI tract differs from mammalian development. Compound heterozygous mice mutant W/W^{v} and $S/Sl^{d.}$ and showed that reduction in the tyrosine kinase activity due to the partial loss of function of KIT signaling slowed or eliminated development of ICC and resulted in uncoordinated motility patterns (Sanders & Ward, 2006). Smooth muscle cells and enteric neurons, the other two components of the intestinal triad, did not appear to have any developmental disruption (Sanders & Ward, 2006). Membrane bound kit ligand

was also shown to be a potent stimulator of ICC development in primary cultures from adult mouse GI tissue (Rich, et al., 2007). Soluble kit ligand did not compensate or substitute for membrane bound kit ligand in primary cultures, suggesting that membrane bound kit ligand is required for ICC development in mature tissues (Rich, et al., 2007). The possibility remains that requirements for soluble and/or membrane bound kit ligand differs during early development,

It is possible that there is so much variability in zebrafish GI motility that it may be impossible to show the effects of motility when lesioning just one part of the intestinal triad. For example, enteric neurons and smooth muscle cells could possibly compensate for deficits in ICC leaving the end result of motility to appear nearly "normal". GI motility is phasic and is controlled by overlapping regulatory mechanisms including ICC, enteric neurons, the autonomic nervous system, the endocrine system, and even circadian rhythms, GI motility is required to maintain life, indicating the importance of a physiological system that can compensate for disturbances. A system with overlapping regulatory mechanisms may not be efficient in the short term but may provide an evolutionary advantage for an organism. Further development of the zebrafish model for GI motility is required and an assay that enabled measurement of ICC density directly, and a method to challenge the system to demonstrate a clear effect are desirable.

Variability in zebrafish GI motility requires experiments designed to produce quantifiable results while eliminating outside variables. MOs effectively

target specific mRNA resulting in the disruption of the translated protein. However, the efficacy of a MO is reduced over time and therefore it is extremely difficult to measure physiological processes that develop slowly. One way to eliminate this problem is to genetically modify zebrafish with inducible promoters on the genes of interest. The inducible promoters enable gene knockdown and better target inhibition of protein expression throughout the entire developmental period being examined and thus eliminate a major experimental flaw of morpholinos. Inducible promoters also allow the modulation of gene transcription. By modulating and measuring the levels of transcription and subsequent protein levels of *kitlb*, it can be better determined how much protein is necessary to maintain a normal GI motility phenotype during developmental periods.

The tyrosine kinase receptors *kita* and *kitb* are activated by their ligands, *kitla* and *kitlb* but the specificity for ligand-receptor interactions is unknown. We anticipate that maintenance and development of ICC in the zebrafish requires stimulation of both *kita* and *kitb* by both *kitla* and *kitlb*. It would be expected that the knockdown of *kitla* or *kitlb* through morpholino injections would result in lower *kita* and *kitb* signaling levels leading to reduced ICC density. However, cellular signaling pathways are made up of a highly complex network of signaling molecules, receptors, secondary messengers, and transcription factors that may act in a redundant manner. If this is the case, it is possible that another signaling molecule may be rescuing expression of *kitlb*

either through direct stimulation of the receptor itself or through secondary activation of its signaling cascade. To explore this possibility further, an assay measuring the transcription products of *kitla* and *kitlb*, as well as an assay calculating total number of ICC and their concentration should be developed and performed on experimental and control larvae. This would allow a better quantitative measurement of *kitla* and *kitlb* knockdown ensuing a more definitive explanation of the role *kitla* and *kitlb* play on GI motility.

Works Cited

Bill, B., Petzold, A., Clark, K., Schimmenti, L., & Ekker, S. (2009 йил November). A Primer for Morpholino Use in Zebrafish. *Zebrafish, 6*(1), 69-77.

Brand, M., Granato, M., Nusslein-Volhard, & Christiane. (2002). Keeping and raising zebrafish. *Zebrafish*, 1-37.

Brand, M., Granato, M., Nusslein-Volhard, & Christiane. (2002). *Zebrafish.* Tubingen.

Broudy, V. (1997). Stem cell factor and hematopoiesis. *Blood*, 1345-1364.

Chen, H., Ordog, T., Chen, J., Young, D. L., Bardsley, M. R., Redelman, D., . . . Sanders, K. M. (2007). Differential gene expression in functional classes of interstitial cells of Cajal in murine small intestine. *Physiol Genomics*, 492-509.

Corey, D. R., & Abrams, J. M. (2001). Morpholino antisense oligonucleotides: tool for investingating vertebrate development. *Genome Biology*, 1015.1 - 1015.3.

Giebel, L., & Spritz, R. (1991). Mutation of the KIT (mast/stem cell growth factor receptor) protooncogene in human piebaldism. *PNAS*, 8696-8699.

GIST Support International- What is GIST? (2011 йил 30-08). Retrieved 2012 йил 30-04 from GIST Support International: www.gistsupport.org/about-gist/what-is-gist.php

Gomez-Pinilla, P. J., Gibbons, S. J., Bardsley, M. R., Lorincz, A., Pozo, M. J., Pasricha, P. J., . . . Farrugia, G. (2009). Ano1 is a selective marker of interstitial cells of Cajal in the human and mouse gastrointestional tract. *J Physiol Gastrointest Liver Physiol*, G1370-G1381.

Hirst, G., & Edwards, F. (2004). Role of Interstitial Cells of Cajal in the Control of Gastric Motility. *Journal of Pharacological Sciences*, 1-10.

Holberg, A., Schwerte, T., Pelster, B., & Holmgren, S. (2004). Ontogeny of the gut motility control system in zebrafish Danio rerio embyros and larave. *The Journal of Experimental Biology*, 4085-4094.

Huang, E. J., Nocka, K. H., Buck, J., & Besmer, P. (1992). Differential Expression and Processing of Two Cell Associated Forms of the Kit-Ligand: KL-1 and KL-2. 349-362.

Huizinga, J. D., Thuneberg, L., kluppel, M. M., Mikkelsen, H. B., & Berstein, A. (1995). W. kit gene required for interstitial cells of Cajal and for intestinal pacemaker activity. *Letters To Nature*, 347-349.

Hultman, K., Bahary, N., Zon, L., & Johnson, S. (2007 йил January). Gene Duplication of the Zebrafish kit ligand and Partitioning of Melanocyte Development Functions to kit ligand a. *PLOS Genetics, 3*(1), 0089-0102.

Hwang, S. J., Blair, P. J., Britton, F. C., O'Driscoll, K. E., Grant, H., Bayguinov, Y. R., . . . Ward, S. M. (2009). Expression of anoctamin 1/ TMEM16A by interstital

cells of Cajal in fundamental for slow wave activity in gastrointestinal muscles. *J Physiology*, 4887-4904.

Hwang, S. J., Blair, P. J., Britton, F. C., O'Driscoll, K. E., Hennig, G., Bayguinov, Y. R., . . . Ward, S. M. (2009). Expression of anoctamin 1/TMEM16A by interstitial cells of Cajal is fundamental for slow wave activity in gastrointestinal muscles. 4887-4904.

Izbeki, F., Asuzu, D. T., Lorincz, A., Bardsley, M. R., Popko, L. N., Choi, K. M., . . . Orgod, T. (2010). Loss of Kit Low progenitors, reduced stem cell factor and high oxidative stress underlie gastric dysfunction in progeric mice. *J Physiol*, 3101-3117.

Kluppel, M., Huizinga, J. D., Malysz, J., & Berstein, A. (1998). Developmental Origin and Kit-Dependent Development of the Interstital Cells of Cajal in the Mammalian Small Intestine. *Developmental Dynamics*, 60-71.

Kluppel, M., Huizinga, J. D., Malysz, J., & Berstein, A. (1998). Developmental Origin and Kit-Dependent Development of the Interstitial Cells of Cajal in the Mammalian Small Intestine. *Developmental Dynamics*, 60-71.

Linnekin, D. (1999). Early signaling pathways activated by c-kit in hematopoietic cells. *The international Journal of Biochemistry & Cell Biology*, 1053-1074.

Linnekin, D. (1999). Review: Early signaling pathways activated by c-Kit in hematopoietic cells. *The International Journal of Biochemistry & Cell Biology*, 1053-1074.

Longley, B. J., Reguera, M. J., & Ma, Y. (2001). Classes of c-KIT activating mutations: proposed mechanisms of action and implications of disease classification and therapy. *Leukemia Research*, 571-576.

Maeda, H., Yamagata, A., Nishikawa, S., Yoshinaga, K., Kobayashi, S., Nishi, K., & Nishikawa, S.-I. (1992). Requirement of c-kit for development of intestional pacemaker system. *Development*, 369-375.

Mouton, J. D., & Jiang, S. (2009). Gene Knockdowns in Adult Animals: PPMOs and Vivo-Morpholinos. *Molecules*, 1304-1323.

Nagata, H., Worobec, A. S., Oh, C. K., Chowdhury, B. A., Tannenbaum, S., Suzuki, Y., & Metcalfe, D. D. (1995). Identification of a point mutation in the catalytic domain of the protooncogene c-kit in peripheral blood mononuclear cells of patients who have mastocytosis with an associated hematologic disorder. *Medical Sciences*, 10560-10564.

Ordog, T., Takayama, I., Cheung, W., Ward, S., & Sanders, K. (2000 йил October). Remodeling of Networks of Interstitial Cells of Cajal in a Murine Model of Diabetic Gastroparesis. *Diabetes, 49*, 1731-1739.

Parichy, D. M., Elizondo, M. R., Mills, M. G., Gordon, T., & Engeszer, R. (2009). Normal Table of Post-Embryonic Zebrfiah Development Staging by Externally Visible Anatomy of the Living Fish. *Developmental Dynamics*, 2975-3015.

Petzold, A. M., Bedell, V. M., Boczek, N. J., Essner, J. J., Balciunas, D., Clark, K. J., & Ekker, S. C. (2010). SCORE Imagine: Specimen in a Corrected OPtical Rotational Enclosure. *Zebrafish*, 149-154.

Rich, A., Leddon, S., Hess, S., Gibbons, S., Miller, S., Xu, X., & Farrugai, G. (2007). Kit-Like Immunoreactivity in the Zebrafish Gastrointestional Tract Reveals Putative ICC. *Developmental Dynamics*, 903-911.

Rich, A., Miller, S., Gibbons, S., Malysz, J., Szurszewski, J., & Farrugia, G. (2003 йил February). Local presentation of Steel factor increases expression of c-kit immunoreactive interstital cells of Cajal in culture. *AJP-Gastrointest Liver Physiol, 284*, G313-.

Sanders, K. M., & Ward, S. M. (2006). Interstitial cells of Cajal: a new perspective on smooth muscle function. *J Physiol*, 721-726.

Sanders, K. M., & Ward, S. M. (2006). Kit Mutants and Gastrointestinal Physiology. *Journal of Physiology Special Issue*, 1-36.

Sanders, K., & Ward, S. (2006). Interstitial cells of Cajal: a new perspective on smooth muscle function. *J Physiol*, 721-726.

Sanders, K., & Ward, S. (2006). Kit mutant and gastrointestinal physiology. *J Physiol*, 33-42.

Scherzer, N. J. (2007 йил April). Scherzer Editorial: companies need patent protection to help with future drug development. *Life Raft Group*, pp. 1-12.

Shen, L. (2009). Functional morphology of the gastrointestinal tract. *Current Topics of Microbiology and Immunology*, 1-35.

Stone, K. D., Prussin, C., & Metcalfe, D. D. (2011). IgE, Mast Cells, Basophils, and Eosinophils. *J Allergy Clin Immunol.*

Streutker, C., Huizinga, J., Driman, D., & Riddell, R. (2007). Interstitial cells of Cajal in health and disease. Part 1: Normal ICC structure and function associated with motility disorders. *Histopathology*, 176-189.

Taniguchi, M., Nishida, T., Hirota, S., Isozaki, K., Ito, T., Nomura, T., . . . Kitamura, Y. (1999). Effect of c-kit Mutation on Prognosis of Gastrointertinal Stromal Tumors. *Cancer Research*, 4297-4300.

Twyman, R. (2002 йил 28-August). *The Human Genome.* Retrieved 2012 йил 28-February from Wellcome trust: http://genome.wellcome.ac.uk/doc_WTD020804.html

Twyman, R. (2002 йил 29-August). *The Human Genome.* Retrieved 2012 йил 28-February from Wellcome trust: http://genome.wellcome.ac.uk/doc_wtd020806.html

Wallace, K. N., Akhter, S., Smith, E. M., Lorent, K., & Pack, M. (2005). Intestinal growth and differentiation in zebrafish. *Elsevier*, 157-173.

Ward, S. M., & Sanders, K. M. (2001). Phsiology and Pathophysiology of the Interstital Cell of Cajal: From Bench to Bedisde I. Functional development and plasticity of interstitial cells of Cajal networks. *Am J Physiol Gastrointest Liver Physiol*, G602-G611.

Ward, S. M., Burns, A. J., Torihashi, S., & Sanders, K. M. (1994). Mutation of the proto-oncogene c-kit blocks development of interstitial cells and electrical rhythmicity in murine intestine. *Journal of Physiology*, 91-97.

Yang, Y. D., Cho, H., Yeon, K. J., Tak, M. H., Cho, Y., Shim, W.-S. S., . . . Oh, U. (2008). TMEM16A confers receptor-activated calcium-dependent chloride conductance. 1210-1215.

Yee, N. S., Langen, H., & Besmer, P. (1993). Mechanism of kit Ligand, Phorbol Ester, and Calcium-induced Down-regulation of c-kit Receptors in Mast Cells. *Journal of Biological Chemistry*, 14189-14201.

Zhu, M. H., Kim, T. W., Ro, S., Yan, W., Ward, S. M., Koh, S. D., & Sanders, K. M. (2009). A Ca2+ activated Cl- conductance in interstitial cells of Cajal linked to slow wave currents and pacemaker activity. *The Journal of Physiology*, 4905-4918.

Appendix

Breeding Zebrafish:

Note: Zebrafish reach sexual maturity at 3 months of age however, optimal results are seen with zebrafish that are crossed between 7 and 18 months of age.

1. The day prior to breeding zebrafish should be fed live food (Preferably more than 1X daily).
2. Crosses need to be set up early in the morning, as soon as the lights turn on in the fish room (this simulates dawn).
3. A ratio of 2 Males: 3 Females are places in breeding boxes filled with system water.
    a. Males appear more slender, torpedo shaped with little white on abdomen.
    b. Females appear more round, with much more white on abdomen.
4. Leave fish room for 20-30 minutes.
5. After this time check from embryos on the bottom of the breeder box.
6. Return adults to designated tanks on system rack.
7. Filter system water in breeder boxes through fine grade filter.
8. Embryos will be collected on filter.
9. Rinse embryos off filter into petri dish with E3.
10. Label petri dish with:
    a. Parent line
    b. Current date
    c. Initials (personal identification)
11. Bring petri dishes containing embryos back to lab.
12. Divide larvae into 25 embryos per petri dish.
13. Using transfer pipette siphon off dirty E2.
14. Fill petri dish ½ full with clean E2.
15. Count total number of embryos, keep ongoing log of embryo viability for each petri dish.
    a. Log should include:
        i. Day post fertilization.
        ii. Embryo/Larvae line.
        iii. Experiment.
        iv. Total number living.
16. Place petri dish in the incubator held at ≈ 28°C.

Larvae Care / Larvae Counting:

Note: Zebrafish embryos / larvae need to be cared for daily.

1. Developing zebrafish embryos / larvae need to be maintained in fresh E2 for 7 days at ≈ 28°C.
2. Using a transfer pipette siphon off as much dirty / day old E2 from petri dish (Be careful not to siphon up embryos / larvae).
3. Disguard dirty /day old E2 in waste container.
4. Refill petri dish ½ way with new E2.
5. Scan embryos/larvae for viability and health.
6. Disguard any embryos / larvae that are dead or unhealthy.
7. Count total number of embryos / larvae viability and add to ongoing fish log.

Recipes:

Egg Water

1. **Stock Solution** (20X E2) in 1L Type 1 Water (Autoclaved)
    i. 17.5g NaCl
    ii. 0.75g KCL
    iii. 2.4g $MgSO_4$
    iv. 0.41g KH_2PO_4
    v. 0.12g Na_2HPO_4
    b. 7.25g $CaCl_2$ in 100mL Type 1 Water (Autoclaved)
    c. 3g $NAHCO_3$ in 100mL Type 1 Water (Autoclaved)

2. **Working Solution** (1X E2)
    a. Mix 50mL of 20X E2 stock, 2mL CaCl2 and 2mL NaHCO3
    b. Bring to 1L volume using Di-ionized Water

50X TAE Buffer:

1. 242g Tris base (Molecular weight: 121.1).
2. 57.1mL glacial acetic acid.
3. 18.6g EDTA (disodium salt) (Molecular weight: 372.24).
4. Add all components to ≈900mL di-H_2O.
5. pH to 8.3 with Tris base or glacial acetic acid.
6. Bring to 1L volume with di-H_2O.

1X TAE Buffer:

1. Add 20mL of 50X TAE to 980mL of di-H_2O.
2. pH to 8.3 with Tris base or glacial acetic acid.

2.0% Agarose Gel:

1. 60mL of 1X TAE Buffer.
2. 1.2g agarose.

3. 6μL Ethidium bromide.
4. Combine all ingredients into 250mL Erlenmeyer flask.
5. Heat in microwave until agarose is dissolved (make sure it does not boil over).
6. Pour into gel mold and place comb into gel.
7. Allow gel to set for 30 minutes at room temperature.
8. Remove comb from gel when gel is almost fully set.
9. Remove gel from mold after 30 minutes and place in electrophoresis chamber containing 1X TAE Buffer.

25X MESAB (anesthestizing):

1. 400mg Trican powder.
2. 97.9mL di-H_2O.
3. ≈ 2.1mL Tris (1M, pH 9).
4. pH to 7.
5. Store in freezer.

.75% MESAB

1. 0.3mL 25X MESAB
2. 9.7mL E2

0.9% Agar:

1. 1.2mL 25X MESAB
2. .36g Agar
3. Bring to 40mL total Volume with E2

Pulling of Micropipette:

1. Open Nitrogen tank.
2. Turn on Flaming Brown micropipette puller
3. Select program 1:
    a. Heat – 750
    b. Pull – 190
    c. Velocity – 170
    d. Time – 170
4. Center a 10cm electrode (Borosilicate glass with filament) over heating filament.
5. Secure electrode by turning metal jaw clips.
6. Press pull.
7. Spring-loaded clamp will retract when electrode has been pulled.
8. Loosen metal jaw clips.
9. Place freshly pulled electrode in pipette storage box.

Note: It is important to wait a minute in between the pulling micropipettes so that the heating filament has time to cool and does not collapse.

Cutting Micropipette for injections:

1. Select one micropipette from pipette storage box.
2. Place on stage of dissecting microscope.
3. Focus microscope.
4. Using a new razor blade cut the tip of the micropipette at the point where the micropipette has a hollow center (the smaller the opening the better!).
5. Handle freshly cut micropipette carefully, it is easy to break!

Loading Micropipette for injection:

1. Select morpholino that will be used.
2. Vortex morpholino.
3. Using a p20 with a 20μL microloader elongated pipette tip, transfer 3μL of morpholino into tip of freshly pulled micropipette.

Attaching Micropipette into Pressure Injector:

1. Turn on Nitrogen tank.
2. Turn Pressure Injector on.
3. Secure morpholino-loaded micropipette into micromanipulator attached to pressure injector.
4. Manually controlling micromanipulator, bring the apparatus into focus under the dissecting microscope.
5. Move micromanipulator close to petri dish containing embryos and some E2.
6. Carefully manipulate micropipette so that it barely pierces the E2.
7. Tap foot needle while looking through eyepiece of microscope.
8. Look for small bolus of morpholino present in E2, if present the micropipette is working properly!
9. Set aside carefully while prepping embryos for injection.

Prepping and Injection of Embryos:

1. Using a new petri dish and clean glass slide, place glass slide into petri dish as far left as possible, secure with piece of masking tape.
2. Using a transfer pipette draw up at least 10 embryos from the petri dish containing all embryos.
3. Dispense embryos in a line on the right side of glass slide in the clean petri dish.
4. Siphon off most of the E2 surrounding the embryos (If too much E2 surround embryos they move around too much while injecting).

5. Place petri dish containing embryos on stage of dissecting microscope and bring into focus.
6. Pick up micromanipulator containing loaded micropipette and without looking though eyepiece bring micropipette as close to the line of embryos as possible.
7. Now, looking through microscope move micropipette so that it is gently touching chorion of one embryo.
8. Once touching, add pressure and with one smooth motion push micropipette through chorion and into yolk behind dividing cells of embryo (CAREFUL not to pierce through diving cells!!)
9. Tap on foot pedal to release morpholino into yolk, until bolus is an estimated 3nL in volume.
10. Draw micropipette out of yolk and chorion and move to the next embryo.
11. Repeat steps 7-10.
12. Once all embryos are injected, gently set down micromanipulator containing micropipette.
13. Obtain a new/clean petri dish.
14. Label petri dish with:
    a. Parent line
    b. Morpholino
    c. Current date
    d. Initials
15. Fill petri dish ½ full with E2.
16. Siphon up injected embryos and release into new petri dish.
17. Place petri dish in the incubator maintained at ≈ 28°C.

Primer Sequences

Name	Sequence (5' – 3')	Accession Number
Beta – actin Forward	ACCTGCTCACCTCTTTTTGG	52150966
Beta- actin Reverse	CATTCTGTCCTCCAGGTCGT	52150967
kitlb Forward	CCCTTGACTTTGAGCACCAG	46418578
kitlb Reverse	ATGCCAATGTTGTCGTTTGA	46418579

Mounting Agar

1. Stock solution of 0.9% agar:
    a. 1.2mL 25X MESAB
    b. .36g Agar
    c. Bring to 40mL total volume with E2
2. Dissolved completely in the microwave (careful to not to boil over).
3. 40mL of agar divided into 15mL conical tubes.
4. Labeled and dated conical tubes can be placed in refrigerator for future use.
5. Agar stored in refrigerator must be warmed before use.
6. Heat refrigerated agar for 10 seconds in microwave with loosened cap. Stirred with transfer pipette. Repeated until agar is fluid.
7. Fluid agar should be placed in a warm water bath at $\approx 42°C$.
8. Fluorinated ethylene propylene (FEP) tubing should be cut (estimate 2" in length) at an angle with razor blade.
9. Place FEP tube and glass slides in beaker of di-H_20, then placed in the water bath ($\approx 42°C$).
10. Place 7pdf larvae in .75% MESAB for about 30 seconds.
11. Removed glass slide from water bath, dry completely.
12. Siphoned larvae up in transfer pipette with as little MESAB as possible, placed into 0.9% agar.
13. Draw up larvae and some agar in transfer pipette.
14. Release larvae and agar onto glass slide.
15. Moving quickly, remove FEP tube from the water bath and placed on the end of a pipette pump.
16. Siphoned larvae and some agar into FEP tube.
17. Place FEP tube containing larvae in homemade foam slide on microscope stage.
18. Adjust tube manually for lateral orientation of the larvae.
19. Surround FEP tube with about 1mL of di- H_20.
20. Imaging larvae.
21. Once imaging complete removed larvae from the FEP tube.
22. Remove larvae from tube by cutting tube at an angle as close to the anterior region of the larvae as possible (Careful not to cut into the larvae).
23. Then with a pair of tweezers squeeze just below the posterior end of the larvae. Place larvae 30μL of RNAlater.
24. Stored larvae in RNAlater (for cDNA synthesis).

RNA Isolation (Qiagen Kit)

1. Zebrafish larvae are placed in 30μL of RNA*later* and stored at room temperature for up to 7 days or in the refrigerator for up to 4 weeks.
2. Place larvae sample in mortar tube and grind with pestle.
3. Add 300μL of buffer RTL (with beta mercaptoethanol) to the sample that is already in 30μL of RNA*later*.
4. Using a 20G needle on a 1cc sterile syringe the sample should be sucked up and ejected 5 times, after the fifth time eject the sample onto a Qiagen Shredder column (purple).
5. Spin shredder column for 2 minutes at max speed.
6. Remove the shredder column, and then spin flow through for 3 minutes at max speed.
7. Remove the supernatant from the first tube using a p1000; be careful not to touch the bottom.
8. Transfer the supernatant to a DNA column, a clear tube with a purple band.
9. Spin gDNA column for 30 seconds at max speed.
10. Keep flow through.
11. Add 300μL of 70% EtOH to flow through. Mix with pipette.
12. Place sample on RNeasy column (pink).
13. Spin for 30 seconds at max speed.
14. Discard flow through.
15. Add 600μL of Buffer RW1 to RNeasy column, and then spin at max speed for 30 seconds.
16. Discard flow through.
17. Repeat steps 15 and 16.
18. Spin RNeasy column at max speed for 2 minutes to remove excess ethanol from the column.
19. Put RNeasy column into a new collection tube, add 30μL of nuclease free water to the column and spin at max speed for 1 minute.
20. Place sample on ice immediately.
21. Measure absorption of sample:
    a. Open NanoDrop 2000 program.
    b. Click on nucleic acid.
    c. Click to open previous file.
    d. Make sure the arm of the NanoDrop is down and then click OK for wavelength verification.
    e. Clean NanoDrop 2000, according to cleaning protocol located above instrument.
    f. Add 1μL of nuclease free water to sampling area, click Blank.
    g. Wipe nuclease free water off sampling area with Kimwipe.
    h. Add 1μL of sample to sampling area and then click Measure.

i. Record concentration of sample in ng/μL.

Ingredients	1X
5X Synthesis Buffer	4μL
dNTP Mix	2μL
Oligo dt	1μL
RT Enhancer	1μL
Template (Total RNA)	20ng (See note below)
Verso Enzyme	1μL
Water	Bring to Volume
Total Volume	**20μL**

Synthesis of cDNA:

Note*: **Volume of RNA** (μL RNA)

- 20ng divided by the Concentration of RNA (ng/μL).
  - If possible use 100ng when possible to enhance PCR experiments for low copy number targets

Thermocycler (iScript cDNA synthesis) Protocol:

Cycle Number	Temperature (°C)	Time (Minutes)
1	42	30
2	95	2
3	10	∞

Verification of RNA isolation and cDNA synthesis:

PCR Reaction: (Master Mix (MM) changes according to the experiment. See notes) Use when possible to avoid pippetting errors):

Master Mix	1X
Master Mix	12.5μL
cDNA Template	1μL
Primer (Forward/Reverse)	1μL
Water	10.5μL
Total Volume	**25μL**

1. Mix all components of Master Mix, except the primers.
2. Divide Master Mix into the number of primer sets that are being tested.
3. Add primer (forward/reverse) to designated tubes and mix.
4. Divide the reaction into PCR tube (25μL volume each).
5. Run PCR using the three-step protocol.

Note* MM Advantages: Using a MM will help to troubleshoot and to interpret experiments. It reduces potential for human errors and for pipetting errors. A MM contains all of the 'constant' components in the experiment.

1. When testing one set of primers the MM contains everything *except* the primers. The MM will be created in a separate tube, and then 24 μl aliquots placed into each experimental tube, plus 1 μl primer. Example shows MM created to test one primer set:

Master Mix (MM)	**1X**
Master Mix	12.5μL
Template	1μL
Water	10.5μL

- PCR reaction tube #1: Add 24μL of MM to 1μL primer set.

2. When testing more than one set of primers the MM contains everything *except* the primers. The MM will be created in a separate tube, and then 24 μL of MM is aliquotted out into each experimental tube containing 1μL of one set of primers. Example shows MM created to test 3 primer sets:

Master Mix (MM)	**3X**
Master Mix	37.5μL
Template	3μL
Water	31.5μL

- PCR reaction tube #1: Add 24μL of MM to 1μL primer set one.
- PCR reaction tube #2: Add 24μL of MM to 1μL primer set two.
- PCR reaction tube #3: Add 24μL of MM to 1μL primer set three.

3. When testing a cDNA template with low copy number a larger volume of template is used. The MM will be created in a separate tube containing

everything *except* the cDNA template. Then 23μL of MM is aliquotted out into each sample tube containing 2μL of template. The example shows MM created for one low copy number template.

Master Mix (MM)	**1X**
Master Mix	12.5μL
Primer	1μL
Water	9.5μL

- PCR reaction tube #1: Add 23μL of MM to 2μL template

4. When testing multiple cDNA templates with low copy number a larger volume of template is used. The MM will be created in a separate tube containing everything *except* the cDNA templates. Then 23μL of MM is aliquoted out into each sample tube, plus 2μL of template. The example shows MM that will be used for 3 different templates:

Master Mix (MM)	3X
Master Mix	37.5μL
Primer	3μL
Water	28.5μL

- PCR reaction tube #1: Add 23μL of MM to 2μL template one.
- PCR reaction tube #2: Add 23μL of MM to 2μL template two.
- PCR reaction tube #3: Add 23μL of MM to 2μL template three.

Conventional PCR (3 Step protocol):

95°	4 minutes
95°	30 seconds
54°	30 seconds
72°	1 minute
72°	7 minutes
10°	∞

6. Load sample (Add 5μL of 10X DNA loading dye to each sample if desired, mix well) into 2.0% agarose gel.
7. Run gel at 80mV for 60 minutes.
8. Use Gel Dock to observe gel with ethidum bromide and UV light.

a. Bands at expected size in each lane confirms the quality of cDNA.

Note*: Annealing temperatures may very for different primers. A temperature gradient is used to determine optimum annealing temperature. Lower temperatures will enhance the reaction, but also increase non-specific amplification.

Maintenance of the NanoDrop

Cleaning NanoDrop

The purpose of this procedure is to ensure that the sampling area is clean and free from old samples or debris that would otherwise affect the absorption measurement.

1. Open NanoDrop 2000 program.
2. Place 2μL of 0.5M HCL on the sampling area.
3. Click on the Measure option located in the tool bar.
4. Allow the HCL to sit on sampling area for 2 minutes.
5. Wipe the sampling area clean with a Kimwipe.
6. Place 2μL of H_2O on the sampling area.
7. Click on the Measure option located in the tool bar.
8. Wipe the sampling area clean with a Kimwipe.

The NanoDrop is now ready to be blanked for the sample that is being tested.

Testing the NanoDrop

1. Place 1μL of H_2O on sampling area.
2. Click the Blank option in the tool bar.
3. Wipe the sampling area clean with a Kimwipe.
4. Place 1μL of a DNA Ladder that is dye free on the sampling area.
5. Click the Measure option located in the tool bar.
    a. If an accurate curve and ratio appear on the screen, then the NanoDrop is working. The sampling area can then be wiped clean with a Kimwipe and Blanked for the sample that is being tested.
    b. If an accurate curve and ratio do not appear; Call Fisher Scientific Tech Support at 302-479-7707.
    c. If an accurate curve and ratio do not appear; Call Fisher Scientific Tech Support at 302-479-7707.

5dpf Count / Distance / Velocity

Control

Anterior	Count	Distance	Velocity
May 15 2012 Control 5df 1	27.00	73.86	-12.63
May 15 2012 Control 5df 2	32.00	74.08	-15.58
May 15 2012 Control 5df 3	No Con.		
May 15 2012 Control 5df 4	38.00	44.66	3.55
May 15 2012 Control 5df 5	32.00	48.99	0.82
Mean	**32.25**	**60.40**	**-5.96**
ttest	**0.34**	**0.76**	**0.08**

kitla/kitlb

Anterior	Count	Distance	Velocity
May 15 2012 kitlakitlb 5dpf 1	40.00	48.99	5.18
May 15 2012 kitlakitlb 5dpf 2	21.00	102.58	7.43
May 15 2012 kitlakitlb 5dpf 3	13.00	46.99	6.67
May 15 2012 kitlakitlb 5dpf 4	No Con.		
Mean	**24.67**	**66.19**	**6.42**

5dpf Count / Distance / Velocity

Control

Posterior	Count	Distance	Velocity
May 15 2012 Control 5df 1	18.00	91.94	4.59
May 15 2012 Control 5df 2	13.00	86.05	5.07
May 15 2012 Control 5df 3	8.00	105.16	6.84
May 15 2012 Control 5df 4	19.00	105.37	7.92
May 15 2012 Control 5df 5	13.00	86.87	4.67
Mean	**14.20**	**95.08**	**5.82**
ttest	**0.22**	**0.20**	**0.89**

kitla/kitlb

Posterior	Count	Distance	Velocity
May 15 2012 kitlakitlb 5dpf 1	40.00	48.99	5.18
May 15 2012 kitlakitlb 5dpf 2	15.00	103.35	5.96
May 15 2012 kitlakitlb 5dpf 3	19.00	91.11	6.52
May 15 2012 kitlakitlb 5dpf 4	14.00	71.45	5.15
Mean	**22.00**	**78.72**	**5.70**

5dpf Count / Frequency / Interval

Control

Anterior	Count	Freq (cpm)	Interval(s)
May 15 2012 5dpf control 1	40	6.13	14.45
May 15 2012 5dpf control 2	29	4.60	15.34
May 15 2012 5dpf control 3	No Con.		
May 15 2012 5dpf control 4	40	6.09	14.23
May 15 2012 5dpf control 5	24	3.88	24.33
Mean	**33.25**	**5.18**	**17.09**
ttest	**0.92**	**0.56**	**0.93**

kitla/kitlb

Anterior	Count	Freq (cpm)	Interval(s)
May 15 2012 5dpf kitla/kitlb 1	53	7.08	10.83
May 15 2012 5dpf kitla/kitlb 2	29	3.93	19.72
May 15 2012 5dpf kitla/kitlb 3	15	6.12	19.80
May 15 2012 5dpf kitla/kitlb 4	No Con.		
Mean	**32.33**	**5.71**	**16.78**

5dpf Count / Frequency / Interval

Control

Posterior	Count	Freq (cpm)	Interval(s)
May 15 2012 5dpf control 1	17	1.89	33.12
May 15 2012 5dpf control 2	12	1.72	35.83
May 15 2012 5dpf control 3	8	1.34	45.75
May 15 2012 5dpf control 4	19	2.22	29.74
May 15 2012 5dpf control 5	14	2.09	32.07
Mean	**14**	**1.85**	**35.30**
ttest	**0.26**	**0.10**	**0.49**

kitla/kitlb

Posterior	Count	Freq (cpm)	Interval(s)
May 15 2012 5dpf kitla/kitlb 1	22	2.44	26.09
May 15 2012 5dpf kitla/kitlb 2	17	3.08	31.47
May 15 2012 5dpf kitla/kitlb 3	19	2.30	29.05
May 15 2012 5dpf kitla/kitlb 4	12	1.79	41.92
Mean	**17.5**	**2.40**	**32.13**

7dpf Count / Distance / Velocity

Control

Anterior	Count	Distance	Velocity
May 15 2012 Control 7df 1	No Contraction		
May 15 2012 Control 7df 2	9	71.91	-3.98
May 15 2012 Control 7df 3	41	85.60	-7.70
May 15 2012 Control 7df 4	18	50.05	-4.91
May 15 2012 Control 7df 5	16	21.29	-3.81
Mean	**21**	**57.21**	**-5.10**
ttest	**0.50**	**0.59**	**0.18**

kitla/kitlb

Anterior	Count	Distance	Velocity
May 15 2012 kitlakitlb 7df 1	33	79.32	-8.87
May 15 2012 kitlakitlb 7df 2	2	49.74	10.11
May 15 2012 kitlakitlb 7df 3	No Contraction		
May 15 2012 kitlakitlb 7df 4	2	73.96	7.23
Mean	**12.33**	**67.67**	**2.82**

7dpf Count / Distance / Velocity

Control

Posterior	Count	Distance	Velocity
May 15 2012 Control 7df 1	13	88.44	5.61
May 15 2012 Control 7df 2	11	96.18	3.60
May 15 2012 Control 7df 3	20	85.53	7.34
May 15 2012 Control 7df 4	5	92.38	3.14
May 15 2012 Control 7df 5	46	26.70	-1.85
Mean	**19**	**77.85**	**3.57**
ttest	**0.42**	**0.59**	**0.70**

kitla/kitlb

Posterior	Count	Distance	Velocity
May 15 2012 kitlakitlb 7df 1	13	98.51	2.85
May 15 2012 kitlakitlb 7df 2	11	82.80	5.33
May 15 2012 kitlakitlb 7df 3	12	99.17	5.77
May 15 2012 kitlakitlb 7df 4	12	67.64	3.32
Mean	**12**	**87.03**	**4.32**

7dpf Count / Frequency / Interval

Control

Anterior	Count	Freq (cpm)	Interval(s)
May 15 2012 Control 7df 1	0.00	0.00	
May 15 2012 Control 7df 2	10.00	3.17	21.50
May 15 2012 Control 7df 3	43.00	4.98	13.58
May 15 2012 Control 7df 4	18.00	2.71	23.94
May 15 2012 Control 7df 5	16.00	2.51	27.75
Mean	**17.40**	**2.67**	**21.69**
ttest	**0.25**	**0.79**	**0.35**

kitla/kitlb

Anterior	Count	Freq (cpm)	Interval(s)
May 15 2012 kitlakitlb 7df 1	21.00	4.79	13.62
May 15 2012 kitlakitlb 7df 2	1.00	4.00	15.00
May 15 2012 kitlakitlb 7df 3	0.00	0.00	
May 15 2012 kitlakitlb 7df 4	1.00	0.32	190.00
Mean	**5.75**	**2.28**	**72.87**

7dpf Count / Frequency / Interval

Control

Posterior	Count	Freq (cpm)	Interval(s)
May 15 2012 Control 7df 1	12.00	4.29	30.08
May 15 2012 Control 7df 2	10.00	1.31	50.40
May 15 2012 Control 7df 3	20.00	3.12	21.25
May 15 2012 Control 7df 4	4.00	0.89	78.75
May 15 2012 Control 7df 5	37.00	12.15	6.24
Mean	**16.60**	**4.35**	**37.35**
ttest	**0.50**	**0.34**	**0.96**

kitla/kitlb

Posterior	Count	Freq (cpm)	Interval(s)
May 15 2012 kitlakitlb 7df 1	12	1.65	44.42
May 15 2012 kitlakitlb 7df 2	11	1.95	35.09
May 15 2012 kitlakitlb 7df 3	13	2.15	30.92
May 15 2012 kitlakitlb 7df 4	12	2.12	36.25
Mean	**12**	**1.97**	**36.67**

7dpf Count/Frequency/Interval

Control			
Filename	**Count**	**Freq (cpm)**	**Interval(s)**
Controlinjected segres seq 1	13	1.41	43
Controlinjected segres seq 2	9	1.02	61.2
Controlinjected 16 March 2011 seq 2	6	0.802	82.1
Controlinjected 16 March 2011 seq 3	14	1.57	39.84
Controlinjected 11 July 2011 Seq 1	8	3.59	16.8
Controlinjected 11 July 2011 Seq 2	15	2.65	33.63
Controlinjected 11 July 2011 Seq 3	12	4.71	18.25
Controlinjected 11 July 2011 Seq 4	7	2.18	33.7
Mean	**11.00**	**2.25**	**42.12**
ttest	**0.06**	**0.10**	**0.24**

kitlb			
Filename	Count	Freq (cpm)	Interval(s)
Kitlbinjected 16 March 2011 seq 1	0		
Kitlbinjected 16 March 2011 seq 2	0		
Kitlbinjected 16 March 2011 seq 3	0		
Kitlbinjected segres seq 1	5	1.32448	49.2
Kitlbinjected segres seq 2	10	1.49	49.3
Kitlbinjected segres seq 3	10	1.04	59.6
Kitlbinjected segres seq 4	14	1.87	36
Kitlbinjected segres seq 5	11	1.16	52.9
Kitlbinjected segres seq 7	8	1.04	58
Kitlbinjected segres seq 8	8	1.21	49.8
Kitlbinjected 11 July 2011 Seq 1	11		46.1
Kitlbinjected 11 July 2011 Seq 2	1		
Kitlbinjected 11 July 2011 Seq 3	8		53.5
Mean	**6.62**	**1.30**	**50.49**

7dpf Count/Velocity/Distance

Control			
Filename	Count	Distance (um)	Velocity (um/s)
Controlinjected segres seq 1	13	128.3	4.56
Controlinjected segres seq 2	9	120.4	6.55
Controlinjected 16 March 2011 seq 2	6	382	8.91
Controlinjected 16 March 2011 seq 3	14	127.2	4.58
Controlinjected 11 July 2011 Seq 1	8	65.5	2.38
Controlinjected 11 July 2011 Seq 2	15	64.1	3.38
Controlinjected 11 July 2011 Seq 3	12	81.4	3.42
Controlinjected 11 July 2011 Seq 4	7	81.4	4.35
Mean	**10.50**	**131.29**	**4.77**
ttest	**0.06**	**0.45**	**0.42**

kitlb			
Filename	Count	Distance (um)	Velocity (um/s)
Kitlbinjected 16 March 2011 seq 1	0		
Kitlbinjected 16 March 2011 seq 2	0		
Kitlbinjected 16 March 2011 seq 3	0		
Kitlbinjected segres seq 1	5	133.9	4.15
Kitlbinjected segres seq 2	10	93.1	3.68
Kitlbinjected segres seq 3	10	91.1	3.42
Kitlbinjected segres seq 4	14	130.1	3.99
Kitlbinjected segres seq 5	11	109.3	4.92
Kitlbinjected segres seq 7	8	108.2	4.42
Kitlbinjected segres seq 8	8	127.7	4.67
Kitlbinjected 11 July 2011 Seq 1	11	68.4	2.18
Kitlbinjected 11 July 2011 Seq 2	1	92.82	5.15
Kitlbinjected 11 July 2011 Seq 3	8	97.02	5.04
Mean	**6.62**	**105.16**	**4.16**

Motility Index 7dpf

Control	
Filename	**MI**
Controlinjected segres seq 1	1
Controlinjected segres seq 2	1
Controlinjected 16 March 2011 seq 2	1
Controlinjected 16 March 2011 seq 3	1
Controlinjected 11 July 2011 Seq 1	1
Controlinjected 11 July 2011 Seq 2	1
Controlinjected 11 July 2011 Seq 3	1
Controlinjected 11 July 2011 Seq 4	0

kitlb	
Filename	**MI**
Kitlbinjected 16 March 2011 seq 1	0
Kitlbinjected 16 March 2011 seq 2	0
Kitlbinjected 16 March 2011 seq 3	0
Kitlbinjected segres seq 1	0
Kitlbinjected segres seq 2	1
Kitlbinjected segres seq 3	1
Kitlbinjected segres seq 4	1
Kitlbinjected segres seq 5	1
Kitlbinjected segres seq 7	0
Kitlbinjected segres seq 8	1
Kitlbinjected 11 July 2011 Seq 1	1
Kitlbinjected 11 July 2011 Seq 2	0
Kitlbinjected 11 July 2011 Seq 3	0

Motility Index 5dpf larvae

Control	
Anterior	**MI**
May 15 2012 Control 5df 1	1
May 15 2012 Control 5df 2	1
May 15 2012 Control 5df 3	0
May 15 2012 Control 5df 4	1
May 15 2012 Control 5df 5	1

kitla/kitlb	
Anterior	**MI**
May 15 2012 kitlakitlb 5dpf 1	1
May 15 2012 kitlakitlb 5dpf 2	1
May 15 2012 kitlakitlb 5dpf 3	1
May 15 2012 kitlakitlb 5dpf 4	0

Control	
Posterior	**MI**
May 15 2012 Control 5df 1	1
May 15 2012 Control 5df 2	1
May 15 2012 Control 5df 3	1
May 15 2012 Control 5df 4	1
May 15 2012 Control 5df 5	1

kitla/kitlb	
Posterior	**MI**
May 15 2012 kitlakitlb 5dpf 1	1
May 15 2012 kitlakitlb 5dpf 2	1
May 15 2012 kitlakitlb 5dpf 3	1
May 15 2012 kitlakitlb 5dpf 4	1

Motility Index 7dpf larvae

Control	
Anterior	**MI**
May 15 2012 Control 7df 1	0
May 15 2012 Control 7df 2	0
May 15 2012 Control 7df 3	1
May 15 2012 Control 7df 4	1
May 15 2012 Control 7df 5	1

kitla/kitlb	
Anterior	**MI**
May 15 2012 kitlakitlb 7df 1	1
May 15 2012 kitlakitlb 7df 2	0
May 15 2012 kitlakitlb 7df 3	0
May 15 2012 kitlakitlb 7df 4	0

Control	
Posterior	**MI**
May 15 2012 Control 7df 1	1
May 15 2012 Control 7df 2	1
May 15 2012 Control 7df 3	1
May 15 2012 Control 7df 4	0
May 15 2012 Control 7df 5	1

kitla/kitlb	
Posterior	**MI**
May 15 2012 kitlakitlb 7df 1	1
May 15 2012 kitlakitlb 7df 2	1
May 15 2012 kitlakitlb 7df 3	1
May 15 2012 kitlakitlb 7df 4	1